Control of Distributed Generation and Storage: Operation and Planning Perspectives

A thesis submitted to The University of Manchester for the degree of

Doctor of Philosophy
In the Faculty of Engineering and Physical Sciences

2015

Sahban Alnaser

Electrical Energy and Power Systems Group
School of Electrical and Electronic Engineering
The University of Manchester

Table of Contents

List of Figures

List of Tables

ACRONYMS

Active Network Management	ANM
Alternating Current	AC
Automatic Voltage and Power Factor Controller	AVPFC
Automatic Voltage Control	AVC
Bulk Supply Point	BSP
Carbon Capture and Storage	CCS
Case Based Reasoning	CBR
Combined Heat and Power	CHP
Constraint Satisfaction Problem	CSP
Coordinated Voltage Control	CVC
Council on Large Electric Systems	CIGRE
Demand Side Management	DSM
Department of Energy & Climate Change	DECC
Depth of Discharge	DoD
Direct Current	DC
Distributed Generation	DG
Distribution Network Operators	DNOs
Distribution State Estimation	DSE
Double Fed Induction Generator	DFIG
Electricity Networks Strategy Group	ENSG
Extra High Voltage	EHV
Fault Current Limiter	FCL
Feed-in Tariffs	FiTs
Generic Distribution System	GDS
Grid Supply Points	GSP
High Voltage	HV
Information, Communication and Control Technology	ICCT
Kirchhoff's Current Law	KCL
Kirchhoff's Voltage Law	KVL
Last In First Out	LIFO
Low Carbon Networks Fund	LCNF
Low Voltage	LV
Medium Voltage	MV
Network Management System	NMS
Normal Open Point	NOP
Office of Gas and Electricity Markets	OFGEM
On-Load Tap Changers	OLTCs
Optimal Power Flow	OPF

Photovoltaic	PV
Plug-in Electrical Vehicles	PEV
Probability density function	Pdf
Remote Terminal Unit	RTU
Renewable Obligation Certificates	ROCs
Revenue = Innovation+ Incentives+ Outputs	RIIO
Standard Test Conditions	STC
Static VAR Compensators	SVC
Supervisory Control and Data Acquisition	SCADA
Tip Speed Ratio	TSR
Transmission System Operator	TSO
Voltage Transformer	VT

ABSTRACT

Title: Control of Distributed Generation and Storage: Operation and Planning Perspectives
Sahban Wael Saeed Alnaser, University of Manchester, February 2015
Doctor of Philosophy (PhD)

Transition towards low-carbon energy systems requires an increase in the volume of renewable Distributed Generation (DG), particularly wind and photovoltaic, connected to distribution networks. To facilitate the connection of renewable DG without the need for expensive and time-consuming network reinforcements, distribution networks should move from passive to active methods of operation, whereby technical network constraints are actively managed in real time. This requires the deployment of control solutions that manage network constraints and, crucially, ensure adequate levels of energy curtailment from DG plants by using other controllable elements to solve network issues rather than resorting to generation curtailment only.

This thesis proposes a deterministic distribution Network Management System (NMS) to facilitate the connections of renewable DG plants (specifically wind) by actively managing network voltages and congestion in real time through the optimal control of on-load tap changers (OLTCs), DG power factor and, then, generation curtailment as a last resort. The set points for the controllable elements are found using an AC Optimal Power Flow (OPF). The proposed NMS considers the realistic modelling of control by adopting one-minute resolution time-series data. To decrease the volumes of control actions from DG plants and OLTCs, the proposed approach departs from multi-second control cycles to multi-minute control cycles. To achieve this, the decision-making algorithm is further improved into a risk-based one to handle the uncertainties in wind power throughout the multi-minute control cycles. The performance of the deterministic and the risk-based NMS are compared using a 33 kV UK distribution network for different control cycles. The results show that the risk-based approach can effectively manage network constraints better than the deterministic approach, particularly for multi-minute control cycles, reducing also the number of control actions but at the expense of higher levels of curtailment.

This thesis also proposes energy storage sizing framework to find the minimum power rating and energy capacity of multiple storage facilities to reduce curtailment from DG plants. A two-stage iterative process is adopted in this framework. The first stage uses a multi-period AC OPF across the studied horizon to obtain initial storage sizes considering hourly wind and load profiles. The second stage adopts a high granularity minute-by-minute control driven by a mono-period bi-level AC OPF to tune the first-stage storage sizes according to the actual curtailment. The application of the proposed planning framework to a 33 kV UK distribution network demonstrates the importance of embedding real-time control aspects into the planning framework so as to accurately size storage facilities. By using reactive power capabilities of storage facilities it is possible to reduce storage sizes. The combined active management of OLTCs and power factor of DG plants resulted in the most significant benefits in terms of the required storage sizes.

DECLARATION

No portion of the work referred to in this thesis has been submitted in support of an application for another degree or qualification of this or any other university or other institute of learning.

COPYRIGHT STATEMENT

DEDICATION

This thesis is dedicated to the memory of my Grandfather Saeed Alnaser

ACKNOWLEDGEMENT

I would like to express my deepest appreciation and special thanks to my Supervisor Dr. Luis (Nando) Ochoa for his great, valuable and continuous support and guidance throughout this research. I really appreciate his valuable comments, suggestions, discussions which have contributed significantly to this research. It has been a great opportunity for me to learn from his knowledge and professional experience.

My gratitude also goes to all my colleagues in the research team of Dr. Luis (Nando) Ochoa for the fruitful and enjoyable discussions during our weekly and monthly meetings.

I would like to acknowledge the University of Jordan for their financial support of my PhD studies.

Finally, special thanks to my wife Sereen and my children Rand and Faisal for their support. Special and sincerest thanks to my parents Wael and Mariam for their support throughout my life.

Chapter 1: Introduction

1.1 Research Background

1.1.1 Environmental and Energy Targets

Governments worldwide are formulating new energy policies in an effort to reduce greenhouse gas emissions and cope with the challenge of climate change [1]. The Climate Change Act 2008 has set a target for UK greenhouse gas emissions to have reduced in 2050 to 80% below the baseline of 1990. To ensure they can meet this target in 2050, the UK government has also placed targets on its volume of carbon emissions for each five year period until 2050. In particular, the UK needs to reduce carbon emissions by 50% during the period 2023-2027 relative to the levels in 1990 [2].

Crucially, the transition towards low-carbon energy systems requires an increase in the contribution of energy produced from renewable energy sources in the total energy consumption from the heating, transport and electrical energy sectors [3]. The UK government is committed by the European Renewable Energy Directive to achieve 15% of the total energy consumption from renewables by 2020[4]. Compliance with these energy targets necessitates an increase in the levels of electricity generated from renewable sources in the total electricity generation mix, to displace electricity generated from conventional fossil fuel power plants (e.g., coal, natural gas). Also, higher levels of renewable generation are required to supply the additional demand resulting from the electrification required in the transport and heat sectors in order to facilitate the adoption of more energy efficient low carbon technologies, for example Plug-in Electrical Vehicle (PEV).

To encourage investment in renewable generation, and to achieve the UK's environmental

and energy targets, financial incentives were introduced. The Renewable Obligation (RO) [6] and Feed-in Tariffs (FiTs) [7] are elements of the government's policy that have been introduced to provide such support. The renewable obligation was introduced in 2002 as the main support for renewable electricity projects larger than 5 MW, to provide additional revenue for renewable generation developers. Renewable Obligation Certificates (ROCs) are issued for energy produced from renewable sources (e.g., one ROC for each 1 MWh of energy generated from onshore wind power technologies), and suppliers in the UK electricity market are obliged to purchase ROCs to meet their renewable energy targets (i.e., a percentage of the sold energy has to be sourced from renewable generation). In addition, a feed-in tariff scheme that was introduced in 2010 rewards small scale low-carbon generation up to 5 MW for both generated and exported energy (back to the grid).

By considering the existing levels of low carbon technologies and the incentive schemes, the National Grid (the UK Transmission System Operator (TSO)) provides the future energy scenarios from 2014 to 2035 and 2050. The *gone green* scenario determines the capacities of low-carbon generation technology required to be connected to the UK electricity networks to achieve both the environmental and energy targets. This includes Carbon Capture and Storage (CCS), i.e. the capture of carbon emissions from fossil fuel generation, nuclear and renewable generation technologies such as wind and solar Photovoltaic (PV). The generation capacities for each five year period in this scenario (presented in Table 1.1) show that most low-carbon generation technology to be connected to the grid will relate to wind generation. In particular, 55 GW of onshore and offshore wind would need to be connected in 2035/2036, which will make up 43% of the total installed capacity [5].

Table 1.1: Generation Capacity (GW) in the Gone Green Scenario [5]

Generation type	2013/2014	2020/2021	2025/2026	2030/2031	2035/2036
Nuclear	9.5	9.0	6.4	9.0	10.7
Coal	20.5	7.2	3.3	-	-
Gas	30.8	34.1	36.6	33.7	31.9
CCS	-	-	0.3	4.5	11.0
Onshore wind	6.7	13.7	18.1	19.1	19.4
Offshore wind	4.1	12.5	26.6	31.9	35.4
Solar PV	2.3	7.5	11.4	15.6	20.1

1.1.2 Passive Distribution Networks

Renewable generation will be connected to the distribution networks in order to achieve the energy and environmental targets. By 2013/2014, the total volume of renewable Distributed Generation (DG) connected to the UK distribution networks is about 8.5 GW. This research will focus on wind power generation since it currently represents the highest share in the total volume of DG technologies used in the UK and it is considered to be a key solution towards the transition to low-carbon energy systems.

The transition towards low-carbon energy systems is placing considerable challenges on Distribution Network Operators (DNOs) to accommodate the increasing levels of renewable DG required to achieve the targets [5]. Distribution networks are traditionally designed and operated as passive circuits used to receive bulk power at the Grid Supply Points (GSP) and then distribute it to the end users, from high voltage levels to low voltage levels. Due to limited observability and controllability in the existing distribution networks, in particular at 11 kV, 6.6 kV and LV levels, they are designed according to the worst case condition so that real-time operational problems are all solved at the planning stage irrespective of their likelihood of occurrence.

The increasing levels of DG may change the traditional power flows in distribution networks, in particular during periods of maximum generation and minimum demand, which in turn may result in voltages above the statutory limits and overloading of network assets (e.g., lines, transformers) [8].

Given the limited observability in the distribution networks, DNOs consider the worst case scenario of maximum generation and minimum demand when connecting DG, such that network constraints (in particular voltages and thermal) are maintained within the network limits for all combinations of generation and demand. Catering adequately for the worst case scenario requires either restriction of the connected DG capacity or reinforcement of the existing network assets (increasing the capex to be paid by DG developers). Therefore, this passive "*fit & forget*" connection approach represents a barrier to the transition towards low carbon energy systems.

1.1.3 Active Distribution Networks

To accelerate the transition towards low carbon energy systems, distribution networks need to be enablers of renewable generation and provide efficient and cost-effective connection solutions, reducing the need for expensive and time consuming network reinforcements. This transition requires DNOs to move from passive to active connection approaches, where controllable devices and network participants are actively managed to increase the utilisation of the existing network assets [9-10]. This also will require a higher level of network visibility, to facilitate the adoption of future control solutions using monitoring elements and communication networks.

Active Network Management (ANM) is the close to real-time monitoring and control of distribution networks and controllable network elements, to solve network issues in close to real-time rather than upgrading the existing network assets. An active approach towards facilitating the deployment of larger volumes of renewable DG with cheaper and quicker connections is the application of curtailment, where set points are defined for multiple DG plants during each control cycle (e.g., one minute) in order to manage network constraints, such as congestion [11]. In those cases, the real power outputs of DG plants are actively controlled based on pre-determined rules to decrease the exports through a particular corridor of the distribution network. However, during high penetrations of DG capacity within the same distribution network, some DG plants could be subject to significant levels of curtailment, since generation curtailment is needed to manage congestion and voltage

issues. This may affect the profitability of DG developers, which in turn may place limits on the benefits of ANM in increasing the hosting capacity of distribution networks.

Hence, to ensure adequate levels of curtailment, advanced technical solutions are required [12] in order to not resort only to DG curtailment for managing network constraints. Therefore, to increase the harvesting of low-carbon electricity and to offer a positive business case to DG developers, the reactive power capabilities of modern wind farms could be used to alleviate voltage rise problems during high wind power injections and low demand. Moreover, the active management of On-Load Tap Changers (OLTCs) at substations could also alleviate voltage issues, thus minimising curtailment [13-14]. Battery energy storage is also considered to be a key technology for the near future. Indeed, network issues could be actively managed in real-time by storing the excess of DG production and releasing it later when constraints are not binding [15]. Storage facilities could also be controlled to absorb or inject reactive power within the rating of the power conversion system, allowing further flexibility to manage voltages [16].

Although rule-based ANM schemes are implementable in practice, the complexity brought about by the connection of multiple DG plants and the incorporation of future controllable network elements to actively manage multiple network constraints increases significantly. This scenario also increases operational overheads since more rules are needed to effectively coordinate the control actions of controllable network elements. Also, coordination between ANM schemes is required to ensure adequate levels of energy harvesting without resorting only to DG curtailment to manage network constraints.

Therefore, the introduction of more advanced control than that offered by a rule-based approach is required. This is a shift towards an intelligent, centralised, advanced Network Management System (NMS) [17] to actively manage network constraints for the benefit of the network and, crucially, to minimise curtailment from DG plants. This represents a transition in relation to distribution control centres, from them dealing only with power restoration to the inclusion of ANM functions.

1.1.4 Advanced Distribution Network Management Systems (NMS)

Advanced or future NMS algorithms have been proposed in the literature within the context of high penetrations of wind power in distribution networks. In [18] real-time measurements are considered using the Constraint Satisfaction Problem (CSP) method to obtain the best DG set points (i.e., curtailment) to solve congestion issues. A decision-making algorithm is proposed in [19] to find the most adequate set points based on a predefined search space generated through simulations or based on historical performance, to manage voltage constraints using OLTCs. However, the algorithms in [18-19] may fail to cope with more complex networks that include a significant number of control devices. In [20], an optimal power flow approach is applied to minimise DG curtailment but without including OLTCs. Moreover, none of the aforementioned NMS approaches provide a complete, integrated solution for both congestion and voltage problems. An integrated approach is considered in [21-22]. However, the optimisation problem is formulated in a simplified manner using linear programming and voltage sensitivity coefficients. The following summarises the key challenges that have not yet been adequately addressed in the literature.

Realistic Modelling of Control Aspects

From the control perspective, the realistic modelling of control aspects is needed to adequately model real-time operation and, thus, evaluate the performance of the controller. The above studies, except those from [18-20], do not consider the system response between successive control actions, making it impossible to adequately to model the real-time control aspects.

Uncertainties in Wind Power

The design of an advanced NMS must handle the uncertainties introduced by wind power (i.e., variability) and avoid/reduce the risk of violating network constraints [23-25]. Indeed, ‘optimal’ decisions taken for a given control cycle might be inadequate for the next one, leading to binding constraints or poor wind energy harvesting.

More specifically, the variability of wind power output for the uncontrollable DG units (firm generation) increases the challenge of actively managing thermal and voltage network constraints in real-time. In this context, the adopted decision may not be suitable for the next time step and may lead to violation of the operating constraints (voltage and thermal), particularly when wind power output changes from that in place at the time the decision was made.

Although in [18, 20, 26] multi-second control cycles are used to quickly react to wind variations, the above decision-making algorithms do not explicitly formulate the uncertainty of wind power. Also, the adoption of such multi-second control cycles may lead to large volumes of control actions from different controllable elements such as the OLTCs and the DG plants which may reduce their potential life cycles. In addition, in practice, there will be practical limitations on the control cycle due to mechanical and communication aspects or due to the response of the controllable elements.

1.1.5 Sizing of Storage Facilities in Active Distribution Networks

As indicated previously that energy storage facilities can be considered as a key technology for the near future to facilitate the connection of renewable DG. Due to the relatively high investment costs of energy storage facilities compared to other ANM control solutions, storage sizing framework is needed to determine the power and energy ratings of storage facilities. The following summarises the key challenges that have not yet been adequately addressed in the literature.

Optimal Sizing for Multiple Storage Facilities

In the literature, sizing of storage in the context of active distribution networks and DG has been proposed, mainly adopting trial and error approaches. In [27-29] this is done by investigating a number of predetermined storage sizes considering different control schemes. The optimal size is that which achieves a trade-off between the cost of the storage facility and the operational cost [27-28] or the volume of curtailment [29]. Although trial and error approaches might seem implementable and practical, they may

need to explore a large search space due to the combinations of power and energy capacities. Adequately covering this search space becomes even more challenging when multiple storage facilities are considered simultaneously.

Storage sizing techniques based on classical and meta-heuristic optimisation approaches are proposed in [30-31] (AC OPF) and [32] (genetic algorithm), allowing a more thorough exploration of the corresponding search space. In [30], although multiple storage facilities are considered, the aggregated capacity is sized for the required daily wind energy curtailment. This approach neglects the discharge periods that, if adequately taken into account, might reduce the required capacity of storage facilities. Another way of sizing these facilities is by considering the corresponding investment cost in the context of the provision of services (i.e., for profit or savings). In [31] and [32], the capital cost of multiple storage facilities was incorporated in addition to potential revenue streams but renewable energy curtailment was not part of the optimisation.

Modelling of High Granularity Control Aspects

Given the ANM context in which these facilities will be used, sizing approaches need to integrate close to real-time operational aspects in order to capture the actual storage needs (i.e., power and energy) [33-35].

Most of the above studies [27, 30-32] consider demand and generation on an hourly basis, neglecting the close to real-time changes that can be exploited by charge and discharge interactions for a more accurate sizing of storage. In addition, hourly intervals (or even intervals of 30-min or 15-min [28-29]) are not adequate for modelling the actual operation of other controllable network elements (e.g., on-load tap changers) that have the potential to bring further benefits in the context of ANM.

1.2 Research Hypothesis, Objectives and Scope

The hypothesis of this research is:

Centralised Network Management System (NMS) will enable the connection of greater volume of renewable DG in distribution networks by the deployment of control solutions that manage simultaneously congestion and voltage rise issues in close to real time and, crucially, ensure adequate levels of energy curtailment from DG plants by using other controllable elements to solve network issues rather than resorting to generation curtailment only. The integration of Battery energy storage in future NMS is a key solution to allow solving network issues and increase the exported energy from DG plants.

The following points summarise the objectives and the scope of this research to tackle the challenges not yet adequately addressed in the literature (discussed in Sections 1.1.4 and 1.1.5):

- Develop a comprehensive distribution NMS in the role of energy harvesting to manage simultaneously voltage and thermal constraints in close to real-time through the optimal control of OLTCs, DG power factor control and generation curtailment as a last resort.

- Develop realistic modelling of the control aspects in the NMS by adopting high granularity time-series data and considering the system response between successive control actions.

- Extend the decision-making algorithm in the proposed distribution NMS to handle the uncertainties introduced by wind power, to allow departure from multi-second control cycles to multi-minute ones so that network constraints are actively managed with less control actions.

- Develop a methodology to assess the performance of the proposed NMS in terms of voltage and congestion management, volume of energy curtailment and effects

of control cycles on the volume of control actions from renewable DG and OLTCs.

- Develop a planning framework to find the minimum sizes (power and energy) of storage facilities at multiple locations, so as to reduce curtailment from DG whilst managing congestion and voltages.

- Quantify the potential benefits of exploiting the reactive power capability of storage, OLTCs and power factor control of wind farms to reduce the overall size of storage facilities required to reduce curtailment.

- Understand to what extent the sizing of energy storage facilities in the context of active distribution networks requires modelling of the high granularity real-time control aspects.

1.3 Research Methodologies

Distribution Network Management Systems

A comprehensive distribution NMS is proposed, aimed at minimising DG curtailment whilst simultaneously managing network voltage rises and congestion close to real-time, considering the realistic modelling of control by adopting 1-min resolution time-series data. The AC Optimal Power Flow (OPF), which has been used within the context of planning in [12, 36-37], is adapted and expanded for realistic operational use in the production of optimal set points for OLTCs, DG reactive power output and generation curtailment as a last resort. Also, the AC OPF is tailored to comply with the existing firm connection agreements.

Risk-Based Distribution Network Management Systems

The deterministic NMS is extended to a risk-based system to allow the adoption of multi-minute control cycles, so that the volume of actions from OLTCs and DG plants can be reduced whilst effectively catering for the effects of wind power uncertainties. The AC

OPF is extended to produce optimal set points for the active elements to both minimise DG curtailment and reduce/avoid operational problems (i.e., risk of thermal overloading and voltage rise) that may result from wind uncertainty. A risk level is used to determine the extent to which congestion and voltage rise could exist during a control cycle.

Optimal Sizing of Storage Facilities to reduce Generation Curtailment

A two-stage planning framework that incorporates real-time control aspects is proposed, aimed at determining the required minimum sizes (power ratings and energy capacities) of storage facilities at multiple locations, in order to reduce curtailment from DG plants whilst managing voltages and congestion. The first stage uses a multi-period AC Optimal Power Flow across the studied horizon to consider simplified hourly wind and load profiles. The second stage adopts a high granularity minute-by-minute control driven by a mono-period bi-level AC OPF. This control minimises the required curtailment using the first-stage storage sizes and so the actual curtailment can be assessed over the studied horizon. This assessment is then used to tune the first-stage storage sizes accordingly. Congestion and voltages are managed through the intelligent control of storage (active and reactive power), OLTCs, DG power factor and DG curtailment as a last resort.

1.4 Research Contributions

Distribution Network Management Systems

An innovative and advanced distribution NMS is developed in this research which bridges the gaps in the literature discussed in Section 1.1.4. The key and the original contributions are summarized as follows:

- For the first time, a risk-based AC OPF decision-making algorithm is developed that allows the adoption of multi-minute control cycles in advanced NMS to reduce the volume of control actions by reducing the effect of wind power uncertainties and controlling the risk of overloading and voltage excursions throughout the control cycle.

- A methodology that allows an investigation in detail of the benefits and impacts of adopting different control cycles (key metrics: voltage compliance with BS EN50160 standard, congestion, capacity factor of wind farms and, crucially, volume of control actions). This provides DNOs with an important tool to understand benefits and challenges of departing from deterministic multi-second-based control cycles into risk-based longer cycles.

Optimal Sizing and Control of Storage Facilities

The proposed planning framework to size storage facilities is innovative and bridges the gaps in previous studies discussed in Section 1.1.5. The key and the original contributions are summarized as follows:

- The development of an innovative planning framework for sizing storage facilities that embeds the high granularity modelling of control aspects to capture accurately the actual power and energy needs of storage facilities. The proposed framework allows determination of the minimum size (power and energy) of multiple storage facilities without the need for a trial and error approach to explore large combinations of power ratings and energy capacities.

- The development of an innovative decision-making algorithm (AC OPF-based), adequate to optimally control in close to real-time the active and reactive power of storage facilities, OLTCs and DG power factor in addition to generation curtailment as a last resort.

1.5 Research Publications

The original contributions in this thesis presented in Section 1.6 related to the modelling of advanced NMS and planning of energy storage lead to the following peer reviewed journal and conference publications:

- S. W. Alnaser and L. F. Ochoa, “Optimal sizing and control of energy storage in

wind power-rich distribution networks", IEEE Trans. on Power Systems, submitted for second round of reviews (Paper TPWRS-01402-2014).

- S. W. Alnaser and L. F. Ochoa, "Advanced network management systems: A risk-based AC OPF approach", IEEE Transactions on Power Systems, vol. 30, pp. 409-418, 2015. DOI Link

- S. W. Alnaser and L. F. Ochoa, "Distribution network management system: An AC OPF approach", in IEEE/PES General Meeting 2013, 2013, p. 5. DOI Link

- S. W. Alnaser and L. F. Ochoa, "Towards distribution energy management systems: Maximising renewable DG", in 22nd International Conference on Electricity Distribution CIRED 2013, 2013, p. 4. DOI Link

- S. W. Alnaser and L. F. Ochoa, "Hybrid controller of energy storage and renewable DG for congestion management", in IEEE/PES General Meeting 2012, 2012, p. 8. DOI Link

1.6 Thesis Structure

The remainder of the thesis is structured as follows:

- **Chapter 2** provides an introduction to DG focusing on wind power generation due to its important role in the achievement of the environmental and energy targets in the UK. Then, the main technical impacts of DG on distribution networks are discussed in detail, particularly voltage and thermal constraints and how the passive operation of distribution networks can restrict the volume of DG capacity.

- **Chapter 3** provides an overview of ANM control solutions used in this work to manage thermal and voltage constraints. This includes generation curtailment, voltage control devices (OLTCs), power factor control of DG plants and energy storage facilities. An extensive literature review concerning the ANM schemes proposed in the literature to manage thermal and voltage constraints is provided.

The gaps in the literature are highlighted.

- **Chapter 4** presents the architecture of proposed deterministic NMS and the formulation of the optimisation engine. Results from the application of the proposed planning framework using a UK 33 kV network in the north-west of England, incorporating multiple wind farms and considering firm and controllable DG, are presented and discussed. To assess the performance of the proposed NMS using different control schemes, performance metrics are adopted (voltage compliance with EN50160 standard, congestion, volume of curtailment from wind farms and volume of control actions).

- **Chapter 5** extends the deterministic NMS in Chapter 4 into risk-based NMS, which allows the adoption of multi-minute control cycles in order that the volume of actions from OLTCs and DG can be reduced whilst effectively catering for the effects of wind power uncertainties. The architecture of proposed risk-based NMS and the formulation of the optimisation engine are presented. Then, the adopted methodology with which to handle the uncertainty due to wind power is given. Results from the application of the proposed NMS to simple and full case studies are presented and discussed, and compared with the deterministic NMS approach.

- **Chapter 6** presents a planning framework to find the minimum storage sizes (power and energy) at multiple locations in distribution networks, to reduce curtailment from renewable DG whilst managing congestion and voltages. Realistic control schemes are embedded within the proposed planning tool using a control cycle of 1-min. Results from the application of the proposed planning framework to multiple case studies are presented and discussed. The effectiveness of the approach in producing smaller sizes of storage facilities is also discussed.

- **Chapter 7** provides the conclusions drawn from the overall research. Also, the limitations of this work and future works are discussed.

Chapter 2: Renewable Distributed Generation in Distribution Networks

2.1 Introduction

This chapter introduces Distributed Generation (DG) and discusses the importance of renewable DG in achieving the environmental and energy targets in the UK. In particular, wind power generation is discussed in detail in terms of technology (wind turbines), characteristics of wind in the UK, and the recent and potential levels of wind power generation. In addition, this chapter introduces UK distribution networks to which DG is connected in terms of voltage levels, components and design. Then, the main technical impacts of DG on distribution networks are discussed and how the passive operation of distribution networks can restrict the volume of DG capacity. This chapter also highlights the need for Active Network Management (ANM) as a building block in the smart grid to facilitate the connection of DG without the need for network reinforcements. The potential characteristics, control functions and technologies of future smart distribution networks are briefly presented at the end of the chapter.

2.2 Renewable Distributed Generation (DG)

Several definitions are used in the literature to refer to DG [8, 38-39]. In most of these studies, DG is defined according to the rating of the generation plant [40-41]. For example, within the context of generation plants with capacities below 50-100 MW, DG is referred to according to the definition provided by the International Council on Large Electric Systems (CIGRE). Additional definitions of DG are based on the location of generation

plants (voltage levels), technology (e.g., fossil fuels, renewables), environmental impact and mode of operation (e.g., centrally dispatched, decentralised controlled and uncontrolled) [39-40]. Embedded generation and dispersed generation are sometimes used as alternative terms for DG [8]. A general definition of DG is provided in [39] as follows:

"Distributed generation is an electric power source connected directly to the distribution network or on the customer side of the meter".

Different DG technologies based on the energy resource have been developed, e.g. Combined Heat and Power (CHP), biomass generation, renewable DG in the form of wind, solar, wave, etc. In particular, renewable DG plays a significant role in the achievement of the UK environmental targets. By the end of 2013, the total capacity of renewable DG connected to the UK distribution networks was 8.5 GW. Wind is the most commonly adopted technology for generation plants above 1 MW, and with total capacities of 4 GW. On the other hand, solar PV is the most commonly adopted technology for generation plants below 1 MW. Indeed, the Feed-in Tariff incentive scheme facilitated considerably the connection of 1.9 GW of solar PV during the period from 2010 to the end of 2013 [5].

The *gone green* scenario produced by National Grid [5] determines the level of renewable DG required to achieve the 2035 and 2050 carbon reduction and energy targets. Fig. 2.1 shows the levels of DG capacity adopted in this scenario in 2035/2036, classified according to the technology and rating of generation plants (above and below 1 MW) and compared to the corresponding existing levels in 2013/2014. It can be seen that the total share of wind generation for generation plants above 1 MW is expected to increase significantly from 4 GW in 2013/2014 to 10 GW in 2035/2036. Also, this scenario shows a significant increase in the total capacities of solar PV to 14 GW by 2035/2036.

This research will focus on wind power generation since it currently represents the highest share in the total volume of DG technologies used in the UK and it is considered to be a key solution towards the transition to low-carbon energy systems. The next sections will present an overview of wind generation in terms of technologies, characteristics of wind

resource in the UK and figures in relation to the total installed capacities. Then, solar PV will be briefly introduced.

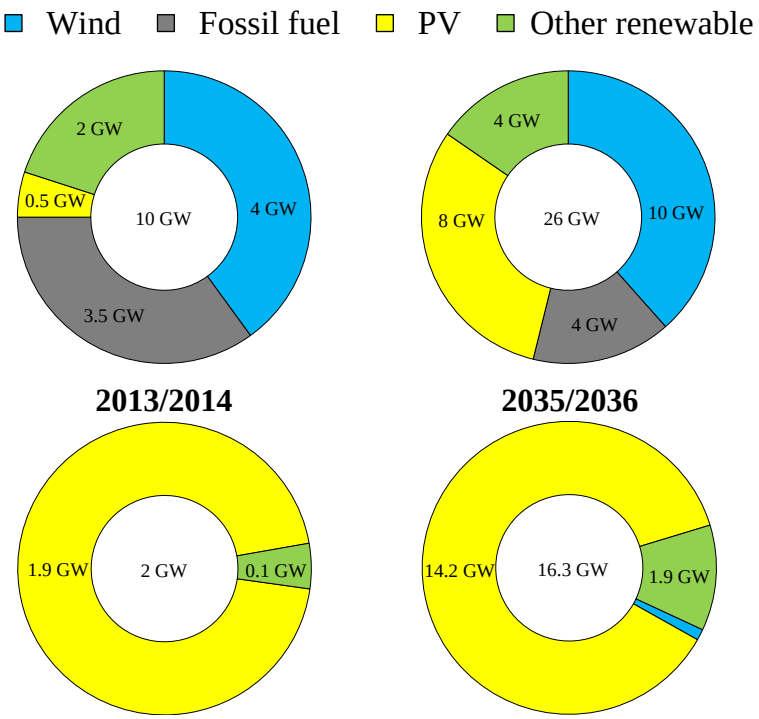

Fig. 2.1 Total installed distributed generation capacity (top) above 1 MW and (bottom) below 1 MW for 2013/2014 and 2035/2036 for the gone green scenario [5]

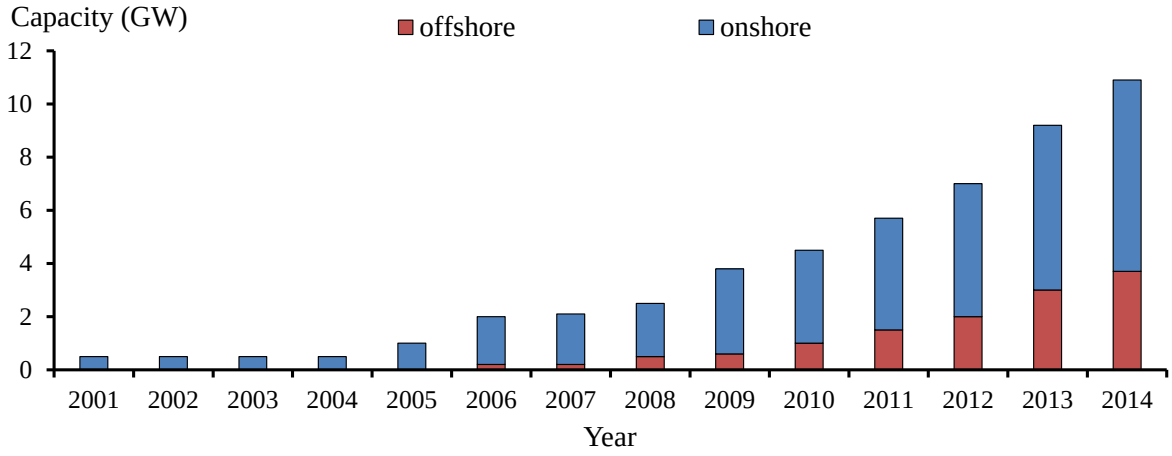

Fig. 2.2 Accumulated wind power deployment in the UK electricity system [42]

2.2.1 Wind

Electricity generation from wind is a central component in the achievement of the environmental targets. As shown in Fig. 2.2, the total installed capacity of wind connected to the UK electricity system has grown significantly from 400 MW to approximately 11 GW in 14 years (between 2000-2014); this consists of 6.7 GW and 4.0 GW of onshore and offshore technologies, respectively [42]. In particular, in 2012-2014, the deployment of wind increased by 57% from 7 GW to 11 GW.

According to the global wind report of 2014, the UK is ranked third in Europe in terms of wind installed capacity, following Germany (34 GW) and Spain (23 GW). Also, the UK has become the sixth country in the world to achieve the 11 GW wind installed capacity connected to transmission and distribution network, which accounts for 3.4% of the worldwide figure (318 GW) [43]. The total capacity of wind generation connected to distribution networks is currently about 4 GW (as shown in Fig. 2.1) that accounts for 36% of the total wind installed capacity in the UK.

Wind Turbines

Wind turbines operate by transforming part of the kinetic energy content that results from the wind blowing over the turbine's blades into electrical energy. Basically, the wind blows across the blades of the turbine and the resultant forces rotate the blades, which in turn rotate the connected low speed shaft. Then, the gearbox increases the rotational speed of the blades to the level required by the generator connected to the high speed shaft. The generator will then convert the mechanical power into electrical power at a voltage level of around 690 V. The generated power can then be fed to the grid using a step-up transformer. The basic components of the wind turbine and the corresponding power flow are shown in Fig. 2.3 [44].

The extracted power of the wind turbine P (in Watts) is given by in Equation (2.1)

$$P = \frac{1}{2}\, C_p\, \rho\, v^3\, A \tag{2.1}$$

where C_p is the power coefficient, ρ is the air density (1.25 kg/m^3), v is the wind speed (m/s) and A is the swept area of the rotor (m^2) that depends on the blade's radius r.

The power coefficient C_p represents the performance of a wind turbine as a fraction of the power that can be harvested from the available wind power resource. The theoretical upper

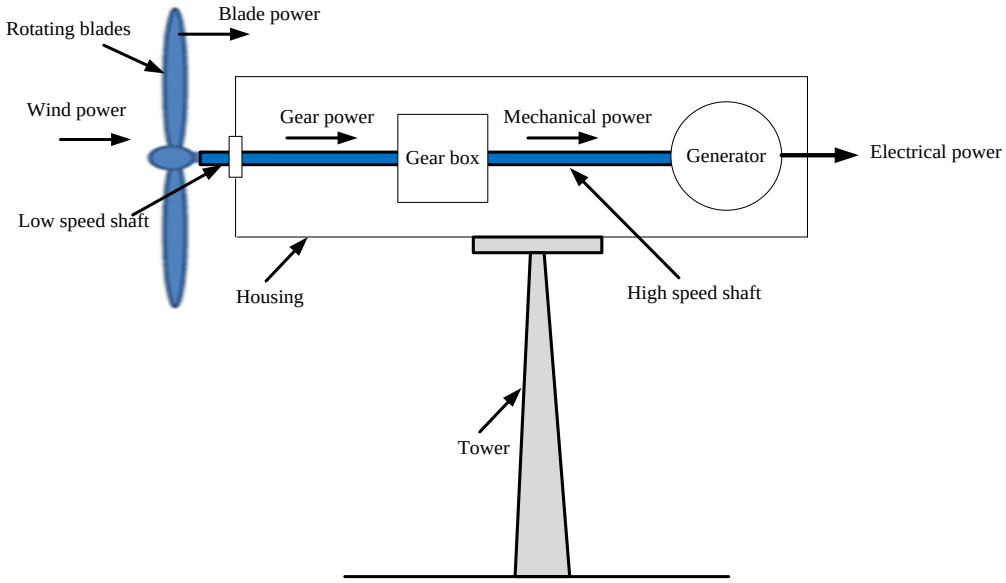

Fig. 2.3 Basic components of a wind turbine [44]

limit of power coefficient C_p^{theory} is 0.59 according to the Betz limit, which states that not all energy from a moving fluid can be extracted. In practice, the maximum value of the power coefficient is in the range of 0.4-0.45. It is a function of the Tip Speed Ratio (TSR) λ, defined as the ratio between the tip velocity v_{tip} and the wind speed v.

The TSR ratio is given in Equation (2.2) in terms of the blade's rotational speed ω, the blade's radius r and the wind speed v [8, 44-45].

$$\lambda = \frac{v_{tip}}{v} = \frac{\omega r}{v} \tag{2.2}$$

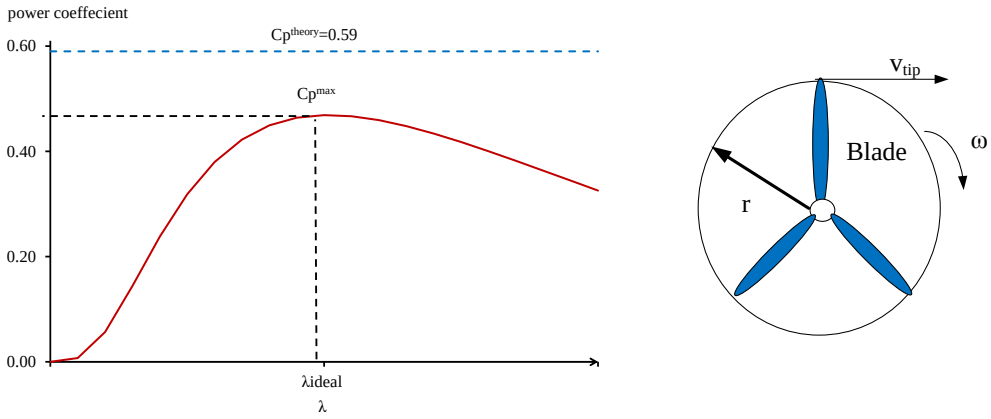

Fig. 2.4 Power coeffecient of a wind tubine as a function of tip speed ratio [44]

It can be seen from the relationship of the power coefficient and the TSR presented in Fig. 2.4 that there is an optimal tip speed ratio λ_{ideal} at which the maximum power coefficient can be obtained. Therefore, to achieve this optimal value of TSR and thus maximise the power coefficient (i.e., maximise the harvested energy), the rotational speed of the turbine's blades needs to be adjusted in response to the wind speed. For example, if the wind turbine is operating at the optimal TSR and wind speed increases, the TSR will decrease according to (2.2), which in turn will reduce energy harvesting. Therefore, if it is possible to increase the rotational speed of the turbine (this depends on the technology), the wind turbine can return to the optimal power coefficient point at λ_{ideal} and therefore increase the energy harvesting [44].

Also, the power coefficient is a function of the blade's pitch angle. Basically, controlling the pitch angle β allows a change in the angle of attack between the wind and the blades, which in turn affects the harvested energy. Fig. 2.5 presents the power coefficient for different values of pitch angle β. It can be seen that for a given TSR, reducing the pitch angle allows an increase in the power coefficients (increasing the perpendicular forces on the turbine blades). This highlights the importance of pitch angle control in achieving a desired power output (active power control) [44, 46].

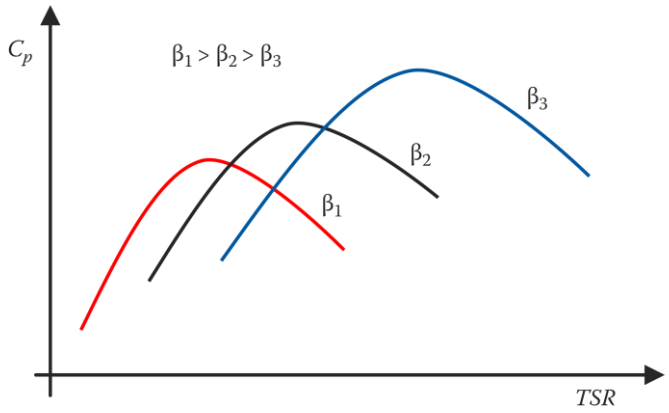

Fig. 2.5 Power coefficients as a function of a blade pitch angle

Wind turbines are classified into four types as follows:

Type 1: Fixed speed turbine: This is the oldest and the simplest design of wind turbine. A simplified schematic diagram of a fixed speed Type 1 turbine is shown in Fig. 2.6. It consists of a squirrel-cage induction generator connected directly to the grid without converters. The generator is connected to the blades by a gearbox, which is required in order to increase the mechanical speed of the generator above its synchronous speed so that power can be injected into the grid. The induction generator operates at a low voltage level – typically 690 V – and is connected to the grid using a step-up transformer. Capacitor banks can be connected to the induction generator to control the power factor of the turbine. However, its reactive power capability is limited compared to other turbine types. Since this type of turbine operates at a fixed speed, the maximum power coefficient can only occur at a single wind speed. This, in turn, highlights the importance of the variable speed operation of wind turbines to track wind speed and maximise harvesting from wind. The other three types of wind turbine provide speed control.

Type 2: Variable speed induction generator: A simplified schematic diagram of a Type 2 wind turbine is presented in Fig. 2.7. It consists of a wound rotor induction generator, gearbox and variable external resistors connected to the rotor windings of the generator. By controlling the power dissipating through the resistors, the speed of the turbine can be controlled to increase its power coefficient. Also, controlling power consumption in the

resistors can be considered a simplified form of controlling the power output of the wind turbine. However, the use of resistors to control the turbine comes at the expense of lost energy, which dissipates in the resistors as heat.

Type 3: Double Fed Induction Generator (DFIG): This type is the most commonly adopted design worldwide. Its basic design is presented in Fig. 2.8. It consists of DFIG, which is a wound induction generator and two power converters connected at both the generator side and the network side. The converters allow for the control of voltage across the rotor of the generator so that a greater range of speed control can be achieved compared to the Type 2 wind turbine. Also, the power converters allow for control of the active and reactive power output of the turbine in addition to voltage at the grid side.

Type 4: Full converter turbine (Fig. 2.9): This is another form of variable speed turbine. The generator may be induction or synchronous. In order to avoid frequent failure of the gearbox, it is omitted from this design. To control the speed of the turbine without affecting the frequency of the grid, the generator is interfaced to the grid using a power electronic converter. Since the power of the generator will pass through the converter, the size of the converter is selected in accordance with the rating of the generator. As with the Type 3 wind turbine, the use of power converters allows control over the active and reactive power outputs of the turbine, as well as voltages. Extended reactive power capability can be obtained compared to Type 3 due to the relatively larger size of the power converter.

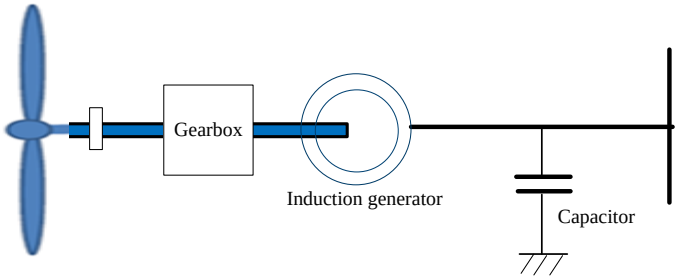

Fig. 2.6 Type 1: Simplified schematic of a fixed speed wind turbine [44]

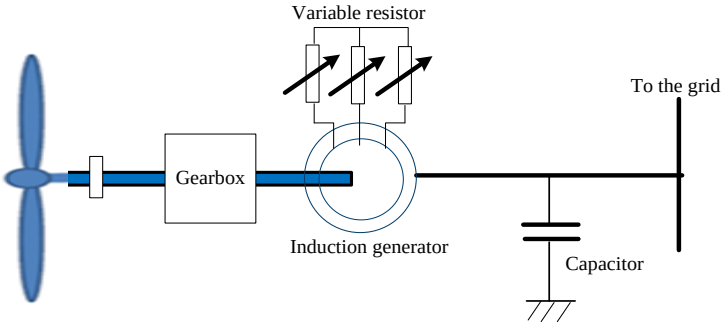

Fig. 2.7 Type 2: Simplified schematic of a variable speed induction generator wind turbine [44]

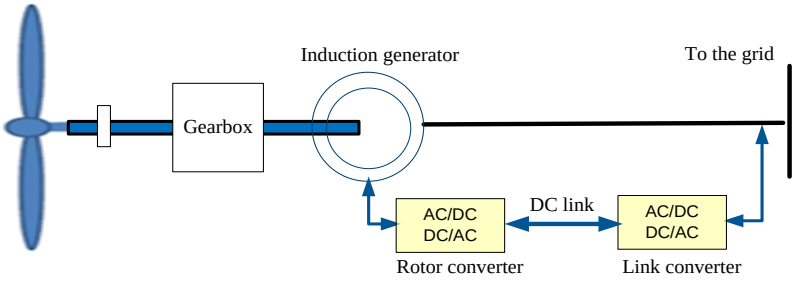

Fig. 2.8 Type 3: Simplified schematic of a Double Fed Induction Generator (DFIG) wind turbine [44]

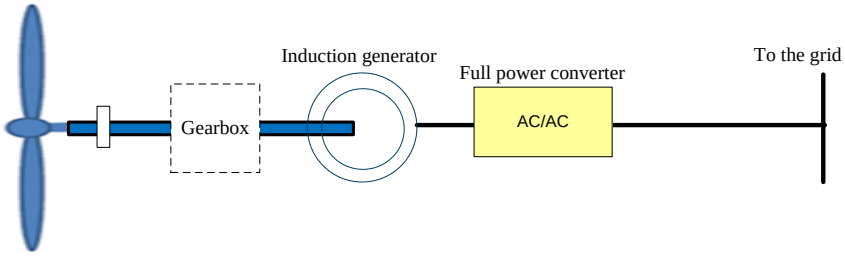

Fig. 2.9 Type 4: Simplified schematic of a full converter wind turbine [44]

Wind Power Curve

The performance of the wind turbine is described using its power curve, which illustrates the relationship between the output power of the turbine against various wind speeds. The power curve is characterised mainly by three wind speeds: cut-in speed, rated speed and cut-out speed. Fig. 2.10 is an example of a wind power curve for a 3 MW wind power turbine [47].

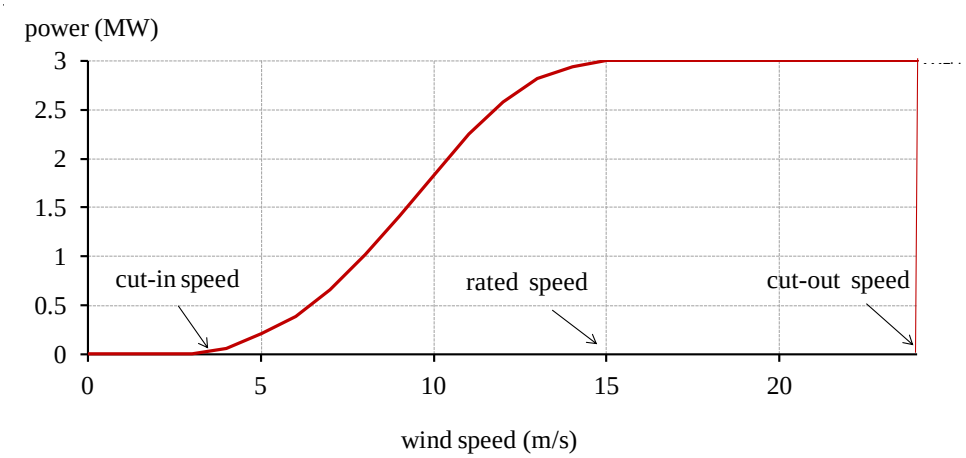

Fig. 2.10 Wind power curve of a 3 MW generator [47]

The wind turbine starts producing power once the speed of the wind becomes higher than the cut-in speed, typically between 4-5 m/s. Then, the wind power increases with the wind speed following an approximately cubic function until the wind speed reaches the rated speed of the turbine. Then, the wind power is limited up to the rated power of the turbine as the wind speed is below the cut-out speed, typically 25 m/s. When the wind speed exceeds the cut-out speed, the turbine will be shut down for safety purposes. Controlling the blade's pitch angle is the common control approach used to maintain the power output below the rating of the generator for wind speeds between the rated speed and the cut-out speed [45].

In order to estimate the potential energy yield from a wind turbine at a particular site, the annual wind speed time series is needed. By combining the wind speed data and the power curve of the turbine, the power output for each time step can be found. Fig. 2.11 shows an

example of the statistical analysis of annual hourly wind speed for a particular site in the UK [45]. The projection of the wind speed data onto the wind power curve (presented in Fig. 2.10) shows that the turbine will only inject its rated power for 2.7% of the year. This corresponds to the wind speed between the rated speed (15 m/s) and the cut out speed (25 m/s) of the turbine. In contrast, it can be seen from the statistical distribution of wind speed that the probability of wind speed above the cut-out speed (25 m/s) in the year is very small. This in turn shows that the wind turbine will block generation during rare wind speed events in the year.

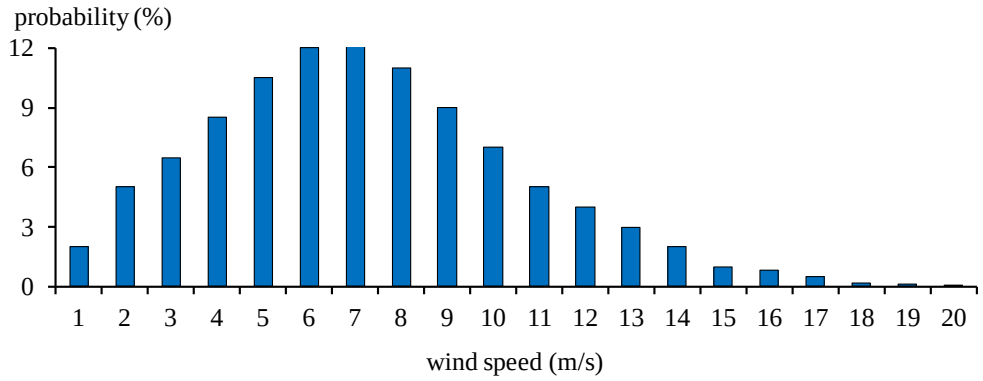

Fig. 2.11 Statistical analysis of annual hourly wind speeds at a site in the UK [45]

However, it is important to note that wind speed measurements are in practice usually taken at a lower height than the height of the turbine. To accurately estimate energy production, it is necessary to estimate the wind speed at the hub height to cater for the effect of hub height on wind speed: the so-called "*shear effect*" [48-49]. Indeed, the log-law or power law has to be used. These laws describe the relationship between the wind speed $v(z_r)$ at a reference height z_r (at which the measurements are taken) and the wind speed $v(z)$ at the hub height z. Equation (2.3) describes the power law with an exponent of α which depends on the type of site (e.g., smooth terrain, urban areas with tall buildings). Its value ranges between 0.1 and 0.4.

$$\frac{v(\mathrm{z})}{v(z_r)} = \left(\frac{z}{z_r}\right)^{\alpha} \tag{2.3}$$

This equation is presented in Fig. 2.12 which considers a power exponent of 1/7 for different hub heights and two reference heights of 30 m and 50 m. The y-axis shows the hub height and the x-axis is the factor required to adjust the wind speed measurements. To illustrate the figure, assume that the height of a wind turbine is 90 m and the wind speed measurements are taken at a lower height of 30 m; the measurements then have to be multiplied by a factor of 1.18 to estimate the wind speed at the hub height (point a). If the measurements are taken at the greater height of 50 m, a smaller factor of 1.1 is needed to adjust the wind speed (point b). Otherwise, if the measurements are taken at the hub height, there is no need to adjust the wind speed [48-49].

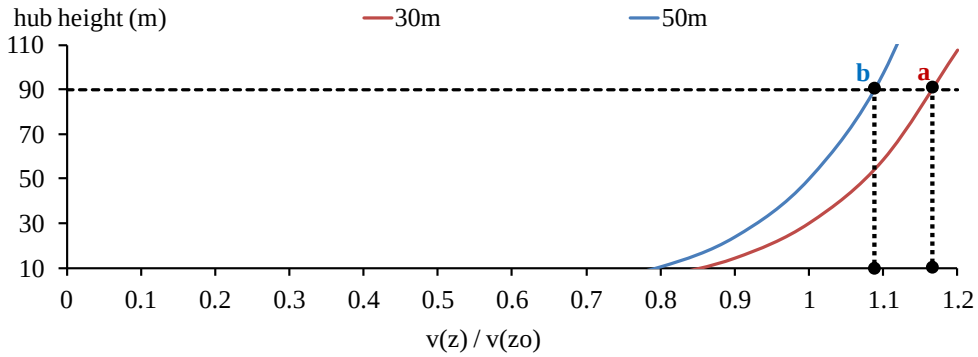

Fig. 2.12 Wind power at 30 m and 50 m reference height [48-49]

Characteristics of Wind Power in the UK

The annual capacity factor of a wind turbine is calculated as the ratio of the actual energy production to the theoretical level that could be produced if the turbine were to generate its full rated power throughout the year. Typically, the average annual capacity factor for onshore wind turbines in the UK is between 28% and 30% [50].

Fig. 2.13 presents the average monthly capacity factor for a number of wind farms in the UK over a period of 34 years (1970-2003) [51]. These figures are based on actual power measurements for a number of offshore and onshore wind farms. The average annual capacity factor is 30%, while the maximum monthly capacity factor is 40% and occurs in January. These figures demonstrate the seasonal effect on the capacity factor. Indeed, the

energy output in winter during December, January and February makes up one-third of the total potential annual available resource. In contrast, 17% of the energy output is generated in summer during June, July and August [51].

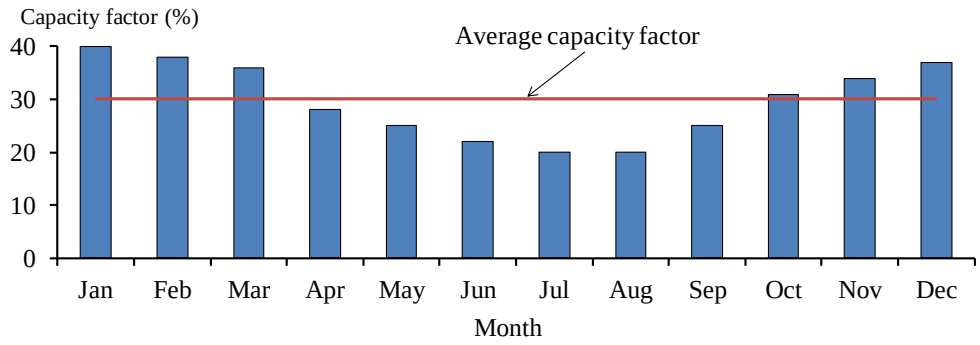

Fig. 2.13 Average monthly wind power capacity factor between 1970-2003 in the UK [51]

2.2.2 Photovoltaic (PV)

This section will briefly present solar PV as another form of DG technology. As indicated previously, solar PV is the most commonly adopted technology for DG plants below 1 MW in the UK. Solar cells are building blocks in the design of the PV system. Basically, they convert solar light into electrical DC power. The performance of a solar cell is obtained by its electrical characteristics which are described by the solar cell's I-V curve. In principle, the I-V curve represents the cell energy conversion capability at a particular irradiance level (W/m^2) and the temperature at which the current varies from a short circuit current (I_{sc}) at zero voltage to a zero current at open circuit voltage (V_{oc}). Fig. 2.14 shows a typical I-V curve and the corresponding power voltage (P-V) curve. It can be seen that the maximum DC power (P_{max}) is produced near the curve knee at I_{mp} and V_{mp}.

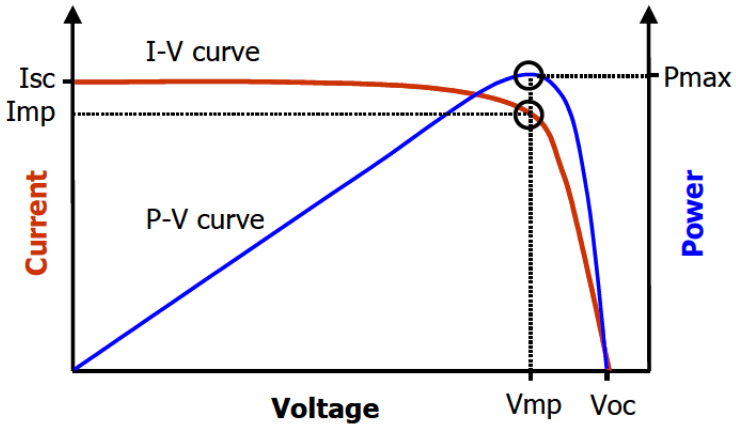

Fig. 2.14 Typical I-V and P-V curves of PV cells [52-53]

The connection of solar cells in series and parallel builds up the peak power rating of a PV panel. As shown in Fig. 2.15, the series connection increases the open circuit voltage while the parallel connection increases the short circuit of the array. The combination of series and parallel connections will in turn increase the maximum produced output power.

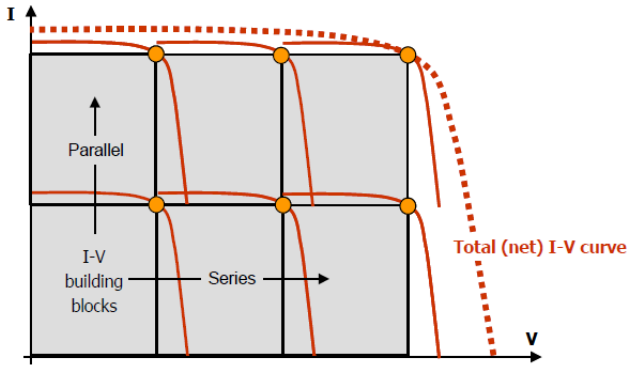

Fig. 2.15 An I-V curve for a PV array [52-53]

The DC power output of PV is rated by the manufacturers under the Standard Test Conditions (STC). The Standard Test Conditions include, but are not limited to, solar irradiance (intensity) (i.e., 1000 W/m^2) and solar cell temperature (i.e., 20°C). Any deviations from these test conditions affect the power output of the solar module. For a given irradiance level, the PV output power will be reduced by a factor according to the panel temperature. For example, considering a 253 W PV panel with a temperature reduction factor of -0.45%/°C, the power output of the PV panel will drop to a level of

30% of the rated capacity as the temperature increases from 20°C to 85°C.

A PV inverter is used to convert DC power into AC power, which is required to supply AC loads. The conversion process from DC-AC results in power losses which vary with different inputs of DC power.

2.3 UK Distribution Networks

The expansion of renewable generation, particularly wind energy, introduces new challenges for distribution networks to accommodate the increased volume of DG. This section presents an overview of UK distribution networks and the following section will present the potential impacts of DG on distribution networks.

The structure of the electricity industry in the UK is shown in Fig. 2.16. Electrical power is generated by centralised large-scale power generation plants connected to the transmission networks, at 400 kV and 275 kV in England and Wales and at 400 kV, 275 kV and 132 kV in Scotland. The transmission networks then transport electrical power towards distribution networks at the Grid Supply Points (GSP), which transform voltages from 275 kV and 400 kV to 132 kV. Distribution networks in England and Wales begin at 132 kV (33 kV in Scotland) and deliver the received bulk power to the end users of the networks at lower voltage levels. The voltage is first transformed from 132 kV to 33 kV at Bulk Supply Points (BSP) and from 33 kV to 11 kV and 6.6 kV at primary substations. Distribution substations then transform voltages into the Low Voltage (LV) levels required to supply single phase users at 230 V and three phase users at 400 V. Larger commercial and industrial consumers could also be connected at High Voltage (HV) levels at 6.6 kV and 11 kV and Extra High Voltage (EHV) levels at 132 kV and 33kV [54].

End users are connected to the substations using overhead lines and underground cables. Typically, underground cables are used for feeders in urban areas with higher load density, while overhead line feeders are used for rural feeders. Different types of switching elements are installed along distribution feeders to maintain and improve the security of the supply by isolating faults quickly and by reducing the number of disconnected users

and the duration of interruptions. Switches are used to reconfigure power flow in the network. They can interrupt the load current but not the fault current. In contrast, breakers can interrupt the fault current and they are combined with protection relays to detect faults and trigger circuit breakers to break fault currents. Reclosers and sectionalisers are also used with MV overhead lines to avoid disconnecting distribution feeders due to temporary faults.

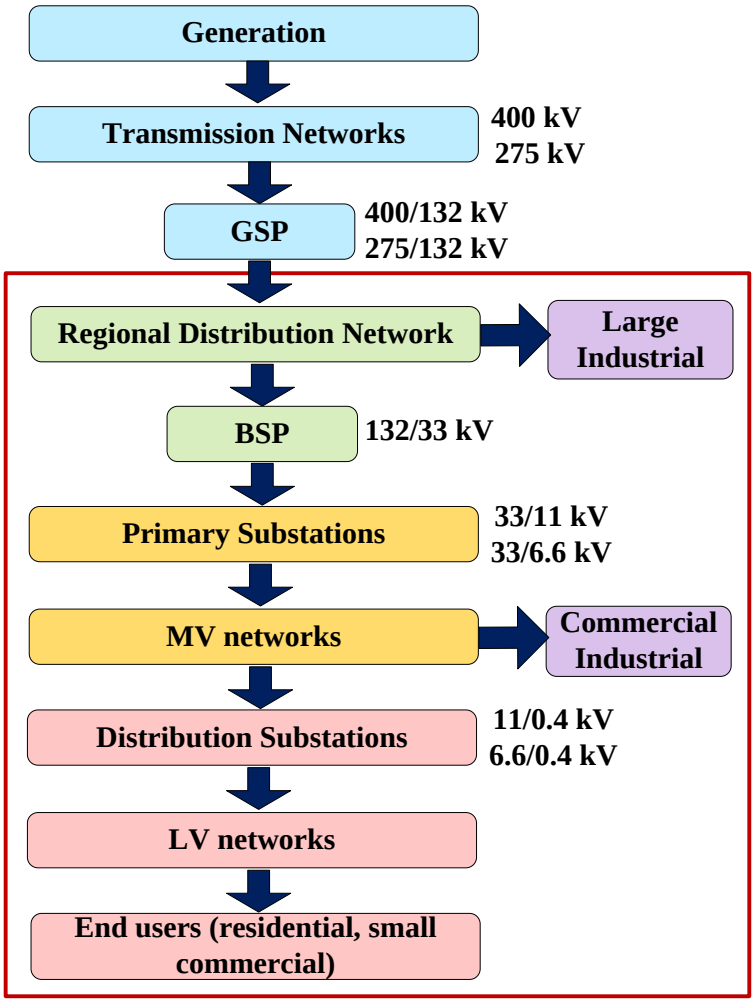

Fig. 2.16 UK electricity industry structure

There are three main topologies used to design distribution networks and they are shown in Fig. 2.17 [55]. Typically, radial network topology is used to design LV distribution networks. Ring topology is adopted in most 11 kV and 33 kV feeders to improve the

security of the supply in the event of circuit outages during faults or scheduled outages due to maintenance. Indeed, the Normal Open Point (NOP) is located between the two interconnected feeders to ensure radial operation for each feeder. The location of the NOP can be moved following the occurrence of a fault, such that the faulty section is isolated and power is restored to all users connected to the two interconnected feeders. Further security could be achieved by the connection of multiple feeders (Interconnected Topology). This is adopted in the 132 kV design due to the large distribution areas and BSP substations fed from the 132 kV feeders. However, the adoption of such a design at lower voltage levels would increase the complexity of the operation in addition to necessitating a relatively high investment.

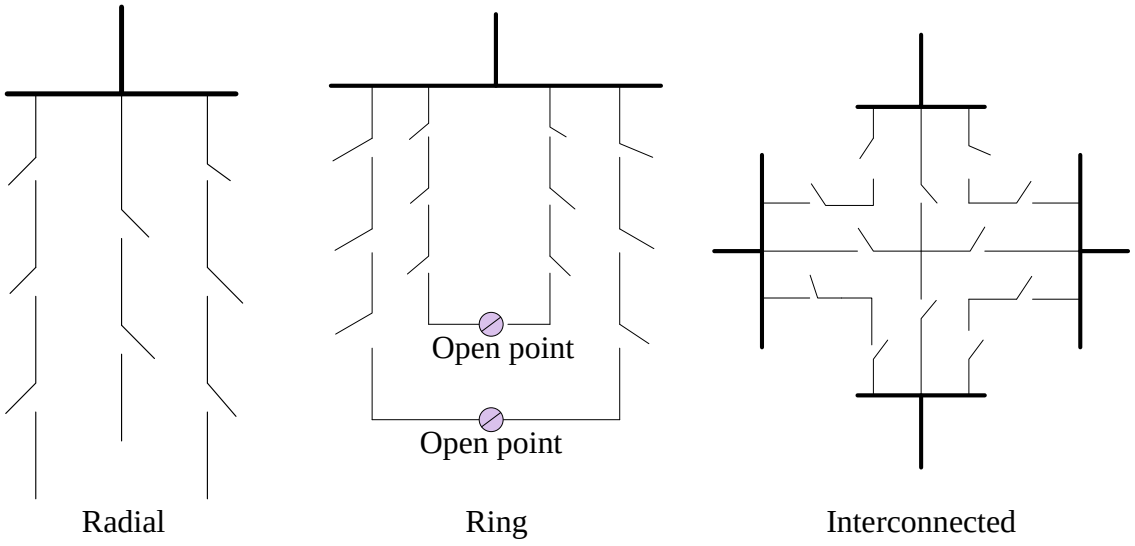

Fig. 2.17 Distribution Network Topologies [55]

Due to the natural monopoly that exists in relation to the operation of distribution networks, where competition is not applicable, distribution networks are operated in each region of the UK by a Distribution Network Operator (DNO) according to a regional distribution license. DNOs are regulated by the Office of Gas and Electricity Markets (OFGEM). DNOs are obliged to comply with the distribution performance standards and to provide reliable and secure power supply to network users. A cap is set on the maximum revenue that the DNOs can collect from the users of distribution networks. In contrast,

incentives are offered to encourage improvement in the performance of distribution services according to predetermined metrics, for example energy losses, connection time and security of supply [56].

2.4 Impacts of Distributed Generation on Distribution Networks

Distribution networks are traditionally passive with limited monitoring and control functions. The power flow in distribution networks is unidirectional, delivering bulk power received at the BSP to the end users. Therefore, distribution networks are designed with respect to peak demand, such that capacities of network assets are selected so as to maintain network constraints within the limits of the worst case scenario. The increasing levels of DG may change the power flow from unidirectional to bi-directional. This in turn will require an understanding of the corresponding technical impacts of DG on distribution networks. The following sections present the main impacts of DG on distribution networks in terms of network voltages, thermal overloads, fault levels, protection and power quality [8, 45, 57-58]. Voltage and thermal constraints are the only constraints considered in this work.

2.4.1 Network Voltages

Distribution network operators are obliged to maintain within statutory limits the voltage level supplied to all network users. According to provision 27 of the Electricity Safety, Quality and Continuity Regulations 2002, the permitted voltage variations limits are classified according to the voltage levels [59]:

Low voltage supply operating at a voltage below 1 kV

Voltage variation should not exceed 10% above or 6% below the nominal voltage at the declared frequency.

MV voltage supply operating at a voltage below 132 kV

Voltage variations should not exceed 6% above or below the declared voltage at the

declared frequency. In addition, DNOs are obliged to comply with the BS EN5010 standard. The standard states that

"during an observation period of a week, 95% of the 10-min Root Mean Square (rms) voltage magnitude measurements at the consumer connection point should be within the statutory limits".

The statutory limits are defined as ±6% for consumers connected to MV networks (33 kV, 11 kV and 6.6 kV) and +10% and -6% for consumers connected to LV networks (0.4 kV).

The connection of DG may change the direction of power flow and will increase the voltage beyond those defined limits in the standards. To demonstrate the impact of DG on distribution network voltages, a simple two-bus system, as shown in Fig. 2.18, is used. The network accommodates a load and generator connected to bus 2. Equation (2.4), proposed in [60], is used to approximate the voltage at bus 2 based on the assumption that the angle between the source bus (bus 1) and the receiving bus (bus 2) is very small; therefore the quadrature component of voltage drop/rise is neglected [60].

$$V_2 \approx V_1 + (P_G - P_L)R + (\pm Q_G - Q_L)\,X \tag{2.4}$$

where V_1, V_2 are the p.u. voltages at the source and the receiving bus, respectively. R and X are the per unit resistance and reactance of the line, and P_L and Q_L are the per unit active and reactive powers of load, respectively. P_G and Q_G are the per unit active and reactive powers injected by the generator, respectively,

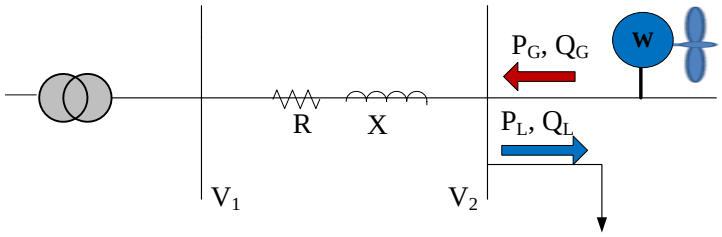

Fig. 2.18 Two-bus system [60]

As indicated by Equation (2.4), the active power injection from the generator above the demand level will create a reverse power flowing upstream towards the source bus, resulting in voltage increase at the connection point of the generator (bus 2).

Due to the limited observability and controllability of distribution networks, DNOs consider the worst case condition to solve voltage rise issues that could result from the connection of DG. Real-time operational problems are all solved at the planning stage. This is achieved by either reinforcing the existing network assets or limiting the maximum DG capacity that can be connected. Under this "*fit and forget*" approach, the maximum DG capacity ${P_G}^{max}$ that can be connected without violating voltages above the maximum tolerance voltage limit ${V_2}^{max}$ for all the combinations of demand and generation can be given in Equation (2.5), assuming the DG operates at unity power factor ($Q_G = 0$) and at no load ($P_L = Q_L = 0$).

$$ {P_G}^{max} \leq \frac{{V_2}^{max} - V_1}{R} \tag{2.5} $$

It is important to highlight the benefits of operating DG in the inductive power factor ($Q_G < 0$) mode (absorbing reactive power) to increase the maximum DG capacity, as given in Equation (2.6):

$$ {P_G}^{max} \leq \frac{{V_2}^{max} - V_1}{R} - Q_G \frac{X}{R} \tag{2.6} $$

Voltage rise issues are more significant in the context of UK low voltage systems due to the relatively high voltage transformation ratio of transformers in distribution substations (11kV/0.433kV, 6.6kV/0.433kV). Indeed, if the voltage received at the primary side of the transformer is 11 kV, the line to neutral voltage at the secondary side is 250 V. Then, the available headroom for any voltage rise that could result from the connection of DG is just 3 V, given the 10% allowance in voltage rise at low voltage distribution networks (1.1% × 230V=253V).

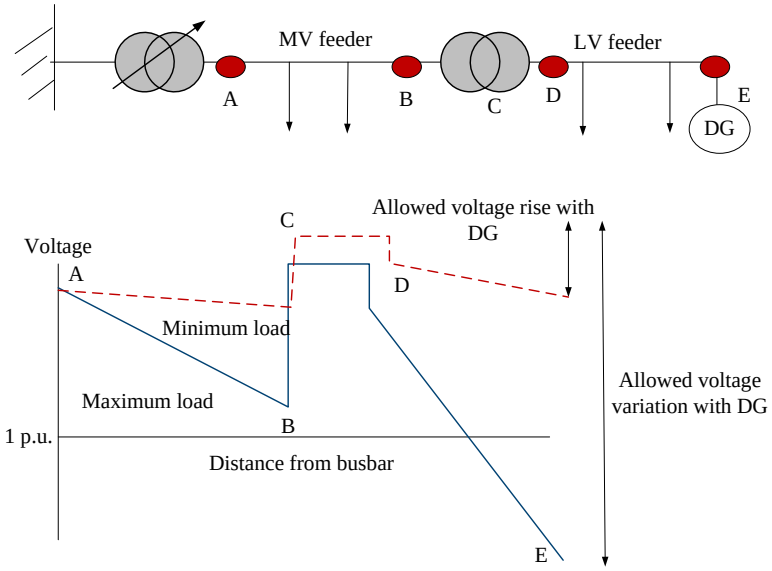

Fig. 2.19 Voltage variation in radial distribution feeder [8]

The existing approach for setting voltage control devices in distribution networks also places restrictions on maximum connected DG capacity. Transformers at primary substations are equipped with on-load tap changers to maintain voltage at the secondary side close to a target voltage above the nominal so that the voltage to all users connected to the networks (particularly at the end of the network) is within the statutory limits during maximum load (i.e., no voltage drop issues). Given the settings of voltage control devices and the relatively high transformation ratio of distribution transformers, the connection of DG may increase voltage significantly above the upper voltage statutory limits during minimum load. This issue is illustrated in Fig. 2.19. It can be seen that, during minimum load, the voltage at the primary substation at point A is above the nominal and the distribution transformer at point C boosts the voltage, resulting in voltage excursion at bus E to which the DG is connected.

2.4.2 Thermal Overloads

Distribution networks may face a reverse current flow upon higher penetrations of DG which may result in overloading the existing network assets above their thermal ratings. Loading cables and transformers above their maximum current capacity may lead to an

increase in the temperature of the insulation above their design limit, which in turn will accelerate ageing or cause damage to the overloaded assets. Also, overloading overhead lines may increase the sag of the line, which in turn may violate the limits determined by the regulation clearance standard.

Given the traditional passive operation of distribution networks, DNOs avoid overloading network assets either by restricting the DG capacity or by upgrading the corresponding assets so that no issues are created for any combination of demand and generation. In this context, the design considers the worst case scenario of maximum generation and minimum demand. The following sections present the thermal ratings that could be adopted in the design of distribution networks [61-62].

Continuous Ratings

Continuous rating relates to the loading that can be applied continuously without affecting the loss of life and safety standard. Loading is applied in terms of the ambient temperature, conductor parameters (cross section and conductor material), weather conditions (e.g., wind speed for overhead lines) and operating voltages. Other particular factors also affect the thermal capacity of cables, including the ground soil resistivity (K.m/Watt) and the presence of other cables (e.g., three single core cables).

Cyclic Ratings

This rating considers the cyclic variations of loading throughout the day between day and night, and throughout the year between summer and winter. Periods of low demand provide a cooling-off period, which allows overloading during peak demand time periods whilst preserving the same level of ageing as would be seen with continuous rating.

Emergency Ratings

During emergency conditions (e.g., replacement of a failed transformer), the magnitude of overloading is allowed to rise above the cyclic rating without causing damage and with acceptable loss of asset life. The allowable emergency loading is inversely proportional to

the duration of the emergency.

2.4.3 Fault Level

The fault level at a particular point in the network is the maximum magnitude of the fault current that could result from a three-phase short circuit at that location. Distribution networks at higher voltage levels (closer to the centralised generation plants) will experience larger fault levels. Also, induction motors can contribute to the fault level. In the existing distribution networks, the magnitude of the fault current depends on the topology of the network where it is higher for meshed networks and it depends on the network characteristics as well as on loads.

Switching components, which are distributed along the distribution feeders, are responsible for clearing the faults. Therefore, the ratings of these switching components are selected to stand the maximum fault current. Fault levels are commonly expressed in MVA based on the nominal voltage level. The typical fault levels used for design in the UK are presented in Table 2.1 [63].

Table 2.1: Typical Fault Levels in UK Distribution Networks [63]

System voltage (kV)	11	33	132
Design fault level (MVA)	250	750	3500
Fault current (KA)	13.1	13.1	15.3

The connection of DG contributes to the fault current, which in turn may necessitate an up-rating of the switching components so as to withstand the maximum peak fault current. Up-rating may be expensive and represents a constraint to the connection of DG. Limiting the fault current by introducing a reactor or transformer between the generator and the network could be a viable solution, but this is at the expense of energy losses [64].

It should be noted that DG connected to the network through power electronic inverters make a smaller contribution to the fault current compared to those using rotating machines such as induction and synchronous generators [8].

In addition, higher levels of DG will affect protection coordination in distribution networks and may require the adoption of more advanced protection relays to cater for the reverse power flow issues [65].

2.4.4 Power Quality

Voltage quality is the main issue in relation to power quality. In this context, power quality is mainly related to the transient voltage variation which includes voltage sag, voltage swell, voltage interruption, voltage flicker, voltage unbalance and harmonics of the network voltage.

DG interfaced with power electronic converters may increase the harmonics voltage distortion. This will place challenges on the DNOs to comply with the limits defined in BS EN 50160 [8].

2.5 Transition towards Smart Distribution Networks

Due to the passive method of operating existing distribution networks, by solving all network issues at the planning stage and implementing limited monitoring and control schemes (in particular at 11 kV, 6.6 kV and LV voltage levels), firm connection agreements are commonly adopted in relation to DG plants. Firm connection agreements allow DG plants to freely operate and generate power up to their installed capacities. However, this passive approach may require a restriction in the size of DG or reinforcement of the existing network assets to cater for the worst case scenario of maximum generation and minimum demand, irrespective of the likelihood of occurrence. In particular, network reinforcements will also be combined with relatively long connection times to undertake the required upgrading; for example, in some cases the connection time may be in excess of two years.

To facilitate efficient and cost-effective connection solutions without costly and time consuming reinforcements to the network, DNOs need to adopt alternative connection approaches that actively manage network constraints in real-time [9-10, 66] so that greater

volumes of renewable DG can be connected. Active Network Management (ANM) is a cyclic process that includes the continuous monitoring of network elements (lines, transformers, buses) so as to solve congestion and voltage rise issues in real-time by actively controlling network elements (e.g., generation curtailment). For example, the ANM scheme adopted in Orkney (the first UK smart grid project) facilitates the connection of 20 MW of DG plants to 33 kV systems, avoiding the capital investment of £30 million required to upgrade a subsea cable [67]. Chapter 3 will provide an extensive review of the ANM schemes proposed in the literature.

However, active network management schemes require an increase in the level of visibility (enhanced monitoring) in distribution networks and the adoption of communication technologies. This in turn increases the operational expenditure required to connect the additional DG capacity. Also, ANM schemes introduce new operational challenges for DNOs in terms of controlling active distribution networks.

OFGEM introduced a new regulatory framework (RIIO, Revenue = Innovation+ Incentives+ Outputs) in 2015 which aims to provide DNOs with stronger incentives than previously on offer, to encourage solutions that defer capital expenditure (i.e., network reinforcements) where technically possible and create an adequate rate of return on the operational cost (not CAPEX biased). Also, this regulatory framework motivates DNOs to adopt solutions that increase the harvested renewable energy [68-70] from DG plants, to provide positive business cases for DG developers [68-70].

Active distribution networks represent a building block towards the so-called *Smart Grid*. The Electricity Networks Strategy Group (ENSG) defines the smart grid as:

"Part of an electricity power system which can intelligently integrate the actions of all users connected to it – generators, consumers and those that do both – in order to efficiently deliver sustainable, economic and secure electricity supplies [71]."

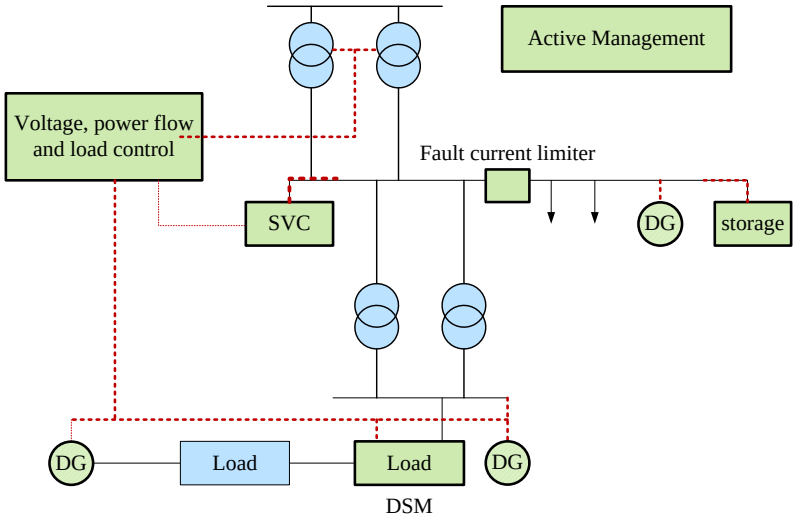

Fig. 2.20 Future Distribution Networks

Fig. 2.20 sets out an example of the potential characteristics, control functions and technologies that may exist in future distribution networks to facilitate the transition towards low carbon energy systems, in addition to the following:

- A higher level of network visibility to facilitate the adoption of future control solutions using monitoring elements and communication networks.

- A transition in relation to distribution control centres, from only dealing with power restoration issues to the inclusion of active network management functions. Crucially, higher speed data acquisition processes than those adopted in the existing control centres are required to closely monitor networks in real-time and solve network issues quickly [72].

- Advanced decision-making algorithms in the role of energy harvesting to coordinate the control actions of future controllable elements (storage, loads, generation and voltage control devices) and consider the uncertainty in inputs (e.g., handle the uncertainties introduced by wind power).

- Active power flow management solutions to maximise the utilisation of the

existing network assets.

- Close to real-time voltage control solutions in distribution networks and at different voltage levels.

- Active fault level management to reduce fault currents by using, for example, Fault Current Limiter (FCL) technology [64] and network reconfiguration.

- Hierarchal coordinated control actions between control centres at different voltage levels to achieve the system wide objectives.

- Reactive power management at the interface between transmission and distribution networks by controlling, for example, the reactive power output of DG plant and Static VAR Compensators (SVC).

- Energy storage facilities will be key network elements in future distribution networks in terms of the active control of thermal and voltage constraints. Also, battery energy can participate in the electricity market and provide ancillary services.

- Demand response that encourages end users to reduce or reschedule their consumption according to the available headroom in the network, and thereby exploiting the roll out of smart meters is a potential solution to facilitating the connection of low-carbon technologies (e.g. electrical vehicles).

2.6 Summary of Chapter 2

This chapter introduces DG, particularly wind power generation, due to the important role it plays in achieving the UK's environmental and energy targets. Then, the main technical impacts of DG on distribution networks are discussed in detail, particularly voltage and thermal constraints and how the passive operation of the existing distribution networks can restrict the volume of DG capacity. The key points in this chapter are as follows:

- Due to the limited observability and control functions in the existing passive distribution networks, DNOs consider the worst case scenario of maximum generation and minimum demand to connect DG so that network constraints are maintained within limits.

- The above passive "*fit and forget*" connection approach places limitations on the volume of DG capacity that the existing distribution network can accommodate.

- To facilitate the connection of DG without the need for costly and time consuming reinforcements to the network, DNOs need to adopt alternative connection approaches that actively manage network constraints in real-time so that greater volumes of renewable DG can be connected.

- The future UK regulatory framework motivates DNOs to adopt smart grid solutions, which in turn will lead to a transition in the operation of future distribution networks.

Chapter 3: Active Network Management (ANM)

3.1 Introduction

The new regulatory framework (RIIO) introduced by ofgem in 2015 motivates DNOs to adopt Active Network Management (ANM) schemes to facilitate the connection of greater volumes of renewable DG without the need for the traditional expensive and time consuming network reinforcements. This chapter introduces active network management and the control solutions adopted in this work to manage voltage and thermal constraints. This includes generation curtailment, voltage control devices (e.g., OLTCs), power factor control of DG plants and energy storage facilities. An extensive review of the ANM schemes proposed in the literature to manage thermal and voltage constraints is provided.

3.2 ANM Control Solutions

Active Network Management (ANM) is considered an economically viable solution to facilitate the connection of the expected large volume of renewable DG to distribution networks by the application of real-time monitoring and control solutions to solve network issues at the operational stage. In the literature, several active network management schemes are proposed to manage technical network constraints that result from the connection of DG. Specifically, this involves ANM schemes that are used to manage voltage and thermal constraints, faults and power quality constraints.

Active control is a cyclic process that involves the continuous monitoring of network elements by taking regular measurements; if the network constraints are outside their limits, a decision-making algorithm (or control logic) is triggered to find new set points for the controllable DG plants and the controllable network elements to keep network

constraints within limits [11].

Different control solutions and technologies are used to manage network constraints including generation curtailment, voltage control devices (OLTCs), power factor control of DG plants, energy storage facilities, dynamic line ratings, dynamic network configuration and demand side response [73].

This work focuses on the use of ANM schemes to manage voltage and thermal constraints through the optimal control of OLTCs, DG power factor, storage devices and generation curtailment. The following presents an overview of the control solutions adopted in this work.

3.2.1 Generation Curtailment

To allow the connection of larger volumes of DG capacity without the need for network reinforcement, the power output of DG plant can be actively controlled by reducing the power injections during periods of constraint issues (voltage rise, congestion) [74]. Although energy curtailment is necessary in this ANM scheme to manage network constraints, DG developers could find such non-firm connection agreements to be economically feasible when compared to the relatively large capital investments that could exist in firm connection agreements (free to operate).

To illustrate generation curtailment, a 33 kV simple feeder (presented in Fig. 3.1) is used. To keep the power flow throughout the line A-B below its thermal capacity of 10 MVA during minimum demand of 1 MW, the maximum DG capacity that could be connected using the *fit and forget* approach to the remote end of the feeder is 11 MW. Therefore, the connection of generation capacity above 11 MW without any form of control would be possible by increasing the capacity of line A-B.

To illustrate the operational aspects of generation curtailment as an ANM solution, it is assumed that a 13 MW controllable DG plant is connected to the remote end of the network (bus B) where its power output is actively controlled to manage the power flows

throughout the line A-B.

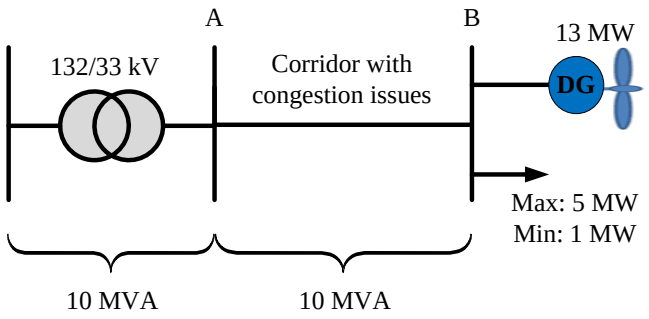

Fig. 3.1 Example of a 33 kV simple feeder with a wind farm

The simple rule-based decision-making algorithm presented in [75] is adopted to control the power output of the wind farm. A control signal (in per unit of the nominal power of the DG plant) is found to determine the maximum allowable power injection from the wind farm. The control signal is varied in a defined step (e.g., +/- 5% of nominal power) in response to the power flow throughout the monitored line. Indeed, if curtailment is required to manage congestion, the control signal is decreased from its value in the last control cycle by a defined step (5% is adopted in this example). Otherwise, the control signal is increased when the power flow is below the thermal limit of the monitored line until the wind farm returns to its normal operation without curtailment (i.e., the control signal is 1 p.u. and the wind farm is allowed to harvest all the available power resource). A time delay of one minute is adopted between the time of decision making and the time of action to cater for the response time of the controllable DG plant, communications, etc. This process is applied at each control cycle of one minute. The demand is held at its minimum level (1 MW) to show the worst case scenario. An arbitrary 1-min wind power profile for one hour is adopted.

Fig. 3.2 shows the loading of line A-B and the control signal issued to the wind farm. At each minute, the control signal is increased or decreased by 5% in response to the power flow throughout line A-B. For example, at minute 0, the controller is activated to solve the overloading issue and a control signal is sent to the wind farm that the maximum allowable

power is 0.95 p.u. (95% × 13= 12.35 MW). The control action is applied at minute 1 and the overloading issue is solved. At minute 7, the power flow falls below the thermal capacity of the line. Thus, the control signal is increased in steps until it reaches 1 p.u. at minute 9 so that the wind farm can harvest all the available power resource (no curtailment from minutes 9 to 16). Then, the wind speed increases resulting in overloading on line A-B at minute 16. Thus, the control signal is decreased in steps until the congestion issue is solved at minute 20 (control signal reaches 0.8 p.u.).

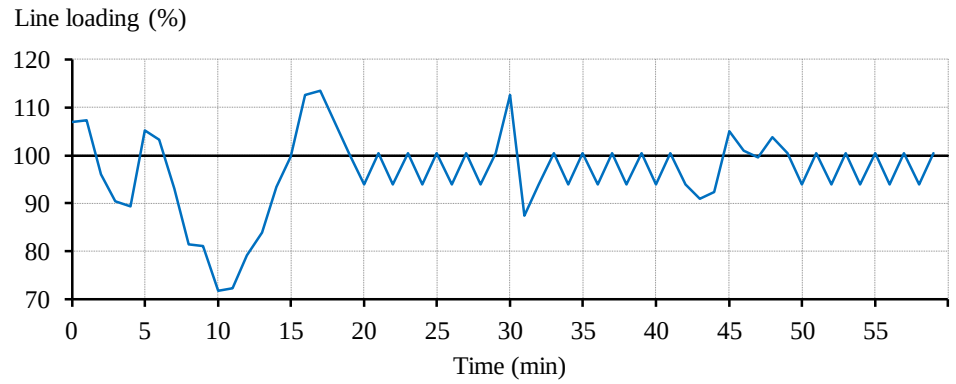

(a)

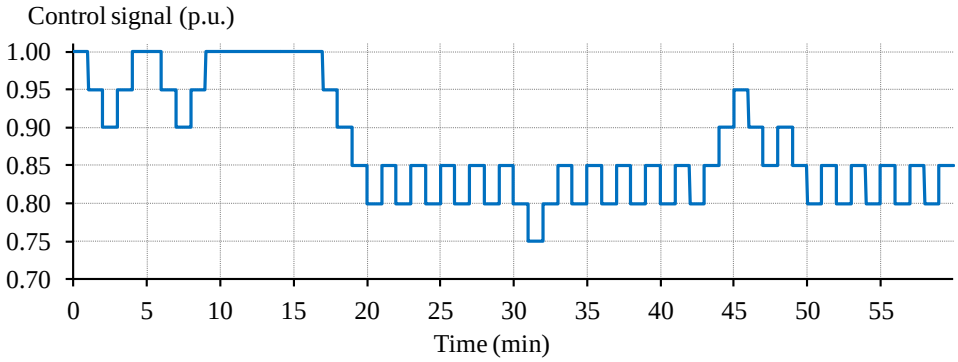

(b)

Fig. 3.2 A 33 kV simple feeder with wind farm and generation curtailment (a) loading of line A-B (%) and (b) control signal in p.u.

This control scheme requires a limited number of measurement points. Indeed, only the power flows throughout the corridor are required to operate this control scheme, with no requirement to collect measurements of demand. However, the complexity of controlling multiple DG plants and multiple network constraints will be increased significantly due to the need for more rules, which in turn introduces operational overheads to update the

settings of the controller. For a scenario of multiple DG plants, an advanced decision-making algorithm is needed but this requires further network visibility (real-time network measurements). Such an ANM scheme is developed in this work and presented in Chapter 4.

It should be highlighted that the adoption of a 1-min control cycle increases the volume of control actions in particular from minute 20 to minute 45. To reduce the volume of control actions (smoother control signal), a larger control cycle than one minute is needed. In addition, an advanced decision-making algorithm is needed to cater for the uncertainty in wind power changes throughout the control cycle, thus effectively managing network constraints within limits. Such a decision-making algorithm is developed in this work and presented in Chapter 5.

3.2.2 On-Load Tap Changers (OLTCs)

Transformers at BSP and primary substations are equipped with on-load tap changers to regulate voltages on MV networks which in turn allows voltages at the end users to be kept within the statutory limits. By controlling the tap position of the OLTCs, the tap ratio of the transformers can be adjusted and, hence, the voltages at the monitored bus can also be maintained within limits. A schematic diagram of the OLTC is provided at Fig. 3.3.

The OLTCs are typically installed at the primary side of the transformer and are controlled using Automatic Voltage Control (AVC) relays in response to the voltage at the secondary bus. Basically, a Voltage Transformer (VT) measures the voltage at the secondary bus and the measured signal is sent to the AVC. If the measured voltage is not within a deadband setting, the AVC sends a raise or lower command to the OLTC. It should be noted that the tap changer is installed at the primary side and so, for example, if the measured voltage is found to be higher than the upper limit (voltage rise), the tap ratio will be increased to reduce the voltage at the secondary of the transformer. The setting of the voltage deadband is determined according to a desired target voltage and a defined deadband (bandwidth) of acceptable voltage variations from the desired voltage. To avoid unnecessary tap changes

due to short periods (e.g., a few seconds) of voltage violation, the tap change is time delayed. Therefore, the OLTC can be used to solve voltage rise issues that result from the connection of DG. Also, the tap operations can be related to the voltages at the DG bus where communication between the AVC and the monitored bus is needed.

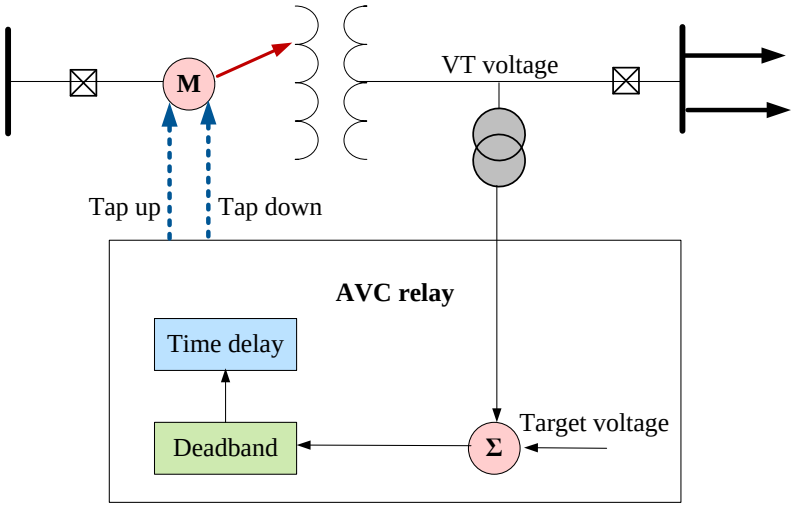

Fig. 3.3 Voltage control using OLTC

To demonstrate the operational aspects of controlling OLTCs to counteract voltage rise issues resulting from the connection of a wind farm, a 5.3 MW wind farm is connected to the end terminal of a 11 kV simple feeder, as shown in Fig. 3.4. The connection of this capacity will increase the voltage at bus B above the upper statutory limit of 1.06 p.u. during the minimum demand period without overloading line A-B. The OLTC at the primary substation is used to solve voltage rise issues at the remote end.

The OLTC is controlled using 16 tap positions to keep voltage at bus B within limits. Its voltage regulation capability is within 0.85 p.u. and 1.05 p.u., meaning that the OLTC can boost voltage by 15% while also reducing the voltage by 5% to solve the voltage rise problem. The voltage regulation capability of one tap change is 0.0125 p.u. ((0.85+0.05)/16). The target voltage at the monitored bus (bus B) is adopted (for demonstration purposes) as 1.03 p.u., considering bandwidth of 2%, and so the range of desired voltages (bus B) is 1.02 p.u. to 1.04 p.u. Also, a time delay of 120 seconds is

adopted from the time step of voltage excursions until a new tap position is triggered.

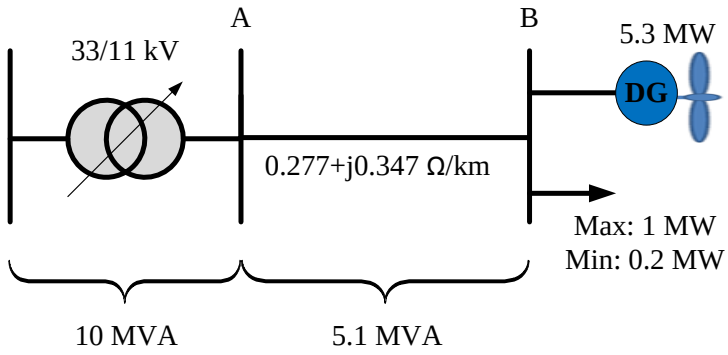

Fig. 3.4 Example of an 11 kV simple feeder with OLTC and a wind farm

Fig. 3.5 shows the voltage profile at bus B and the tap ratio of the OLTC for one hour using 1-min resolution. The demand is held at its minimum level (0.2 MW) to show the operation of the OLTC in the worst case scenario. In contrast, an arbitrary 1-min wind power profile for one hour is adopted. A control cycle of one minute is used (a maximum of one tap change each minute).

It can be seen from Fig. 3.5 that the OLTC can effectively counteract voltage rise issues by increasing the tap ratio in steps of 0.0125 (voltage regulation capability of one tap change). After a time delay of 120 seconds from the voltage excursion at minute 0 (out of the desired voltage range of 1.02 p.u. to 1.04 p.u.), the tap ratio starts increasing until the voltage at bus B falls within the desired range. The tap ratio reaches 1.025 per unit at minute 3 which corresponds to two tap changes. Then, the voltage is maintained within the desired target (no change in tap position) until the occurrence of a voltage excursion at minute 16, resulting in a tap change at minute 18 (time delay of 120 seconds). Although this simple scheme can effectively manage voltages for single DG and one voltage constraint, the complexity of setting the controller is increased with multiple DG plants and the need to coordinate its operation with other control schemes (for example, generation curtailment).

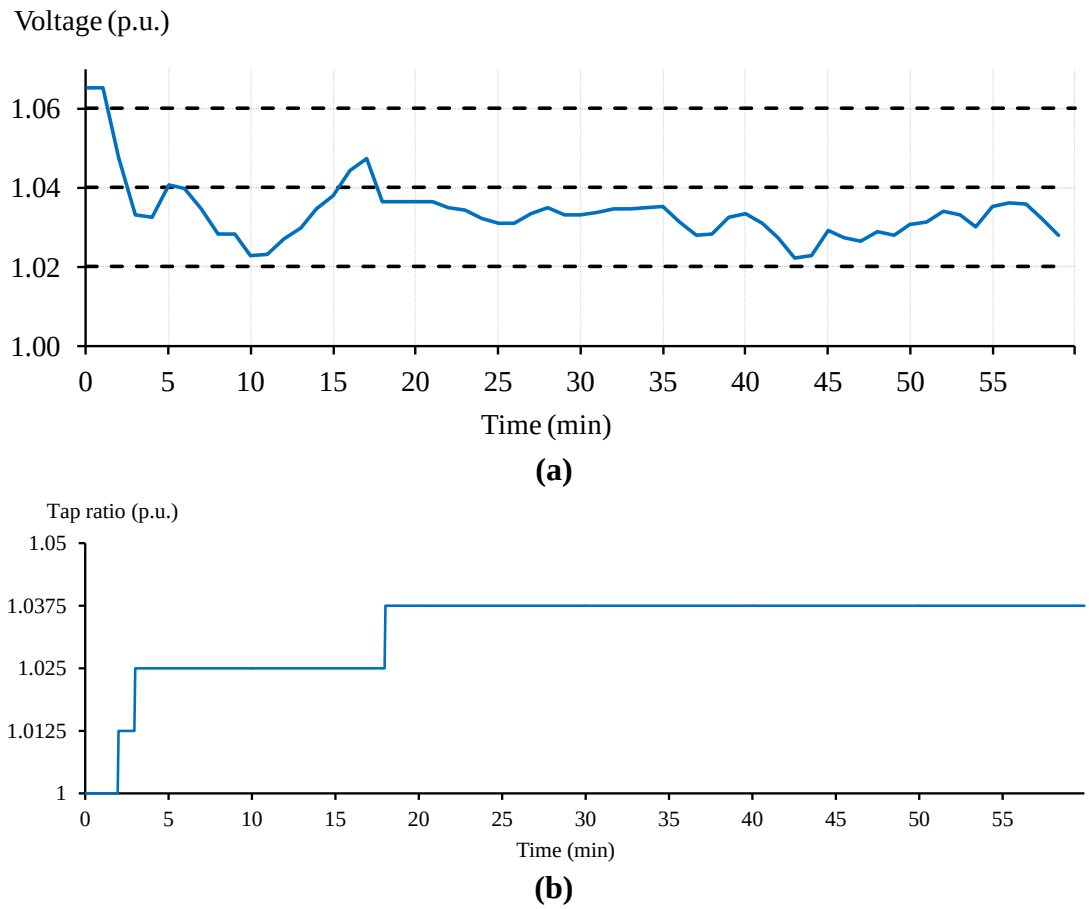

Fig. 3.5 An 11 kV simple feeder with wind farm and controlling of the OLTC (a) voltage at bus B in p.u. and (b) tap ratio

3.2.3 DG Reactive Power Capability

Wind farms can provide dynamic reactive power to keep network voltages within statutory limits. The reactive power capability depends on the type of the turbine [76-77]. For fixed speed squirrel-cage induction generators that typically operate at an inductive power factor (absorbing reactive power), shunt capacitor banks can be combined with the induction generator and controlled to improve the power factor. However, the reactive power capability from fixed speed wind power turbines is limited.

In contrast, extended reactive power capability can be obtained from DFIG and full converter wind power turbines (type three and type four) since they are interfaced with the grid using power electronic converters. The reactive power capability depends on the P-Q

chart of the wind turbine. Fig. 3.6 shows an example of a P-Q chart for a 3 MW DFIG wind power turbine obtained from [47]. Indeed, due to the size of the converter, it can be seen that there are limitations on the maximum reactive power that can be injected or absorbed from the wind turbine (e.g., 1500 kVAr in Fig. 3.6). In particular, the converter size has to be adequately determined to allow reactive power injection/consumption at full active power output. Also, it can be seen that there is no reactive power capability at zero active power output or at relatively small active power output.

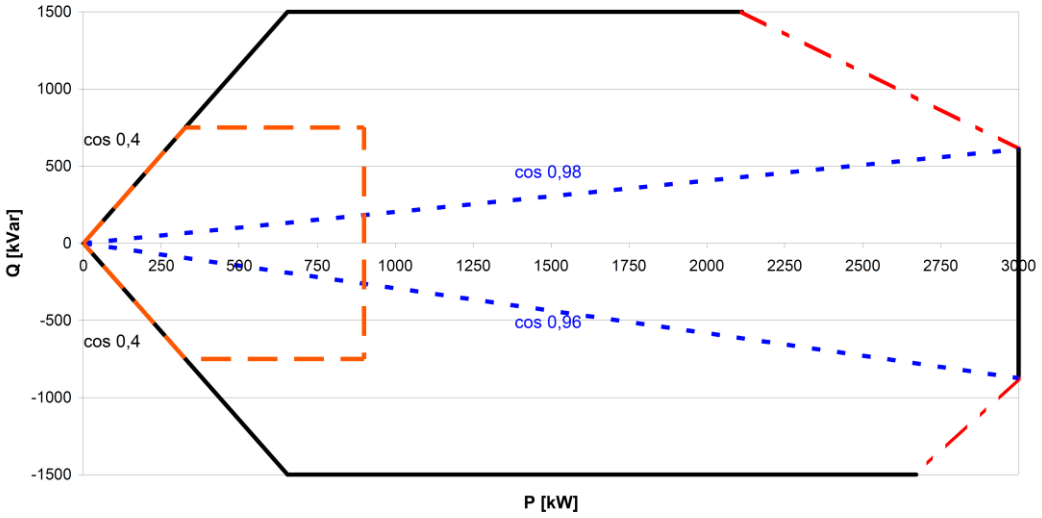

Fig. 3.6 Example of a reactive power capability chart of a 3 MW wind power turbine [47]

The reactive power output of the wind turbine can be controlled using the following three control modes [77]:

- **Power factor control mode**: The reactive power is controlled to produce a desired power factor at the DG terminal bus. Also, it can be seen that the ability to absorb reactive power (inductive power factor) is higher than from injecting (capacitive power factor). Fig. 3.6 shows 0.98 inductive and 0.96 capacitive power factor (blue lines).

- **Reactive power control mode**: The wind turbine is controlled to achieve a

desired reactive power output at the DG terminal bus. However, there is a limitation on the maximum level of reactive power that can be contributed and there is no reactive power capability at zero or at relatively small active power.

- **Voltage control mode**: The reactive power output is controlled to maintain the voltage at the DG terminal bus within desired limits. For example, once the voltage exceeds the limits, reactive power will be absorbed (inductive power factor) proportionally to the magnitude of voltage excursion.

In this work, a power factor control mode is adopted and the desired power factor is obtained from a centralised decision-making algorithm that considers other controllable elements. A larger size of converter is selected than the rating of the generator to allow for the injecting/absorbing of reactive power at full active power at a power factor of +/-0.95. More details can be found in Chapter 4.

It is important to highlight that the benefits of using the inductive power factor to solve voltage rise issues resulting from the connection of a wind farm depend on the X/R ratio of the line. This ratio depends on the type of the line (cable or overhead) and the voltage level. Indeed, the resistance depends on the cross section of the lines, while the reactance is higher for overhead lines with typical values of 0.4 Ω/km compared to 0.1 Ω/km for cables at 33 kV [60]. Therefore, use of the inductive power factor is more efficient in overhead lines than cables for the same cross section. However, the use of reactive power may lead to increased energy losses; in addition it may create congestion in lines as the reactive power will be imported from the source bus.

3.2.4 Integration of Storage Facilities

To increase further the harvesting of low-carbon electricity or, in other words, to minimise the volume of curtailment required to manage network constraints, a key technology that could be integrated into the ANM approach is energy storage. Indeed, network issues could be actively managed in real-time by storing the excess generation and releasing it later when constraints are not binding. If the storage system reaches its maximum energy, or the

power required to solve congestion (or voltage rise) is larger than the power rating of storage, the controller has to apply curtailment to the wind farm [15]. Storage facilities could also be controlled to absorb or inject reactive power within the rating of the power conversion system, allowing further flexibility in managing voltages [78].

Energy storage technologies can be classified according to the store medium. This includes battery energy storage, kinetic energy storage systems (i.e., flywheel energy storage), super conducting magnetic energy storage, super capacitors and potential energy storage in the form of either pumped hydro or compressed air energy storage. The last two technologies are mainly used in large scale in the range between 50 MW and 400 MW and they can only be adopted in specific environmental conditions (water reservoirs), which in turn limits their application in distribution networks [79-81].

The technology of storage facilities should have a response time adequate for use in the context of ANM and to be controlled in close to real-time. Battery energy storage, flywheel storage, super conducting magnetic storage and super capacitors have such characteristics. However, apart from battery energy storage, all of these storage facilities offer smaller energy storage capacities, making them unsuitable for charging excess generation (i.e., curtailment reduction) at their power ratings for in excess of one hour. Therefore, battery energy storage is currently the most suitable technology for the ANM application.

The following summarises the main technical parameters of battery energy storage facilities [79-81].

- **Apparent power rating**: The maximum apparent power output (active and reactive power) of the storage facility, expressed in kVA or MVA.
- **Energy capacity**: The maximum energy that can be stored, expressed in kWh or MWh.
- **State of charge**: The stored energy at a particular time, expressed as a percentage of the energy capacity.

- **Round-trip efficiency**: The energy losses during a full cycle of charging and discharging.

- **Self-discharge**: The losses during the idling state. Batteries tend to discharge energy even when the facility is not in operation.

- **Storage discharge duration**: The time (hour) required to fully discharge the stored energy at the rating power of the storage facility.

- **Energy and power density**: Described in terms of kW/kg and kWh/kg. The importance of these parameters is in the selection of adequate battery technology when space and weight are issues for the installation.

- **Life cycle**: Expressed in terms of the number of full charge and discharge cycles [82] before replacement of the battery. Also, the life cycle depends on the battery temperature.

- **Maximum Depth of Discharge (DOD)**: To preserve the life cycle of the battery, the stored energy is not allowed to fall below a particular percentage of the energy capacity [80]. This is known as the maximum Depth of Discharge. For example, a 80% maximum DoD means that the minimum allowable store level of the battery should be higher than 20% of the energy capacity.

Various commercially available technologies of battery energy storage are available, such as Lead-acid, Sodium/sulfur, Zinc/bromine, Vanadium Redox and Lithium-ion. In this work, a lithium-ion battery is adopted due to such characteristics as its relatively high life cycle and high round-trip efficiency compared to other technologies.

The cost of storage facilities is expressed in terms of the unit cost of the converter's apparent rating and the unit cost of energy capacity (£/MVA and £/MWh) [80]. This represents the largest barrier for the adoption of storage in future distribution networks. In this context, an adequate control solution is needed to maximise the utilisation of storage

[83]. In this work, storage facilities are used to provide multiple services as follows: active power flow control, voltage control and curtailment minimisation. It is important to note that the cost of battery energy storage is expected to decrease in the future (in particular the lithium-ion battery) since this technology will be adopted in many different applications, in particular in electrical vehicles.

A significant challenge in the adoption of storage facilities, similar to other assets, relates to adequate sizing. Given the ANM context in which these facilities will be used, sizing approaches need to integrate (close to) real-time operational aspects to capture the actual storage needs (i.e., power and energy) of distribution networks. A storage sizing framework is developed in this work and presented in Chapter 6.

3.3 Active Network Management Activities

In the literature, several active network management schemes are proposed to manage technical network constraints that result from the connection of DG. Specifically, this involves using ANM schemes to manage voltage and thermal constraints, faults and power quality constraints. This work will consider the active management of thermal and voltage constraints that drive network investments in distribution networks. This section presents a literature review about the functions of ANM schemes using the above control solutions to manage thermal and voltage constraints.

3.3.1 Active Management of Thermal Constraints

In the literature, several ANM schemes are proposed to control the active power output of a single DG plant in response to power flow measurements through a single line [10], [75, 84]. The ANM scheme adopted in those studies is presented in Fig. 3.7.

A simple ANM scheme is presented in [10] whereby the DG plant is disconnected when the power flow exceeds the seasonal thermal rating of the monitored line. To provide more flexible solutions and increase the harvested energy, rather than switching off the DG plant, generation curtailment is used in [10] and [75, 84]. Indeed, a control signal is issued

to the DG plant as illustrated in Section 3.2.1. Should the DG plant fail to achieve the desired power output within a defined response time, and the power flow continues to violate the limit, the DG plant will be disconnected.

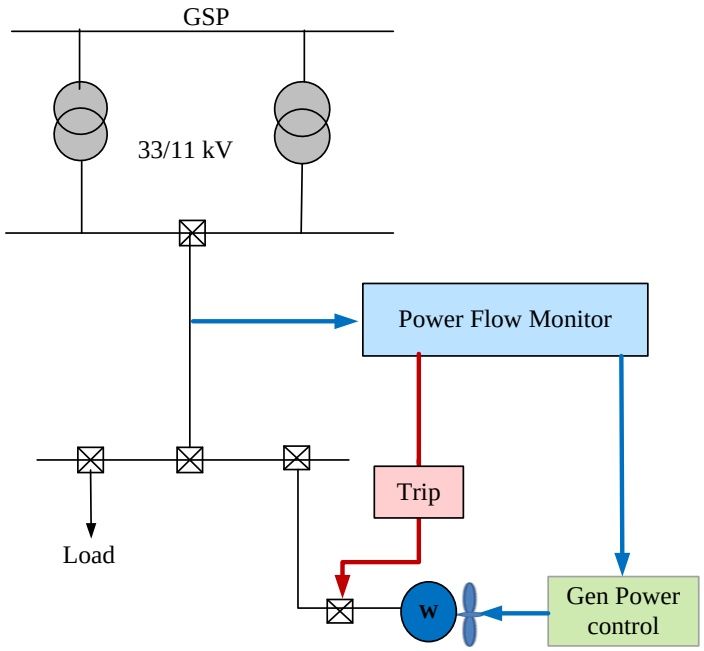

Fig. 3.7 DG power control based on real-time power flow measurements [10]

An advanced rule-based ANM scheme is proposed in [11, 85] to control multiple DG plants and manage multiple thermal constraints. A rule-based decision-making algorithm is proposed to identify the required curtailment from each controllable DG plant to solve congestion issues, based on the Last In First Out (LIFO) principle of network access. The most recently connected generator will be the first to be curtailed; thereafter, generators will be called upon for curtailment in succession according to their order of connection until the congestion is solved. Although this rule-based approach is applied in practice, the complexity introduced by the incorporation of future network elements will place operational overheads on DNOs in terms of updating the rules and the corresponding operating margins.

A Constraint Satisfaction Problem (CSP) method is applied in [18, 86-87] to find the best set points with which to solve congestion at multiple DG plants. A finite number of set

points is defined for each controllable DG plant (e.g., 0%, 20%, 40%, 60%, 80% and 100% of nominal power) and power flows throughout the lines in the network are found for all possible combinations of the DG set points. The best set points are those that minimise the overall volume of curtailment whilst satisfying thermal constraints. Although this approach can be extended to solve other constraints in addition to thermal issues, the corresponding computational burden will increase dramatically with the number of controllable DG plants and other network controllable elements. In addition, the selection of set points from discrete levels may lead to the neglect of better solutions that would be available if the entire continuous range were to be effectively explored.

A DC Optimal Power Flow (OPF) approach is adopted in [20, 88] as the decision-making algorithm to solve only thermal issues. The OPF allows an exploration of the continuous range of controllable DG set points, which in turn enhances the opportunity to find a better solution for minimising curtailment from multiple DG than the CSP approach.

3.3.2 Active Management of Voltage Constraints

The connection of DG may increase voltages above the upper statutory limits, which in turn will limit the maximum capacity of DG connected to the network or will require upgrading of the existing network assets. The application of ANM schemes can maintain voltages within limits by controlling the real and reactive power output of DG plants and the tap position of OLTCs which allows the connection of larger volumes of DG [89]. The following summarises the proposed ANM solutions in the literature to control voltages in medium voltage distribution networks.

In [10], the real power output of a single DG is controlled according to the local voltage measurements at the bus to which the DG is connected. When the voltage at the DG terminal bus rises above the upper statutory limits, the DG is subjected to curtailment or disconnection according to a set of rules.

Controlling the power factor of DG also allows the management of voltages. Indeed, by operating the DG at an inductive power factor to absorb reactive power, voltage rise issues

can be solved. A rule-based ANM scheme, termed an Automatic Voltage and Power Factor Controller (AVPFC), is proposed in [90] to solve voltage rise issues in a rural 11 kV distribution network resulting from the connection of DG. In this ANM scheme, when the terminal voltage is within the statutory limits, the power factor of DG is held constant (fixed power factor control mode). When the voltage rises beyond the upper statutory limit, the DG goes into voltage control mode where its reactive power is adjusted to keep the terminal voltage within limits. During the voltage control mode, the power factor is restricted within the reactive power capability of the DG. A similar control approach is adopted in [91] and the controller is validated using time-series data analysis. Although such approaches can increase the capacity of DG without extensive communication, the complexity in the setting of the controller is increased when coordination with the operation of OLTCs and other DG controllers in the networks is required [92].

The studies in [93-95] present a rule-based voltage control method which actively manages the OLTC transformer in primary substations (33/11 kV). The adopted controller, known as SuperTAPP, has been proven in practice within real UK 11 kV distribution networks. A schematic diagram is shown in Fig. 3.8. To solve voltage rise issues that could arise from the connection of DG, the target voltage of the Automatic Voltage Control Relay (AVC) (used to control OLTC) is adjusted by estimating the voltage at the DG bus using both the voltage measured at the 11 kV busbar and the current at the head of the feeder to which the DG is connected.

One of the advantages of this method is that it does not require the taking of remote measurements since the voltage at the DG terminal bus is estimated using local measurements. However, the estimation of voltages may become more challenging as more DG plants are connected along the 11 kV feeders. In addition, it is important to ensure that lowering the voltage at the 11 kV busbar to reduce voltage rise issues at one particular feeder would not lead to voltage drop issues at the other feeders connected to same 11 kV busbar.

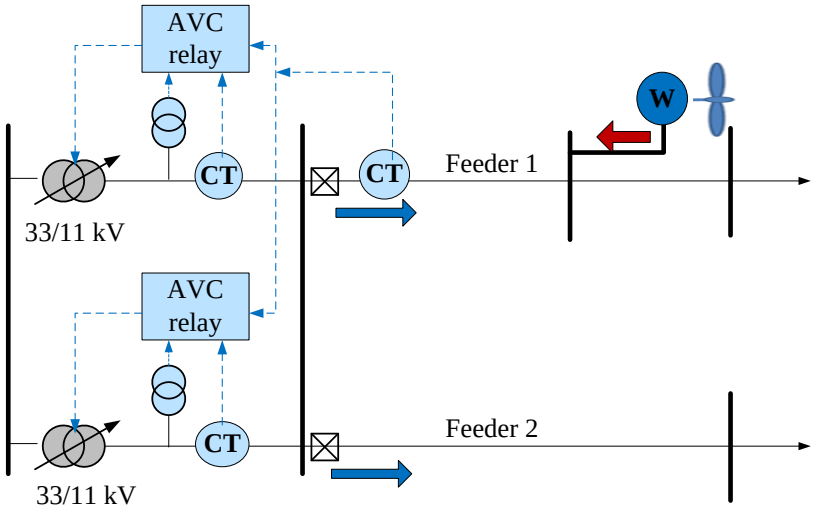

Fig. 3.8 SuperTAPP control scheme [93]

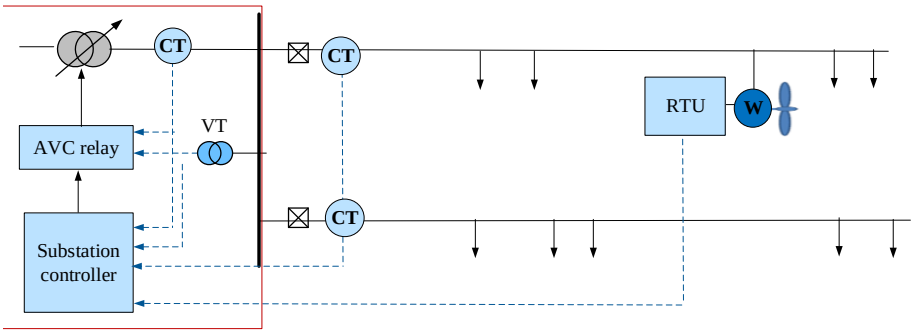

Fig. 3.9 GenAVC system [98]

To ensure that voltages are kept within limits for all the feeders connected to the 11 kV busbar, the studies in [96-99] propose more advanced voltage control schemes. A schematic diagram is presented in Fig. 3.9. The setting of the target voltage of the AVC depends on both the local measurements at primary substations and remote voltage measurements at the DG terminal bus, as well as measurements from other buses in the network. One of these methods, known as *GenAVC*, is commercially available to control voltages in UK distribution networks [98]. However, such a simple rule-based decision-making algorithm becomes more challenging at high DG penetration and when it is required to coordinate the operation of different controllable elements.

All the above ANM schemes are limited to the control of DG plant. The following studies propose ANM schemes to control multiple DG plants. In this context, generation curtailment is used in the ANM scheme in [100] to manage voltages in distribution networks considering multiple DG plants. The approach is demonstrated for a number of scenarios of demand and generation, but time-series analysis is not carried out. To determine the curtailment from each DG plant, sensitivity factors need to be computed to calculate the contribution from each DG to the voltage constraint. However, this requires frequent computation of the sensitivity matrix so as to follow the changes in network topology, generation and demand.

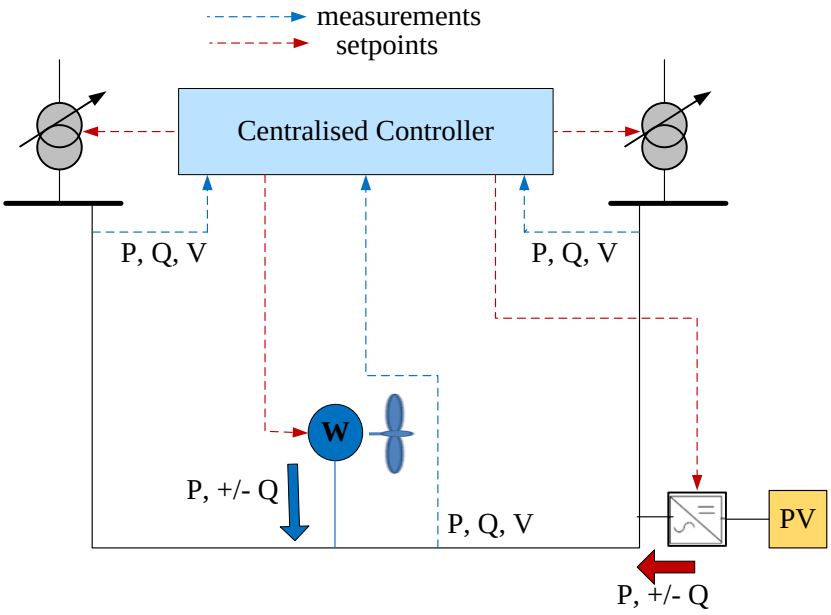

Fig. 3.10 Architecture of DMS controller [101]

A Case Based Reasoning (CBR) decision-making approach is proposed in [19, 102] to provide coordinated voltage control between OLTC transformers, considering multiple DG plants. CBR is an artificial intelligence technique that solves a problem by retrieving similar cases generated by simulations from historical data. The stored cases consider different network configurations. However, the approach does not consider generation curtailment to solve voltage rise issues. Also, the approach has not been demonstrated using real-time series data. A simplified linear programming optimal power flow approach

is presented in [101] (as shown in Fig. 3.10) to manage voltages only through the optimal control of OLTCs, DG power factor control and generation curtailment as a last resort.

3.3.3 Simultaneous Management of Thermal and Voltage Constraints

The above ANM approaches consider the active management of either voltage or thermal constraints. As more DG is connected, the need for ANM solutions that solve voltage and thermal constraints simultaneously is required; however, few studies in the literature consider this. An integrated approach is considered in [21-22]. However, the optimisation problem is formulated in a simplified manner using linear programming and voltage sensitivity coefficients. A decentralised control approach that considers realistic modelling of the control aspects using 1-min control cycles is presented in [14]. Although this scheme considers the integration of OLTCs, and control of the power factor of DG plants, thermal and voltage management are limited for a single line and a single bus.

None of the above studies offer a comprehensive control approach that provides coordinated control actions between controllable DG plants and other controllable network elements to minimise generation curtailment. One of the potential solutions is the use of AC OPF.

Multi-period AC OPF has been adopted in [12, 37] using hourly time-series data that are not adequate to model control aspects. A time-series AC OPF approach is presented in [103] to determine the volume of curtailment required from DG plants, using hourly generation and load.

An AC OPF-based receding horizon ANM scheme that considers realistic modelling of the control aspects is presented in [104]. This ANM scheme also considers minimising the volume of control actions from DG plants and controllable elements. However, the proposed approach requires perfect wind power forecasting for relatively long horizons (e.g., 30-min).

3.3.4 Control of Storage Facilities

The relatively high investment costs of energy storage facilities compared to other ANM control solutions necessitates more advanced control solutions. Storage control schemes are presented in the literature in the context of curtailment minimisation. Rule-based decision-making algorithms are proposed in [27, 105-106]. However, these schemes are limited to a single storage system to solve either congestion or voltage rise issues. An AC OPF is proposed in [30, 107] to coordinate the operation of multiple storage facilities, using predefined periods of daily charging and discharging operations. A more flexible OPF operation is proposed in [28, 108] [32] to determine the optimal scheduling of storage active and reactive power across a day. However, the proposed approaches assume perfect daily wind power forecasting for long periods (i.e., no errors) which is not adequate for such a relatively long horizon. A close to real-time control algorithm is proposed in [29] to capture wind power variations without the need for forecasting. However, the formulation is not general where all storage facilities should have the same operation state (e.g., charging). In addition, the reactive capability of storage is not explicitly formulated.

None of the above OPF-based studies consider the use of storage with high granularity modelling of control. Also, none of them offer coordination between the control actions of storage facilities and OLTCs and DG power factor control as well as storage reactive power capabilities; it is important to use other controllable elements to solve network issues rather than charging storage which in turn allows the adoption of smaller sized storage facilities.

3.4 Summary of Chapter 3

This chapter introduces the ANM control solutions used in this work to manage thermal and voltage constraints, including generation curtailment, voltage control devices (OLTCs), power factor control of DG plants and energy storage facilities. An extensive review of the ANM schemes proposed in the literature to manage thermal and voltage constraints is provided. The following summarises the key points in this chapter.

- Active Network Management facilitates the connection of the expected large volume of renewable DG in distribution networks by the application of real-time monitoring and control solutions to solve network issues at the operational stage. This work will focus on the active management of voltage and thermal constraints.

- Generation curtailment can effectively manage voltage rise and congestion issues in close to real-time. However, at high penetrations of DG, some DG plants could be subjected to significant levels of curtailment.

- The future deployment of a significant number of ANM control schemes will require a comprehensive intelligent coordination approach in order to exploit the potential benefits of control solutions in the reduction of energy curtailment. This requires the implementation of a Network Management System (NMS) that aims to simultaneously manage network voltages and congestion (thermal overloads) through the optimally coordinated control of OLTCs, DG reactive power output, storage facilities, and generation curtailment as a last resort. Such an NMS has not been adequately presented in the literature. Also, to adequately assess the benefits of the NMS, realistic modelling of the control aspects is required.

- The expected high investment costs of energy storage facilities compared to other ANM control solutions necessitates more advanced control solutions to effectively utilise the installed capacities in reducing curtailment and offer coordination between the control actions of storage facilities and OLTCs and DG power factor control as well as storage reactive power capabilities.

Chapter 4: Network Management Systems – A Deterministic Approach

4.1 Introduction

It was highlighted in the previous chapter that a comprehensive network management system is required to manage simultaneously voltage and thermal constraints and reduce the volume of generation curtailment from multiple DG plants by controlling other controllable network elements. In this context, this chapter presents a comprehensive distribution NMS aimed at minimising DG curtailment whilst managing network constraints (i.e., voltage rise and thermal overloads) in close to real-time, adopting 1-min resolution data for both demand and generation. A centralised AC OPF is adopted in [12] to produce the optimal set points for OLTCs, DG reactive power output and generation curtailment as a last resort. The AC OPF in [12] is tailored to comply with the existing connection agreements which might allow some DG plants to deliver power up to their rated capacity (i.e., firm connection agreement).

First, this chapter presents the architecture of the proposed deterministic NMS and the formulation of the optimisation engine. Then, the proposed NMS is applied to a UK 33 kV network in the north-west of England, incorporating multiple wind farms and considering controllable and uncontrollable DG. A control cycle of one minute is adopted. To assess the performance of the proposed NMS using different control schemes, performance metrics are proposed (voltage compliance with the EN50160 standard, congestion and volume of curtailment from wind farms).

4.2 Network Management Systems: Overview

A distribution NMS is proposed aimed at minimising generation curtailment from controllable DG plants whilst managing network constraints (i.e., voltage rise and thermal overloads) in close to real-time. The proposed NMS platform is shown in Fig. 4.1. Measurements are collected from monitored elements to determine the new set points of the controllable elements for each control cycle. When the power flows throughout the monitored lines and transformers exceed their thermal capacities, or when the voltages at the monitored buses exceed the statutory limits, the decision-making algorithm is triggered to find new set points for the controllable elements. To increase the energy harvested from controllable DG plants (minimise curtailment), the decision-making algorithm is also triggered when the DG plants are subject to curtailment while power flows and voltages are within limits. Here, the time interval between two consecutive checks of constraints and the existence of curtailment is defined as the "*control cycle*".

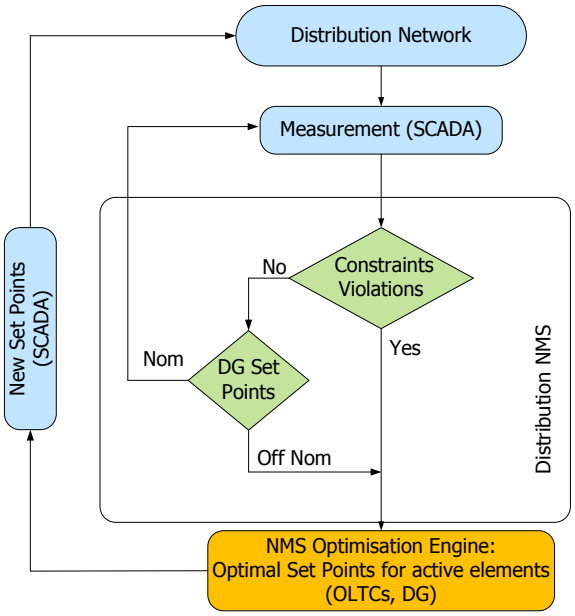

Fig. 4.1 Flow diagram of the proposed Distribution NMS

The AC OPF presented in [12, 36-37] from a planning perspective in the context of maximising the capacity of DG connected to distribution networks is adopted as the

decision-making algorithm to actively manage congestion and voltage rise issues and provide coordinated control actions between the controllable elements in the network. It is adapted and modified to be applicable for realistic operational purposes. Also, it is tailored to comply with the existing firm connection agreements that allow DG plants to deliver power up to their rated capacity.

From an operational perspective, Fig. 4.2 shows details of the adopted parameters for the control cycle. At the start of each control cycle, T_c, the NMS observes the measurements in the network. When constraints are violated (e.g., minute 1), a decision is made to produce the best set points for the operation of voltage control devices (i.e., OLTCs at substations) and the reactive power output of DG plants in such a way that curtailment is considered as the last resort. Because of the short time horizon needed by the NMS (control cycles from 1 to 15 minutes), it is assumed that the availability of the wind resource and demand remains constant throughout the control cycle, i.e., same value as previous one, which also known as persistence forecasting,. Indeed, persistence model is considered as the most adequate short term wind power prediction for short time horizon [125].

The set points found by the OPF are then applied (action) after a delay of T_σ (e,g., at the end of minute 2). The time response for the controllable elements and communication delays limit the practical length of the control cycle. Based on this, the shortest control cycle considered in this work is 1 minute.

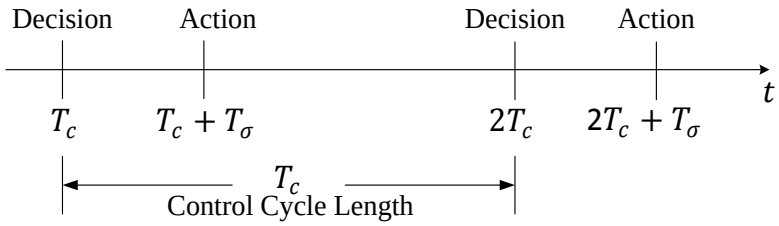

Fig. 4.2 Control cycle of the proposed network management system

The deterministic decision-making process considers only the actual network state (observed) at T_c meaning that the set points are implemented to solve network issues seen

at the start of the control cycle. The decision making process does not consider potential changes in the network state throughout the control cycles due to the variability of wind. However, the network response throughout the control cycle is modelled. In Chapter 5, the advanced NMS approach will be presented to cater for the wind power changes throughout the control cycle.

4.3 Network Management Systems: Components

4.3.1 Supervisory Control and Data Acquisition Systems (SCADA)

Supervisory Control and Data Acquisition Systems (SCADA) involve data acquisition, communication and control systems. SCADA systems collect real-time measurements of voltages, currents and power from monitoring devices on a regular basis and send them to the control room using communication networks. The existing SCADA systems in distribution networks are mainly adopted for power restoration purposes to reconfigure the operation of distribution networks following faults, so that the duration of interruptions and the number of affected network users can be reduced. The introduction of new functions in the role of active network management and in the role of energy harvesting (as presented in this work) will require more advanced decision-making algorithms than those already in existence. Crucially, a faster data acquisition process is also required to follow the changes in the network and solve the potential network issues quickly [72].

Different communication channels, including pilot cables, microwave, mobile networks and fiber optics, could be used between the control room and the monitoring devices and the controllable elements. In the existing SCADA systems adopted in distribution networks, selection of the communication channels and the design of communication networks is a trade-off between costs (capital and operational) and reliability (speed and communication failures). Reliable and high speed communication channels (e.g., fiber optics) are usually used at 132 kV and 33 kV. To avoid the risk of communication failure and to further improve upon the reliability of the communication networks at these voltage levels, point to point communication links and multiple communication routes are

commonly used to connect BSP and primary substations with the control room. In contrast, lower speed communication channels can be used to connect monitoring devices at voltage levels of 11 kV and 6.6 kV and the control room. Other design approaches can be adopted by the usage of data concentrators at 132/33 kV substations to collect data from a group of downstream monitoring devices instead of direct point to point communication links [72].

In practice, given the need for accurate information and high level observability to actively control active network elements, the SCADA system should interface with a more intelligent way of monitoring data and extending network observability (i.e., a state estimator using fewer numbers of monitoring devices [109]). However, this is outside the scope of this work and it is assumed that the measurements are perfectly received (i.e., without errors) and correctly time stamped, and that the network is fully observed. The next section will provide an overview of distribution state estimation as a mandatory element in the proposed NMS.

4.3.2 Distribution State Estimation (DSE)

Real-time control requires determining the state of the network. A distribution state estimator can provide the best values of network state variables based on the available real-time measurements and pseudo measurements so that power flows and voltages in the network can be estimated. A state estimator can be described as an optimisation problem that aims to minimise the residual values between the real-time measurements and the corresponding estimated values determined by measurement functions. By solving the optimisation problem, the best coefficients of the measurement functions can be found and, thus, so can the network state variables. The measurements are weighted in the objective function of the estimator according to the accuracy of the meters, so that measurements coming from more accurate meters will have higher weight compared to those coming from less accurate meters [110].

Weighted Least Square (WLS) is a traditional method used to model the state estimation

problem. It is expressed mathematically as follows:

$$min \sum_{i=1}^{N_m} \frac{\left[z_i^{meas} - h_i(x_1, x_2, .., x_{N_s})\right]^2}{\sigma_i} \tag{4.1}$$

where z_i^{meas} is the value of measurement *i*, $h_i\ (x)$ is the measurement function that models the measurement *i* in terms of the state variables *X* and σ_i is the variance in the error of the measurement i. Its reciprocal represents the weighting coefficient for each measurement. N_s is the number of state variables. The state variables are usually the magnitude of voltages at all network buses and the corresponding angles. N_m is the number of real-time measurements, which may include the active and reactive power flow throughout the lines, bus injections of real and active power (generation and demand), line current magnitudes and the voltage magnitude of buses.

To solve the problem, the number of real-time measurements needs to be at least equal to the number of network states so that the network can be considered observable. If the network state cannot be determined, the system cannot be controllable. However, due to the limited number of real-time measurements available in distribution networks, state estimation is considered to be an under-determined "unobservable". This requires a large number of pseudo measurements to be obtained from historical data or short-term prediction, so as to provide measurements for the unknown parameters and estimate the network state. More specifically, pseudo measurements can be derived in distribution networks using typical load profiles to specify the unmeasured loads at network buses. Other sources of pseudo measurements could also be utilised, using load allocation approaches [111]. Also, smart meters could potentially become an important future solution in solving the issue of observability in distribution networks and providing another source of pseudo measurements [112-113].

However, since pseudo measurements are typically based on historical data, there is a greater potential for errors compared to monitoring devices. Therefore, the state estimation

should be robust to errors and bad data. Indeed, bad data could be detected by applying a threshold to the difference between the measured values and those calculated using the measurement function. If the difference is above this threshold, the measurement is neglected and will not be considered in the estimation. Another approach could be to dynamically tune the weighting coefficients to filter out bad data [114].

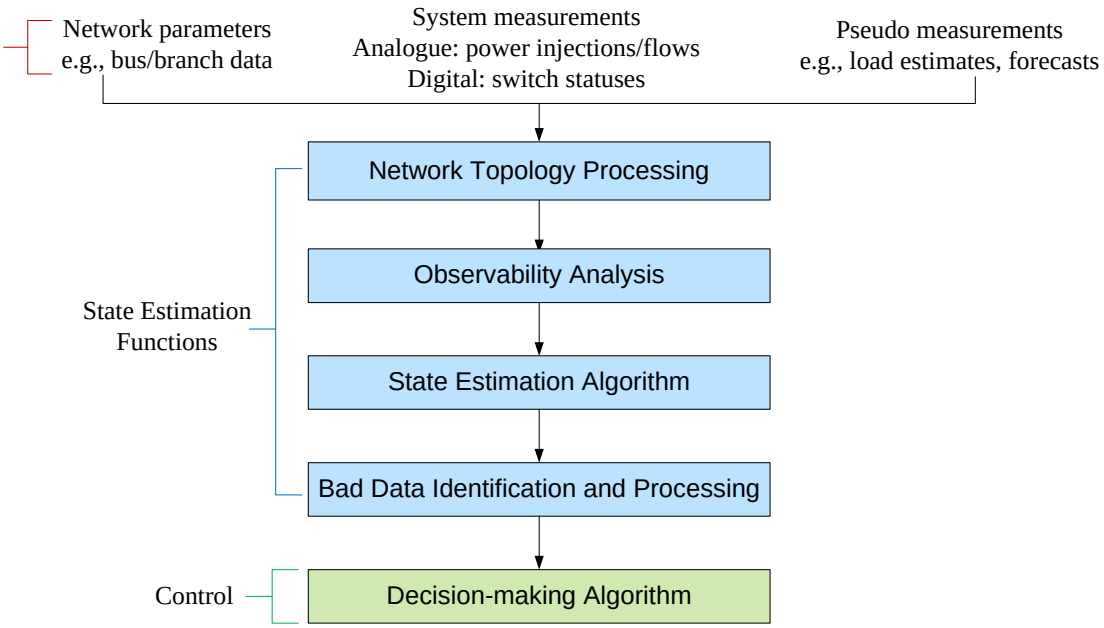

Fig. 4.3 Block diagram of distribution state estimation [115-116]

Fig. 4.3 presents a block diagram of a distribution state estimator and its functions. The parameters of the network have to be defined including the topology, line impedances, etc. As indicated previously, available real-time measurements are collected (e.g., loads, power injections of generators, switch status) and input to the state estimator in addition to the pseudo measurements. The state estimator mainly has three functions. The first function is network observability, to ensure that the number of real-time and pseudo measurements are at least equal to the number of network states (without considering the redundant measurements). If it is found that the system is not observable, then more pseudo measurements will be needed (although this would affect the accuracy of the results). Secondly, a state estimation algorithm (second function) is applied to find the network states. The third function is the identification of bad data and gross error. Finally, the

obtained network states are then passed to the decision-making algorithm in order to find the best set points.

It should be noted that the relatively large volume of distribution networks (number of nodes) and the unbalanced nature of distribution networks (in particular at low voltage) places more challenges on the implementation of DSE in addition to the lack of real-time measurements. The design of the DSE is outside the scope of this research and it is assumed that the measurements are perfectly received (i.e., without errors) and that the network is fully observed (i.e., measurement devices are installed throughout the test network).

4.3.3 Remote Terminal Units (RTUs)

RTUs act as the interface between the controllable elements and the control centre by deploying the set points found by the decision-making algorithm and sending real-time measurements to the control centre. Also, control logics (rule-based) can be programmed in advanced RTUs to provide control functions. RTUs can notify the control room if there is any significant change in the measurements, for example when the loading of a monitored line increases above a defined threshold. This feature of RTUs is important to reduce the traffic of information required to monitor networks and therefore reduce the need for high-speed communication channels [72].

4.4 Network Management Systems: Modelling

Real-time measurements, to be managed by a SCADA system in practice, are obtained from time-series simulations run by a distribution network modelled in OpenDSS [117]. The AC OPF-based optimisation engine is implemented in the modelling language AIMMS [118], to find the best set points for the available controllable elements (i.e., OLTCs, DG power factor and DG curtailment) upon the violation of constraints or the existence of curtailment. To run the AC OPF, in addition to the states above, an identical network representation is considered (i.e., topology, impedances, nominal capacity of loads and generators, etc.).

To identify the need to invoke the optimisation engine, voltage measurements at each bus and the power flow throughout lines and transformers are obtained from OpenDSS (in practice, the SCADA system). As the optimisation engine is invoked, the state of the network is sent for a given instant (start of a control cycle) from OpenDSS to the proposed AC OPF-based NMS optimisation engine. The state of the network includes the following:

- Active and reactive power of loads.
- Active and reactive power output of firm and controllable generation plants.
- Tap positions for centralised and locally controlled OLTCs.

The integration between OpenDSS and AIMMS allows modelling of the system response between successive control actions in OpenDSS. This is important to adequately model the real-time operation (in particular the time delay between decision and action) and the changes in demand and generation and, thus, evaluate the performance of the controller. Also, the benefits and impacts of adopting different control cycles can be assessed. Locally controlled OLTCs can also be modelled in OpenDSS.

To allow communication between OpenDSS and AIMMS and the flow of information, an interface is modelled in Visual Basic using the Component Object Model (COM) interface as shown in Fig. 4.4.

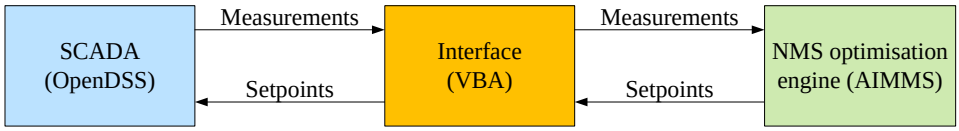

Fig. 4.4 NMS modelling

4.5 Network Management Systems: AC OPF Formulation

The AC OPF formulation, as a proxy to minimising DG curtailment, maximises the total active power that could be injected by the controllable wind farms (set N indexed by n), as given below.

$$max \quad \sum_{n \in N} SP_n \left(\frac{p_n}{SP_n^0} \right) \tag{4.2}$$

where SP_n represents the new set point for the corresponding control cycle, p_n is the active power output and SP_n^0 is the original set point for the last control cycle, $\left(\frac{p_n}{SP_n^0}\right)$ is the potential available wind resource.

With this objective function, the OPF will find the set point that harvests as much of the available wind resource $\left(\frac{p_n}{SP_n^0}\right)$ (active power injection is divided by the set point used throughout the last control cycle) as possible. In practice, the available wind resource can be obtained by either directly measuring the wind power output or indirectly using wind speed measurements and the power characteristics of the wind turbines.

$$0 \leq SP_n \leq 1 \quad \forall n \in N \tag{4.3}$$

This objective is subject to a range of constraints including those related to traditional AC OPF constraints (i.e., Kirchhoff's voltage law and power balance), controllable DG plants and OLTCs as well as the voltage and thermal limits.

4.5.1 General AC OPF constraints

Active, $f_{l,t}^{(1,2),(P)}$, and reactive power, $f_{l,t}^{(1,2),(Q)}$, injections at the start and end buses (denoted as 1 and 2) into each line and transformer (all represented by the set *L* indexed by *l*) are calculated according to the standard Kirchhoff Voltage Law (KVL) expressions as presented below [12].

At the start bus of line l, $f_l^{(1),(P)}$ and $f_l^{(1),(Q)}$ are given in Equations (4.4) and (4.5), respectively

$$f_l^{(1),(P)} = g_l V_{\beta_l^1}^2 - V_{\beta_l^1} V_{\beta_l^2} \left(g_l cos\left(\delta_{\beta_l^1} - \delta_{\beta_l^2}\right) + b_l sin\left(\delta_{\beta_l^1} - \delta_{\beta_l^2}\right)\right) \quad (4.4)$$

$$f_l^{(1),(Q)} = -b_l V_{\beta_l^1}^2 - V_{\beta_l^1} V_{\beta_l^2} \left(g_l sin\left(\delta_{\beta_l^1} - \delta_{\beta_l^2}\right) - b_l cos\left(\delta_{\beta_l^1} - \delta_{\beta_l^2}\right)\right) \quad (4.5)$$

At the end bus of line l, $f_l^{(2),(P)}$ and $f_l^{(2),(Q)}$ are given in Equations (4.6) and (4.7), respectively

$$f_l^{(2),(P)} = g_l V_{\beta_l^2}^2 - V_{\beta_l^1} V_{\beta_l^2} \left(g_l cos\left(\delta_{\beta_l^2} - \delta_{\beta_l^1}\right) + b_l sin\left(\delta_{\beta_l^2} - \delta_{\beta_l^1}\right)\right) \quad (4.6)$$

$$f_l^{(2),(Q)} = -b_l V_{\beta_l^2}^2 - V_{\beta_l^1} V_{\beta_l^2} \left(g_l sin\left(\delta_{\beta_l^2} - \delta_{\beta_l^1}\right) - b_l cos\left(\delta_{\beta_l^2} - \delta_{\beta_l^1}\right)\right) \quad (4.7)$$

where $V_{b,}$ δ_b are the voltage magnitude and voltage angle of bus b (set *B* indexed by *b),* g_l and b_l are the conductance and susceptance of line l, respectively, and $\beta_l^{(1,2)}$ are the start and end bus of line *l*.

If the transformers are equipped with voltage regulation devices, the corresponding terms in Equations (4.4) to (4.7) for voltage at the start bus of the transformer will be divided by the tap ratio τ_l assuming that the taps are located at the primary side of the transformer (i.e., the start bus). Therefore, the corresponding active and reactive power injections at the start and end buses are given in Equations (4.8) to (4.11), respectively.

$$f_l^{(1),(P)} = g_l \left(\frac{V_{\beta_l^1}}{\tau_{l.}}\right)^2 - \frac{V_{\beta_l^1}}{\tau_{l.}} V_{\beta_l^2} \left(g_l cos\left(\delta_{\beta_l^1} - \delta_{\beta_l^2}\right) + b_l sin\left(\delta_{\beta_l^1} - \delta_{\beta_l^2}\right)\right) \quad (4.8)$$

$$f_l^{(1),(Q)} = -b_l \left(\frac{V_{\beta_l^1}}{\tau_{l.}}\right)^2 - \frac{V_{\beta_l^1}}{\tau_{l.}} V_{\beta_l^2} \left(g_l sin\left(\delta_{\beta_l^1} - \delta_{\beta_l^2}\right) - b_l cos\left(\delta_{\beta_l^1} - \delta_{\beta_l^2}\right)\right) \quad (4.9)$$

$$f_l^{(2),(P)} = g_l V_{\beta_l^2}^2 - \frac{V_{\beta_l^1}}{\tau_{l.}} V_{\beta_l^2} \left(g_l cos\left(\delta_{\beta_l^2} - \delta_{\beta_l^1}\right) + b_l sin\left(\delta_{\beta_l^2} - \delta_{\beta_l^1}\right)\right) \quad (4.10)$$

$$f_l^{(2),(Q)} = -b_l V_{\beta_l^2}^2 - \frac{V_{\beta_l^1}}{\tau_{l.}} V_{\beta_l^2} \left(g_l sin\left(\delta_{\beta_l^2} - \delta_{\beta_l^1}\right) - b_l cos\left(\delta_{\beta_l^2} - \delta_{\beta_l^1}\right)\right) \quad (4.11)$$

For the OLTCs that are remotely controlled by the NMS optimisation engine, the corresponding tap ratios τ_l are considered in the optimisation problem as decision variables. On the other hand, for OLTCs that are locally controlled with respect to the measurements at the regulated terminal, the values of the tap ratios τ_l can be included as fixed parameters obtained from OpenDSS. Indeed, a parameter is defined for each line and transformer *l* to determine whether the element in the set is a line, a transformer equipped with OLTC controlled by the NMS or a transformer controlled locally.

The distribution network will be supplied by at least one point interfacing with the upstream grid. It is assumed that this point x (X, set of external connections) can import/export real and reactive power p_x, q_x, respectively, within limits $p_x^{-,+}$, $q_x^{-,+}$. One of these external connections will be taken as the slack bus with voltage angle, δ_{slack}, equal to zero and voltage magnitude, V_{slack}, (e.g., equal to 1 p.u).

$$p_x^- \leq p_x \leq p_x^+ \quad \forall x \in X \quad (4.12)$$

$$q_x^- \leq q_x \leq q_x^+ \; \forall x \in X \quad (4.13)$$

The balance of real and reactive power at each bus (set *B* indexed *b*), described by Kirchhoff's Current Law (KCL), is formulated according to Equations (4.14) and (4.15), respectively. The modelling considers firm generation (set *G* indexed by *g*), whose power output, p_g, is not controllable. They are assumed to have fixed power factor, $\emptyset_g$. Indeed, the inclusion of firm generation plants introduces more challenges to the management of network constraints since the power output is not controllable and may be increased throughout the control cycle above the observed value at the decision time (start of control

cycle), which in turn may violate network constraints.

$$\sum_{n\in N|\beta_{n=b}} SP_n\left(\frac{p_n}{SP_n^0}\right) + \sum_{g\in G|\beta_{g=b}} p_g + \sum_{x\in X|\beta_{x=b}} p_x = d_b^P + \sum_{l\in L|\beta_l^{(1)}=b} f_l^{(1),(P)} + \sum_{l\in L|\beta_l^{(2)}=b} f_l^{(2),(P)} \tag{4.14}$$

$$\sum_{n\in N|\beta_{n=b}} SP_n\left(\frac{p_n}{SP_n^0}\right) tan(\emptyset_n) + \sum_{g\in G|\beta_{g=b}} q_g + \sum_{x\in X|\beta_{x=b}} q_x = d_b^Q + \sum_{l\in L|\beta_l^{(1)}=b} f_l^{(1),(Q)} + \sum_{l\in L|\beta_l^{(2)}=b} f_l^{(2),(Q)} \tag{4.15}$$

where β_m maps the location of each network element ($m \subset \{n, g, x, l\}$) to its associated bus and $d_b^{(P,Q)}$ are the active and reactive demand at the same bus obtained from the measurements at the instant of triggering the optimisation engine.

The apparent power flow at the start and end of the lines and the transformer are limited to the corresponding capacity f_l^+,

$$\left(f_l^{(1,2),P}\right)^2 + \left(f_l^{(1,2),Q}\right)^2 \leq (f_l^+)^2 \quad \forall l \in L \tag{4.16}$$

Furthermore, the voltage magnitude at bus b (B, set of buses) should be maintained within the statutory limits $V_b^{(+,-)}$.

$$V_b^- \leq V_b \leq V_b^+ \quad \forall b \in B \tag{4.17}$$

4.5.2 On-Load Tap Changers

The OLTCs controlled by the NMS optimisation engine are controlled using min and max

tap positions $M^{(-,+)}$ to achieve voltage regulation capabilities in the range of $\tau_l^{(-,+)}$. To avoid tap changes beyond the actual operational capabilities of the OLTCs (mechanical response time to change tap position considering 1-min resolution), and to reduce the effects of wearing, the tap change is limited to one (up or down) from the initial tap position at the start of the control cycle. Given that the AC OPF is formulated as a non-linear programming problem (i.e., continuous variables), this constraint is modelled in terms of the tap ratio and the corresponding regulation equivalent R_l (per unit, e.g. 0.0167). The change in the tap ratio should be below the regulation equivalent value for a single tap change.

$$\left|\tau_l - \tau_l^0\right| \leq R_l \quad \forall l \in L \tag{4.18}$$

$$R_l = \frac{(\tau_l^+ - \tau_l^-)}{(M^+ - M^-)} \tag{4.19}$$

To find the tap position, the tap ratio obtained from the NMS optimisation engine requires adjustment. It should be converted to the nearest discrete value that reflects a feasible integer tap position $m_l \in \{M^-, \ldots, -1, 0, 1, \ldots M^+\}$. In the case of two feasible tap positions, the larger tap position will be selected to better managing voltage rise issues. For example, let assume τ_l is 1.04175 and R_l is 0.0167, then m_l will be set to the tap position number three since $\left(\frac{\tau_l - 1}{R_l}\right)$=2.5. This is equivalent for a tap ratio of 1.0501.

$$m_l = nearest\ integer\ \left(\frac{\tau_l - 1}{R_l}\right) \tag{4.20}$$

It should be mentioned that it is possible to formulate the tap as an integer variable in the optimisation problem so that the optimisation engine finds the best tap position m_l and given the voltage regulation capabilities $M^{(-,+)}$ as given in Equation (4.21). However, this converts the optimisation problem into Mixed Integer Non Linear Programming (MINLP), which in turn will require a relatively long computation time which is not suitable for real-

time application.

$$\tau_l = 1 + m_l \; R_l \tag{4.21}$$

4.5.3 DG Power Factor Control

Controllable DG units can also operate at different power factor, making reactive power "dispatchable" [13] within the MVA capability of the DG plants S_n^{rated}. To incorporate this into the AC OPF framework, the power factor angle for each controlled DG, $\emptyset_n$, is considered as a variable and is required to operate within the DG plant's capability. It is important to note that only the power factor control from the reactive power capability charts is adopted in this work.

$$\emptyset_n^- \leq \emptyset_n \leq \emptyset_n^+ \quad \forall n \in N \tag{4.22}$$

$$\left(SP_n\left(\frac{p_n}{SP_n^0}\right)\right)^2 + \left(SP_n\left(\frac{p_n}{SP_n^0}\right) tan(\emptyset_n)\right)^2 \leq (S_n^{rated})^2 \quad \forall n \in N \tag{4.23}$$

4.6 Case Study: Network Description

The proposed distribution NMS is applied to a 33 kV network in the north-west of England in order to assess its effectiveness in managing a distribution network with a high penetration of DG. This section presents the network description and the load and generation profiles. The network description is obtained from the database of the DNOs in the north-west of England and is modelled in the power system software IPSA [119]. A single line representation of the network is given in Fig. 4.5.

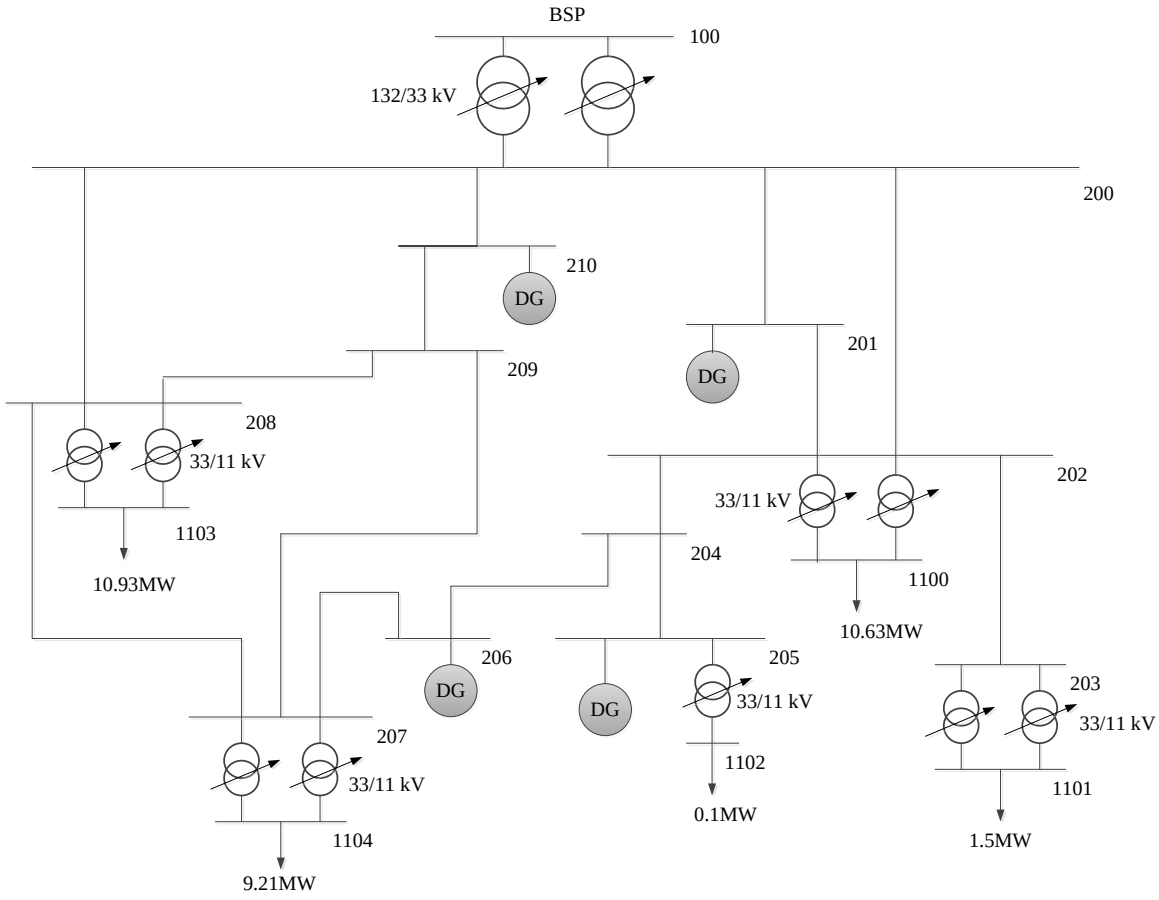

Fig. 4.5 A 33 kV network in the north-west of England

The corresponding lines, transformers and load data are included in Appendix A. The 33 kV feeders of the test network are supplied by two 63 MVA 132/33 kV power transformers at the BSP. The voltage of the 33 kV system is regulated by the OLTCs in the BSP using the regulation range of +10% to -20%, in 18 steps of 1.67%. Similarly, the primary substations (33/11 kV) are equipped with OLTCs with a predefined target of 1.0 p.u. at the 11 kV terminals. The regulation range for the OLTCs in the primary substations is –17.16% to +5.72%, in 16 steps of 1.43%. The network accommodates four wind farms with firm connection agreements at buses 201, 205, 206 and 210 and with capacities of 9.1, 10.6, 12 and 7.5 MW, respectively.

4.6.1 Load Profiles

The profiles for loads in the real network are needed to model the proposed NMS and assess its effectiveness in managing network constraints in close to real-time. However, real monitoring data are unavailable. Therefore, the load profiles have to be produced for the loads at each primary substation (33/11 kV).

The available data from which load profiles can be generated consist of the peak demand and the day of its occurrence for each primary substation, the number of consumers and their metering types at each primary substation and the half-hourly load profiles for consumers in the north-west of England in 2011. These half-hourly load profiles are used in the UK electricity settlement market to represent consumers whose maximum demand is below 100 kW. Indeed, eight types of half-hourly profile classes are used, presented briefly as follows [120].

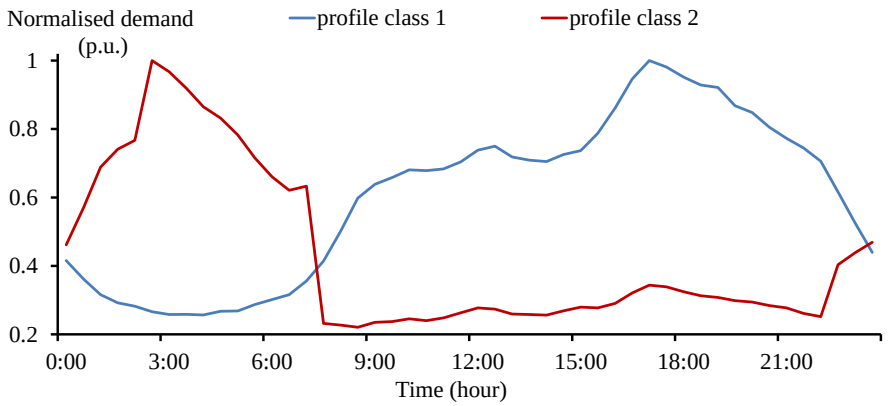

Fig. 4.6 Half-hourly normalised load profiles (p.u.) on a winter weekday

Profile class 1 is used to represent the electricity consumption pattern for domestic unrestricted consumers who have a flat electricity tariff rate. Profile class 2 is used for domestic restricted consumers whose metering systems have a time of use tariff rate (e.g., Economy 7). Indeed, a higher price is applied during on-peak time intervals than off-peak periods (e.g., 00:30-07:30) to encourage consumption during off-peak periods. Fig. 4.6 compares the normalised half-hourly load profiles for profile class 1 and profile class 2 per unit (in respect to their peak demand) on a winter weekday. It can be seen that the peak

demand for profile class 1, defined as 'unrestricted', occurs during the peak periods while the power consumption of profile class 2 occurs during the off-peak time periods (lower price intervals) between 00:30 and 07:30.

Profile classes 3 and 4 are used to represent unrestricted and restricted non-domestic consumers, respectively. Profile classes 5 to 8 represent larger non-domestic consumers whose metering systems record the maximum demand for a given defined period. The consumers are classified into these profile classes 5 to 8 according to their peak load factor, defined as the ratio between the total energy consumption for a given period and the energy consumption that could exist if the maximum demand extended throughout the same period. In this context, profile class 5 includes consumers whose annual peak load factor is less than 20%. Profile class 6 refers to consumers with peak load factor in the range between 20% and 30%. Profile class 7 includes consumers with peak load factor ranging from 30% to 40%, while customers with peak load factor higher than 40% are grouped within class 8.

Based on the above available data, the procedure adopted to produce the load profile for each primary substation can be described as follows. First, the yearly load profile for a typical single consumer within each profile class in the north-west of England is found. This is obtained by dividing the yearly aggregated half-hourly load profiles for each profile class in the north-west of England by the corresponding number of consumers.

For each primary substation, the corresponding number of consumers within each profile class is multiplied by the corresponding yearly typical profile of a single consumer (found in the first process). The resultant yearly half-hourly profiles are then aggregated to form the profile of the primary substation. It should be noted that some consumers do not follow a specific profile class and, for simplicity, these consumers are all assumed to be profile class 1.

The peak demand for the aggregated profile may be below that registered (from actual measurements) in the database for primary substations. To cater for this issue, the data in

the aggregated load profiles are then scaled up so that the peak demand of the aggregated profile at each primary substation matches the registered peak demand.

The obtained normalised load profile for bus 1101 using the above methodology is presented in Fig. 4.7 in per unit (based on the maximum demand of the load). The seasonal effect is clear in that the peak demand occurs in December (winter), while the minimum demand occurs in summer.

The maximum and minimum demand for the whole network are 31 MW and 15 MW, respectively. The yearly peak load factor for the loads in primary substations are presented in Table 4.1, in the range of 0.44 and 0.52, close to the yearly peak load factor of unrestricted domestic loads (0.44).

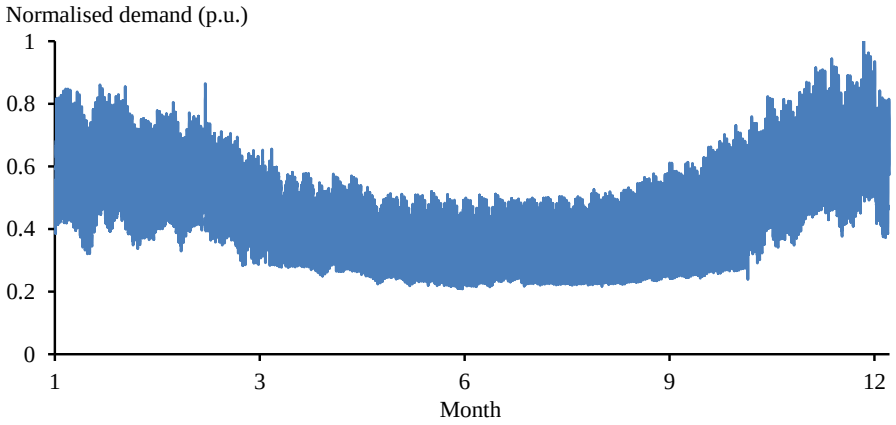

Fig. 4.7 Annual half-hourly normalised load profile (p.u.) at bus 1101

Table 4.1: Annual Peak Load Factor at Primary Substations

Bus location	Annual peak load factor
1100	0.51
1101	0.52
1102	0.44
1103	0.47
1104	0.50

4.6.2 Wind Power Profiles

One-minute resolution historical normalised wind power data from a site in England for February 2010 is adopted to drive all the firm and controllable generators in the network. According to this wind power profile, the capacity factor for the wind farms in the network during the analysed month is 24.2%. This capacity factor is lower than the UK average capacity factor of 30% for February (see Fig. 2.13 in Chapter 2). The highest energy production occurs during the first week of February 2010 and represents 39% of the potential energy production of the analysed month. The energy content in each week is shown in Fig. 4.8.

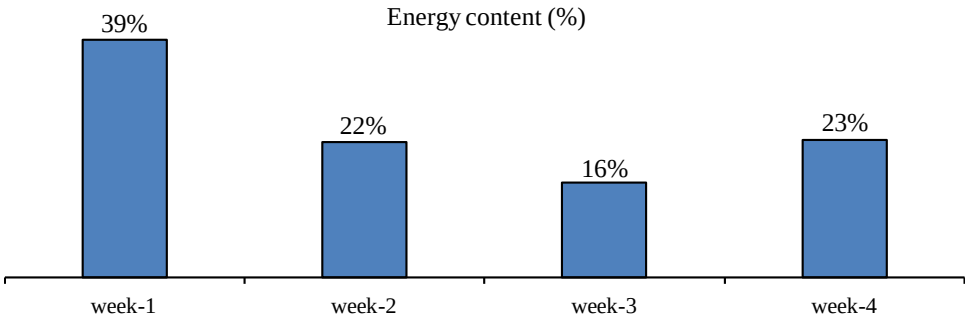

Fig. 4.8 Proportion of wind energy content (%) during the four weeks of February 2010

A demonstration of the NMS operation will be presented considering the wind data for the first week of February (the week of the highest energy content) and using the corresponding data of load profiles. To increase the granularity of the load profiles to a 1-min time resolution (similar to the available wind power data), each sample in the half-hourly load profiles is extended for the next half an hour (30 time steps).

The normalised half-hourly demand (load 1101) and the 1-min wind profiles for 1st February 2010 are shown in Fig. 4.9. The high variability in the wind power profile is clearly shown in this figure compared to the load profile. Indeed, wind power can change significantly within one hour. Chapter 5 provides further statistical analysis in relation to the variability of this wind power profile and how wind power changes throughout

different control cycles of one, five and 15 minutes.

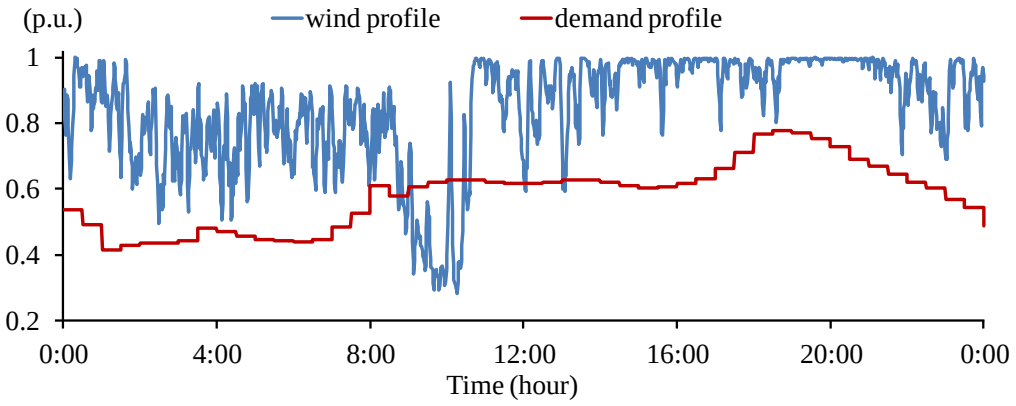

Fig. 4.9 Normalised wind and demand profiles on 1st February 2010

4.7 Simple Case Study 1: Congestion Management

In this section, the effectiveness of the proposed NMS to manage congestion issues is demonstrated for 1st February 2010. In order to do so, a new 9 MW wind power plant is connected as firm generation to bus 201. This capacity corresponds to the maximum extra firm generation that could be connected to the network at bus 201 so that no constraint issues arise during the worst case scenario of maximum generation and minimum demand. Furthermore, a 6 MW controllable DG plant is connected to bus 201. The connection of this capacity without any form of control would create congestion throughout line 200-201 (thermal capacity of 20 MVA) of 27% during the analysed day.

NMS: Curtailment-Only Scheme

Here, the AC OPF-based distribution NMS is continuously monitoring network elements and controlling (if necessary) the output of DG plants during each control cycle (one minute). Fig. 4.10 illustrates the operation of the curtailment-only NMS over one hour. The wind power profile is presented in Fig. 4.10 (a) to illustrate the operation of the control scheme. To show the benefits of the adopted control scheme, the potential loading that would occur without any form of control throughout line is shown in Fig. 4.10 (b). The loading of line 200-201 with control is presented in Fig. 4.10 (b). The set points SP_{201} for

the controllable wind farm at bus 201 are also presented in Fig. 4.10 (c). The set points represent the mechanical variations of the wind farm. For example, a set point of 0.5 p.u. means that wind farm has to extract 50% of the potential available wind resource. As discussed in Section 4.5, the potential available resource at each control cycle is found by dividing the active power injection of the wind farm by the corresponding set point used throughout the last control cycle.

It can be seen that the loading of line 200-201 is actively managed by controlling the new 6 MW controllable DG plant. For example, at minute 0, the controller is activated to solve the overloading at line 200-201. Based on the optimisation engine, the NMS sends a control signal to the wind farm at bus 201 to change its set point (SP_n) from 100% to 14%.

At minute 2 there is no constraint violation for line 200-201. However, given that curtailment has been applied to the wind farm, the NMS triggers the optimisation to find a new set point to minimise curtailment. It can be seen that it is indeed improved at minute 3 from 51% to unity. Nonetheless, at minute 5 the wind speed increases (see the normalised wind power profile in Fig. 4.10 (a)), congesting line 200-201 beyond its limit. This is due to the wind power changes between the time of decision and the action time (application of the set points), and in particular is due to the changes in the power output of the uncontrollable firm DG plants (total capacity of 49 MW). However, the use of short control cycles (such as 1 minute) allows a close following of wind power changes, which in turn prevents any substantial overloading of line 200-201 over a sustained time period. Indeed, the longest period of overload during the analysed day lasts for one minute, at a magnitude of 19%. The volume of curtailment required to manage congestion at line 200-201 is 43% of the available wind resource during the analysed day.

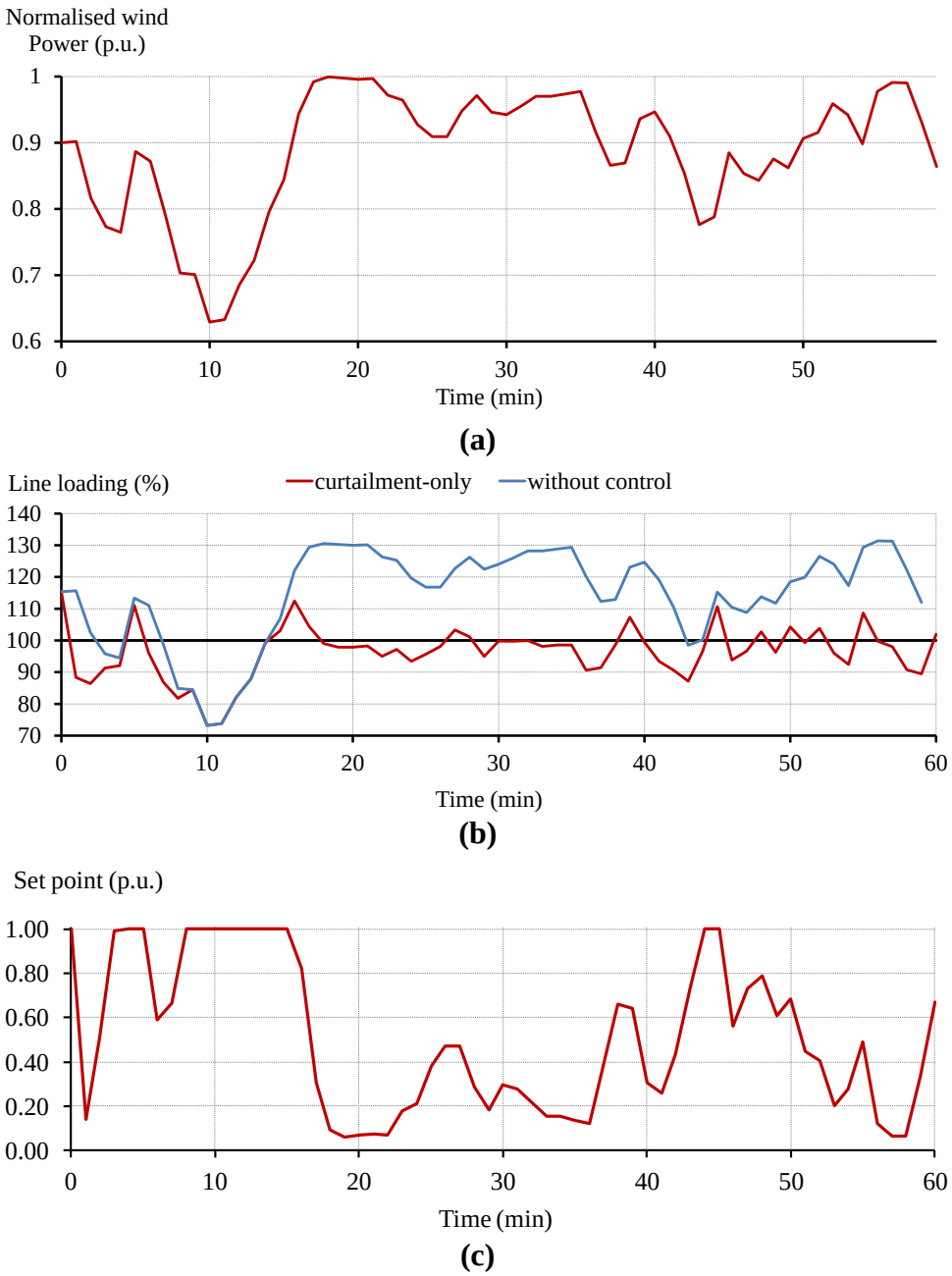

Fig. 4.10 Curtailment-only NMS: (a) wind profile (p.u.) (b) line 200-201 loading (%) and (c) set point at DG 201

4.8 Simple Case Study 2: Voltage and Congestion Management

A new case study is presented to demonstrate the real-time operation of the NMS controller to simultaneously manage congestion and voltage rise issues. Two controllable

DG plants with capacities of 20 MW and 15 MW, respectively, are connected to the real network at buses 205 and 206. Connection of these new DG plants without any form of control would create significant congestion, of 30%, at line 204-205 (thermal capacity of 23 MVA). Also, the voltage at bus 205 would reach 1.09 p.u. It should be noted that, in this case study, no extra firm generation plants are connected to the network.

To examine the benefits of the distribution NMS to managing simultaneously congestion and voltage rise issues, different control schemes are presented. First, the operational aspects of the *curtailment-only* NMS are presented. To reduce the volume of curtailment from the controllable DG plants, the NMS is then extended to control the power factor of the controllable DG plants in addition to generation curtailment. Also, the NMS is demonstrated to control the tap ratio of OLTC at the BSP (132/33 kV) and generation curtailment. Finally, the optimal management of OLTC, DG power factor control and generation curtailment (full NMS) as a last resort are presented. The simulations are carried out with 1-min resolution, and the analysed period is limited to the first day of February 2010. The volume of curtailment required to manage network constraints is found for all the above control schemes during the analysed day.

In this case study, all the firm generators are operating at unity power factor. The controllable DG plants are capable of operating with power factor between 0.95 inductive and capacitive according to UK requirements [121].

4.8.1 NMS: Curtailment-Only Scheme

To illustrate the operation of the curtailment-only NMS, the loading of line 204-205, the voltage profile at bus 205 and the set points of the controllable wind farm at bus 205 are all shown in Fig. 4.11 for the same hour on 1st February 2010. To show the benefits of the adopted control scheme, the potential loading and voltage profiles that would occur without any form of control are also shown in Fig. 4.11. It should be highlighted that the DG plant at bus 206 is not subject to curtailment (i.e., it is allowed to harvest all the available wind resource during the analysed day). It can be seen that in minute 0, the

controller is activated to solve thermal and voltage issues. The NMS sends a control signal to the wind farm at bus 205 to change its set point to 47%. The corresponding response is shown clearly in minute 1 where the line loading and the voltage are within limits. Then, the loading of lines and voltage buses are maintained within limits between minute 1 and minute 4. During this time interval, the set points are increased progressively, reaching (SP_n = 97%) at minute 5. However, the set point obtained at minute 4 (based on the state of the network at this minute) and applied at minute 5 (due to the adopted time delay) congests line 204-205 by 13% and increases the voltage at bus 205 to 1.07 p.u. This is due to the increase in wind power during the control cycle, as previously indicated. Therefore, new set points are obtained to solve the congestion and voltage issues. The obtained set point of 66% allows the network issues at minute 6 to be solved. At minute 8, there is no constraint violation and, thus, the NMS triggers the optimisation engine to find new set points in order to maximise the total active power of the controllable DG units, given that curtailment has been applied to the wind farm at bus 205 (SP_{205} = 89%). The total output of the DG plants is indeed improved until minute 14 and, so, the DG plant is not curtailed (SP_{205} = 100%) and is able to harvest all the available wind power resource.

The curtailment-only scheme allows the maintenance of the voltage profile at bus 205 within the statutory limits, and maintains the loading of line 204-205 below the thermal limits. As discussed above in Section 4.7, the adoption of a 1-min control cycle allows following the changes in the network state and solving for network issues quickly. Indeed, the longest overload during the analysed day lasts for one minute with a 16% magnitude of violation. The maximum voltage rise (1.07 p.u.) also lasts for one minute. To assess the performance of this control scheme in the management of voltages in relative to the BS EN 50160, the analysed period should be extended to one week so that the voltage excursions can be quantified and assessed against the 5% tolerance limit of voltage excusrisons. This performance assessment will be carried out in Section 4.9. The volume of curtailment required to manage congestion at line 204-205 is 16% of the available wind resource during the analysed day. It is important to note that although voltage excursion above the upper statutory limits (+6%) exists during the analysed hour, the

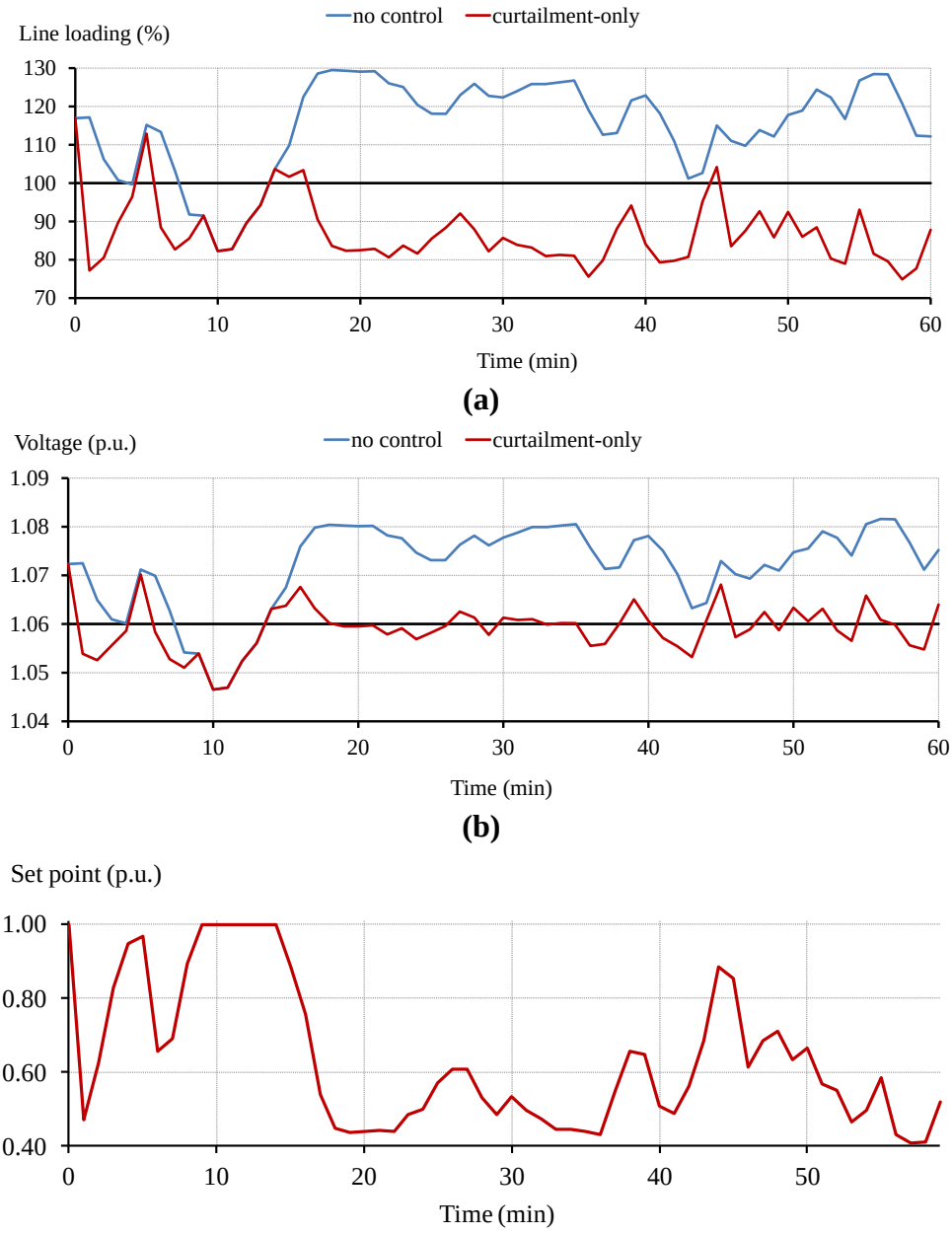

Fig. 4.11 Curtailment-only NMS: (a) loading of line 204-205 (%) (b) voltage profile at bus 205 and (c) set point at DG 205

4.8.2 NMS: Curtailment and DG Power Factor Control

Controlling the power factor of wind farms allows voltage rise issues to be resolved and reduces the volume of curtailment. Indeed, controlling the wind farms to consume reactive power will counteract the voltage rise resulting from high power injection. In this ANM

scheme, the NMS optimisation engine finds the best power factor angle $\emptyset_n$ of wind farms in addition to the set points SP_n. As previously indicated, the power factor is controlled between 0.95 inductive and capacitive. The apparent power capacity S_n^{rated} of the DG plants are selected such that reactive power can be consumed and injected at their full active power output with a power factor of 0.95. Therefore, the apparent power capacity of the DG plants at buses 205 and 206 are 21.05 MVA and 15.8 MVA, respectively.

The DG plant at bus 206 is not curtailed during the analysed day, similar to the case study in Section 4.8.1. However, the NMS controls this DG plant to consume reactive power so that voltage at bus 205 can be managed below the upper statutory limit. In contrast, the DG plant at bus 205 run with unity power factor (i.e., zero reactive power output) due to the available headroom in line 204-205, which places limitations on the imported or injected reactive power from the DG plant at bus 205. The loading of line 204-205, the voltage profile at bus 205, the set points of the controllable DG plant at bus 205 and the reactive power output of the DG plant at bus 206 are all shown in Fig. 4.12 for the first hour of 1st February 2010.

It can be seen from Fig. 4.12 that, by controlling the power factor, the set points of the DG plant at bus 205 are improved compared to those in the *curtailment-only* scheme. For example, at minute 0 the optimisation engine is triggered to solve a voltage rise issue at bus 205 and congestion at line 204-205. The obtained set point for the DG at bus 205 is 64%, which shows a 17% improvement over the set point found in the *curtailment-only* scheme (47%), whilst the DG at bus 206 is controlled to consume reactive power of 1.7 MVAr. For the analysed day, the controlling power factor allows a reduction in the volume of curtailment from 16% in the curtailment-only scheme to 13%. However, the improvement in set points will result in an increase in constraint violations due to the changes in wind power throughout the control cycle.

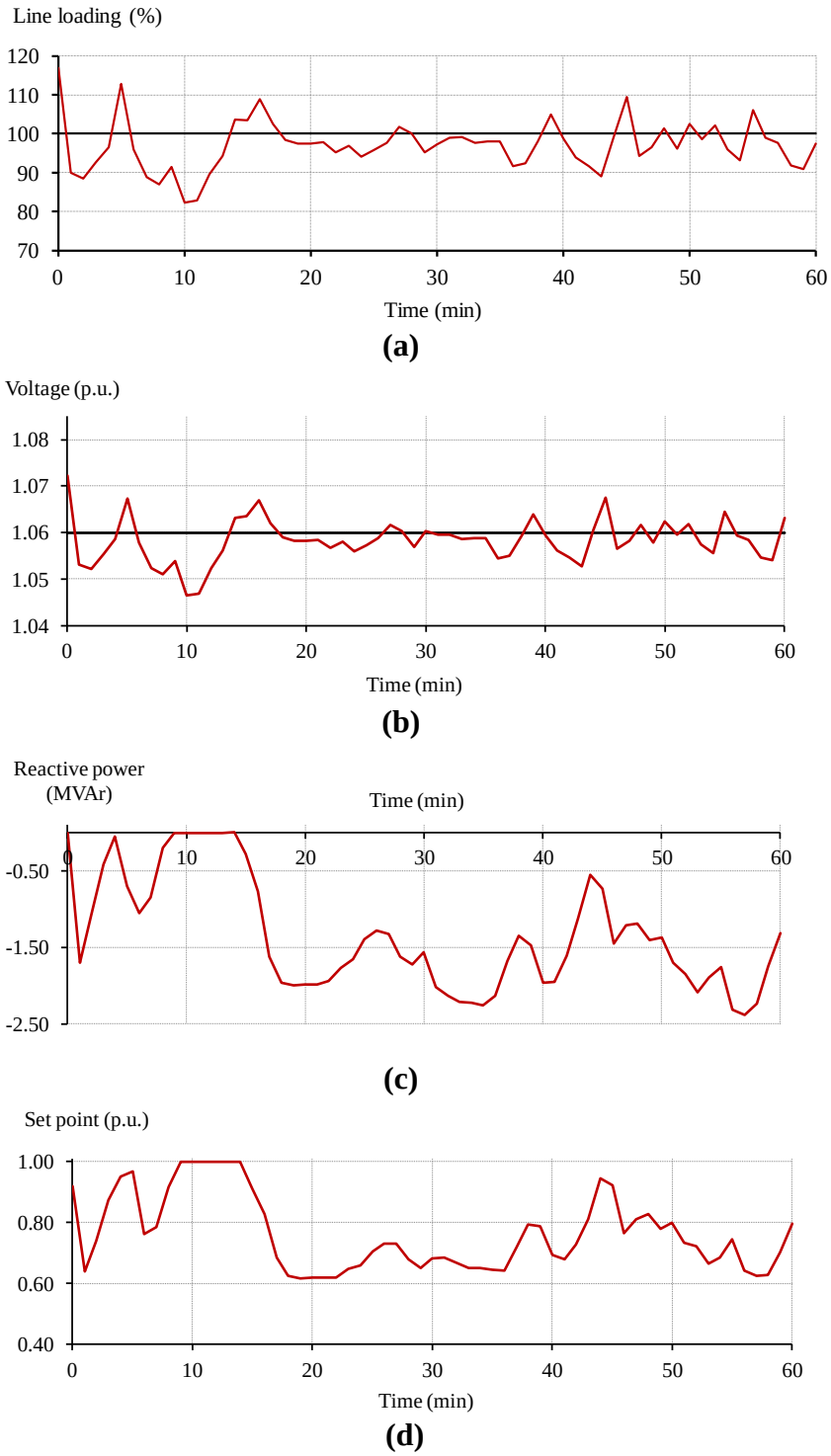

Fig. 4.12 Curtailment and DG PF control NMS: (a) loading of line 204-205 (b) voltage profile at bus 205 (c) reactive power at DG 206 and (d) set point at DG 205

4.8.3 NMS: Curtailment and OLTC Control

This section presents another solution to managing voltages, by controlling the tap position of the OLTC at the BSP so that the volume of curtailment from the DG plants can be decreased. Given the objective function adopted for the optimisation engine, controllable OLTC will be activated first, leaving curtailment as the last resort. The NMS optimisation engine finds the best tap ratio τ_l and the set points of wind farms. The tap ratio is controlled within the voltage regulation capability of the OLTC, between 0.8 p.u. and 1.1 p.u. The maximum tap change is limited to one from the tap position at the start of the control cycle, and the corresponding voltage regulation is 0.0167 p.u. The loading of line 204-205, the voltage profile at bus 205 and the tap ratio at the BSP, in addition to the set points of the DG at bus 205, are all shown in Fig. 4.13 for the first hour of the analysed day.

It can be seen that controlling the OLTC keeps voltages within the statutory limits and improves the DG set point compared to the curtailment-only scheme. It can be seen that after minute 0, the NMS manages the thermal and voltage constraints and improves the set point significantly for the DG at bus 205 from 47% in the curtailment-only scheme to 64% (allowing more power injection).

The tap ratio of the OLTC is increased from 1 to 1.01667 p.u. to manage voltages. Indeed, controlling the OLTC allows a reduction in the volume of curtailment from 16% in the curtailment-only scheme to 13% for the analysed day. Although the reduction in curtailment achieved by controlling the OLTC is the same as that achieved by controlling the power factor, the voltages are effectively managed during the analysed day compared to the voltage excursion issues that exist when controlling the power factor.

It is important to note that, for networks with relatively higher demand than the network adopted in this case study, the flexibility to reduce curtailment using OLTC may be limited to avoid creating voltage drop issues by increasing the tap ratio.

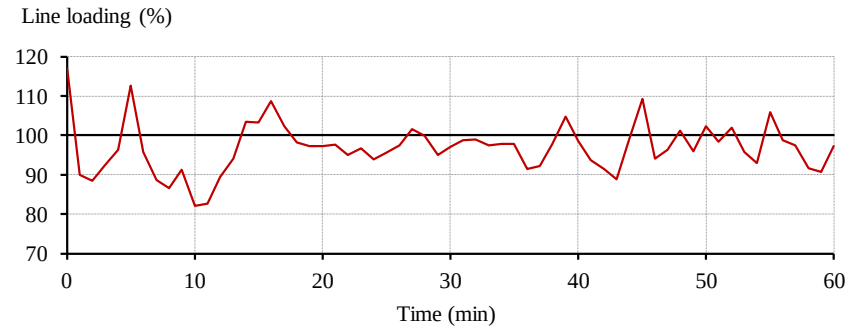

(a)

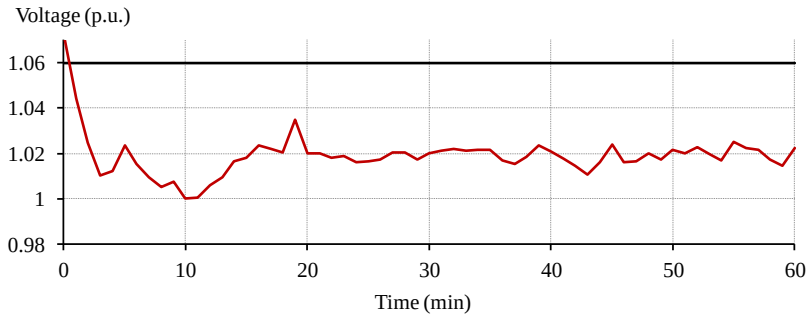

(b)

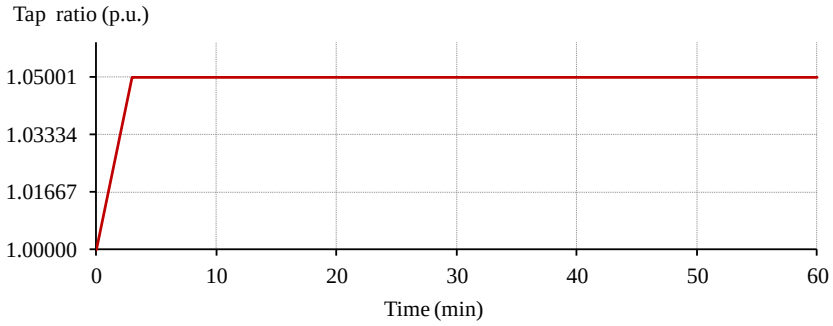

(c)

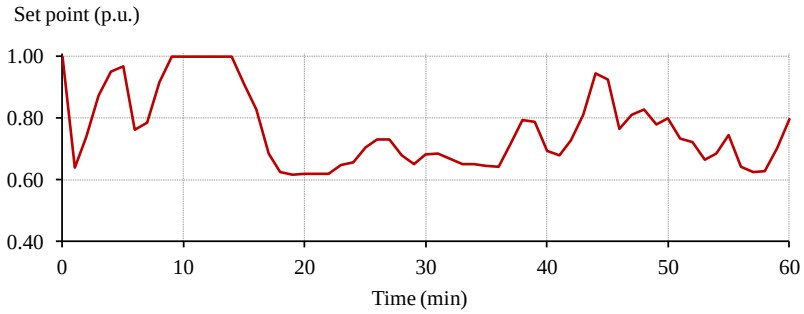

(d)

Fig. 4.13 Curtailment and OLTC control NMS: (a) loading of line 204-205 (b) voltage profile at bus 205 (c) tap ratio of the OLTC at the BSP and (d) set point at DG 205

4.8.4 Full NMS: Curtailment, OLTC and DG Power Factor Control

In this full NMS scheme, once the optimisation engine is triggered, it finds the best set points SP_n and power factor angle $\emptyset_n$ of the controllable DG plants as well as the tap ratio of OLTC τ_l.

For this case study, the application of the full NMS over the analysed day does not provide further improvement in terms of curtailment reduction over the above NMS schemes to control only the OLTC or the DG power factor (the total volume of curtailment across the analysed day is 13%). The maximum voltage rise that can occur without control is 1.09 p.u. which is within the voltage regulation capability of the OLTC (i.e., $\tau_l^{(+)}$=1.1 p.u.). Therefore, most of the voltage rise issues are managed by increasing the tap ratio of the OLTC, so that the benefits of controlling the DG power factor to reduce curtailment in this particular network is limited.

Thus, if voltage rise problems become more significant, controlling the power factor of wind farms simultaneously with the OLTCs could avoid further curtailment. This issue is demonstrated using a generic UK rural distribution network to which additional controllable DG plants are connected so that voltages are increased significantly to 1.18 p.u. before adopting any form of control. Indeed, the results show that the volume of curtailment is reduced by 1% for the full NMS compared to only controlling the OLTCs. The UK generic rural distribution network and the results of the full NMS control are all presented in [66] (one of the conference publications resulting from this project).

It should also be highlighted that the use of power factor control could provide more flexibility to increase the tap ratio (so that curtailment can be further reduced), in order that reactive power (capacitive power factor) can be injected into the network to avoid voltage drop issues that may result from reducing voltages by the OLTC. However, the benefit of controlling the DG power factor depends on the active power of wind resource due to the coupling between the active and reactive power of wind farms, as modelled in this work and following the UK requirements.

4.9 Full Case Study

To demonstrate the effectiveness of the NMS in a more complex environment, the network in Fig. 4.5 will now be studied considering a significantly higher wind penetration and the studied horizon is extended to one week to demonstrate the performance of the NMS optimisation engine considering different ANM schemes. In order to do so and test the NMS, the multi-period AC OPF planning tool developed in [12] is applied in Section 4.9.1 to find the DG capacity that could be connected considering power factor control, the active management of OLTC, 2% energy curtailment and a 10% congestion allowance.. The planning tool suggests the connection of extra 53 MW controllable DG plants. Performance metrics are also defined to test the performance of different ANM schemes.

4.9.1 Multi-period AC OPF Planning

The multi-period AC OPF planning tool developed in [12] is applied to this network in order to calculate the maximum additional DG capacity that can be connected to the four locations with firm DG (buses 201, 205, 206 and 210). This multi-period AC OPF adopts a range of ANM schemes to allow the capacity of controllable DG plants connected to distribution networks to be maximised whilst maintaining voltages within statutory limits and the loadings of lines and transformers within thermal limits, as well as keeping the volume of energy curtailment from the additional controllable DG plants across the planning horizon below a defined curtailment level. It is important to note that this planning approach neglects real-time operational aspects.

To reduce the potential computational burden required to model the time-series data of generation and load profiles, the number of periods to be considered by the multi-period AC OPF (all at once) are reduced by using scenarios of generation and load instead of considering the full time-series data. Based on the volume of curtailment within each period (scenario) and the frequency of occurrence for each scenario, the aggregated volume of curtailment across the planning horizon can be found.

To create scenarios of load and generation, the time-series data for the 1-min wind power

generation profile and the demand profiles at the primary substations (bus 1100, bus 1101, bus 1102, bus 1103 and bus 1104) are all mapped into ranges. For the load profiles, five ranges are adopted as follows [0, 0.2], (0.2, 0.4], (0.4, 0.6], (0.6, 0.8] and (0.8, 1] per unit, and ten ranges are adopted for the wind power profile as follows: [0, 0.1], (0.1, 0.2], (0.2, 0.3], …, (0.9, 1] per unit. Thus, the possible number of scenarios that could exist from the coincidence of loads (five ranges for each of the five load profiles) and wind generation (ten ranges for one wind power profile) is $5^5 \times 10^1 = 31250$. Each scenario consists of the demand level at each primary substation and the wind power level (one for all the wind farms in the network). It is found that the feasible number of scenarios (i.e., non-zero frequency of occurrence) from the adopted methodology is 100. The scenarios are presented in Appendix B.

It is found that, during most of the time periods in February 2010, the generation levels lie at relatively low levels (below 20% of the nominal) for 50% of the month. The demand levels for all the loads in the network are higher than 30% of the peak demand, which in turn implies that larger capacities can be connected to the network before any network issues are created. In contrast, the probability of the occurrence of scenarios resulting from the coincidence of high generation levels (above 70%) and low load levels (between 30-40%) is relatively low (approximately 10%). This highlights the fact that the adoption of the worst case scenario to determine the maximum capacity of firm generation to cater for the relatively low time periods of congestion and/or voltage rise issues will underestimate significantly the hosting capacity of distribution networks (without any NMS scheme). This in turn implies that, even if generation curtailment is adopted to manage network constraints during those relatively low time periods, DG developers could consider such an ANM solution to be economically viable instead of limiting the DG capacity or upgrading the existing network assets.

Adopting wind and generation data for February 2010, power factor control, the active management of OLTC, 2% energy curtailment and a 10% congestion allowance (to increase DG capacity), this planning approach supports the connection of additional

53 MW (135% increased DG capacity) controllable DG plants to the network (with capacities of 5, 17, 22 and 9 MW at buses 201, 205, 206 and 210, respectively). Given that the planning tool neglects the actual real-time operational aspects of the ANM schemes, these values will test the performance of the distribution NMS. All the generators are considered to be capable of operating with power factor between 0.95 inductive and capacitive. It is assumed that all the DG (firm and new) in the network has the same wind resource (availability of time-series data with 1-min resolution).

4.9.2 No Control

Given that simulations are carried out with 1-min resolution, and the analysed period is extended to the first week of February 2010, the connection of extra wind farms with capacities of 53 MW to the distribution network under study without any form of control creates a significant reverse power flow through the lines in the network during minimum demand.

The maximum thermal violations occur at line 200-210, exceeding its thermal limit (17 MVA) by 36%. In addition, the voltage at bus 205 exceeds the statutory upper limit of 6%, reaching 1.09 p.u. Voltage excursions at this bus occur for 26% of the analysed week.

4.9.3 Curtailment-Only Scheme

This section presents the operation of the curtailment-only NMS to actively control the power output of multiple DG plants. To illustrate the operation of the curtailment-only NMS, the loading of line 200-201, the voltage profile at bus 205 and the set points of the controllable DG plants are all shown in Fig. 4.14 for the same hour on 1st February 2010.

It should be highlighted that the DG plant at bus 206 is not subject to curtailment (i.e., it is allowed to harvest all the available wind resource during the analysed day). It can be seen that the DG plant at bus 205 is, crucially, given the lowest set point of the controllable DG plants to solve voltage rise issues, which in turn affects the set points of the other DG plants. Indeed, curtailing the DG plant at bus 205 to solve voltage rise issues reduces the

volume of curtailment from the DG plants at bus 201 and bus 210 (i.e., higher set points) required to manage congestion in lines 200-201 and 200-210, respectively (since the injected power of the DG plant at bus 205 contributes to the complex power flow throughout these lines).

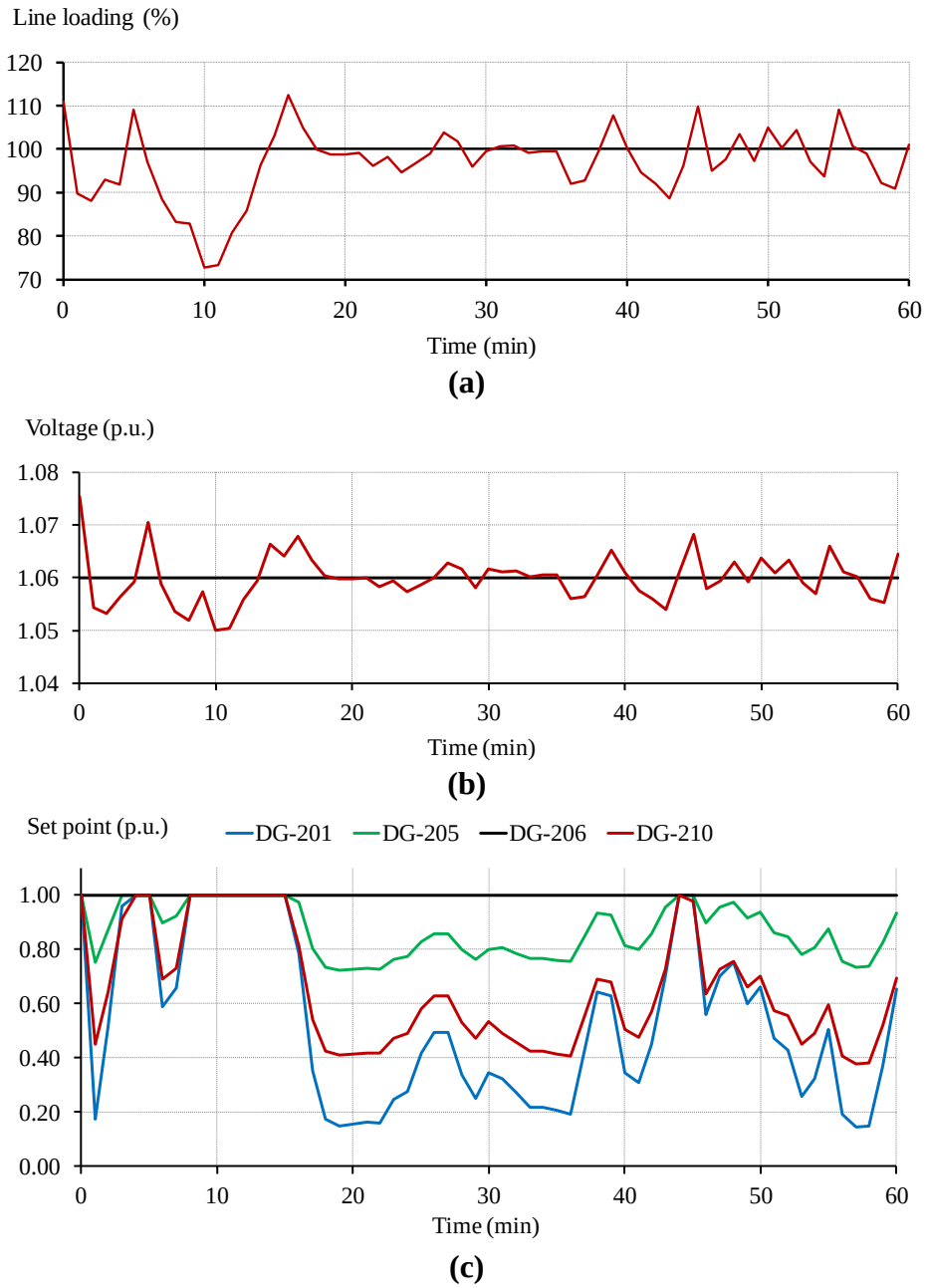

Fig. 4.14 Curtailment-only NMS: (a) loading of line 200-201 (b) voltage profile at bus 205 and (c) set points for all the controllable DG plants

4.9.4 Performance Metrics and Assessment

Considering the usage of different ANM schemes and 1-min resolution simulations, four metrics are applied to assess the performance of the NMS optimisation engine in terms of the management of congestion and voltage rise issues, and the volume of energy curtailment. The analysed period is the first week of February 2010. The adopted metrics are as follows.

- Congestion management: To assess the effectiveness of the approach in managing congestion, two metrics are used: (1) the total duration of overloads (in minutes); and (2) the longest duration and the corresponding average magnitude of overloads larger than 15%. Indeed, the 15% overloading refers to the normal cyclic ratings from 10% to 15% above the continuous rating (more details on cyclic ratings are discussed in Section 2.4.2).

- Voltage management: To assess the NMS performance in maintaining voltage profiles within statutory limits, the BS EN50160 standard is adopted. This standard states that, during an observation period of a week, 95% of the 10-min voltage magnitudes should be within the statutory limits of (in the UK) ±6% and the voltage magnitude should not deviate by more than ±10% of the nominal voltage [59].

- Volume of energy curtailment: The volume of energy curtailment is found during the planning horizon assessing the benefits of controlling more active network elements.

Table 4.2 compares the performance of different NMS approaches; the curtailment-only scheme, the ANM scheme of controlling OLTC and generation curtailment and the full NMS schemes, considering control of the OLTC, power factor control and generation curtailment. To show the benefits of the NMS in the management of network constraints, the performance before control is also provided (i.e., no-control is not a feasible option to be adopted). The effectiveness to manage congestion for line 200-201 and voltages at bus

205 (they were the most affected), the volumes of curtailed energy are all presented by using the above adopted metrics.

It can be seen from Table 4.2 that the power flows throughout the lines 200-201 are effectively managed below their thermal capacities by all the NMS control schemes. In particular, the lines are overloaded above 15% for only one minute. Also, the percentage of overloading during the analysed week for all the NMS control approaches is less than 6%. This is due to the adoption of a 1-min control cycle which allows more frequent monitoring of the network status and closely follows the variability of wind resource. However, the usage of the 1-min control cycle leads to frequent adjustments of the set points of the active network elements. For example, the number of tap changes from the OLTC in the BSP reaches 306 which in turn may affect the cycle life of the OLTC.

In addition, the curtailment-only scheme does not comply with the EN50160 standard since only 90.6% of the 10-min voltage magnitudes during the analysed week are within the statutory limits. In contrast, the NMS scheme of controlling the OLTC and generation curtailment (as a last resort) complies with the EN50160 standard (voltages within limits for 100% of the analysed week). In addition, the volume of curtailment is decreased from 14.5% in the curtailment-only scheme to 10.7% when the OLTC is controlled by the NMS optimisation engine. The volume of curtailment is slightly reduced to 10.2% for the full NMS scheme. It should be highlighted that the use of OLTC and the DG power factor NMS scheme may decrease the percentage of the 10-min voltage magnitudes within limits compared to only using the OLTC. This is since the OPF opts between using OLTC or DG power factor to solve for voltage rise issues. In the case of using DG power factor, the wind speed may increase throughout the control cycle and the power factor found by the OPF at the start of the control cycle is not enough to solve for voltage issues. However, the OLTC and the DG power factor NMS scheme still complies with the EN 50160 standard, where 96.5% of the of the 10-min voltage magnitudes during the analyzed week are within limits.

Table 4.2: Deterministic-Based NMS Performance Assessment – Congestion and Voltage Management and Curtailed Energy (%)

NMS Scheme	Performance metrics			
	Total Duration of Overloads for line 200-201 (min)	Longest Overload >15% for line 200-201 (min, avg overload)	EN50160 compliance of bus 205 (%)	Curtailed Energy (%)
No Control (non-feasible)	2315	1447; 21.2	73.5 (no)	-
Curtailment Only	702	1 ; 15.6%	90.6 (no)	14.5
Curtailment + OLTC	741	1 ; 18.6%	100 (yes)	10.7
Curtailment + OLTC + PFc	727	1 ; 18.6%	96.5 (yes)	10.2

Fig. 4.15 presents the total energy harvested from each DG plant for different NMS control schemes during the analysed week. The potential available wind resource at all DG sites is also presented to show the volume of curtailment within each NMS scheme.

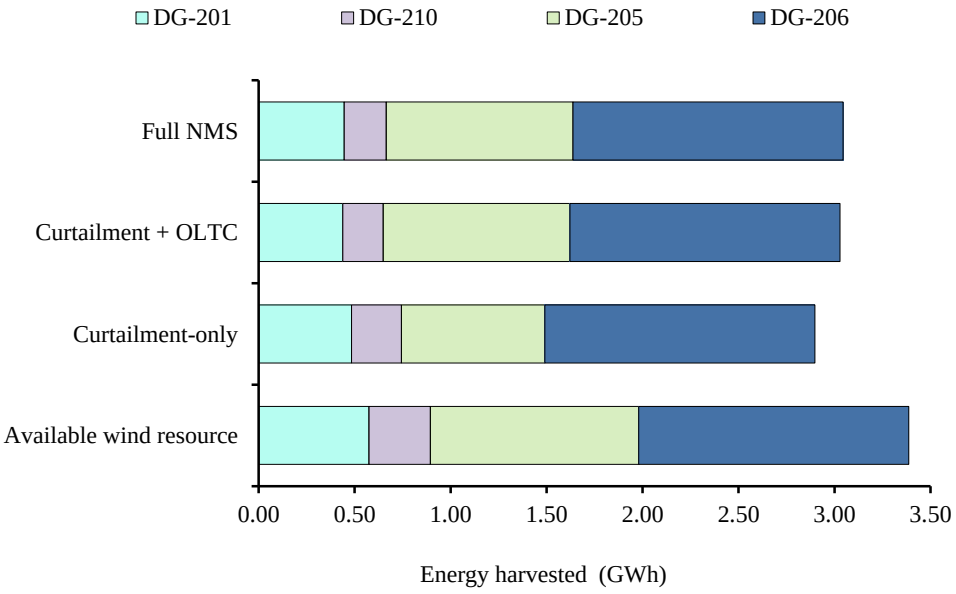

Fig. 4.15 Energy harvested per DG plant for different NMS control schemes

It can be seen that the harvested energy from the DG plant at bus 205 is increased after

controlling OLTC which solves all the voltage issues. The total energy harvested from all the DG sites is increased from 2.9 GWh in the curtailment-only scheme to 3.1 GWh in the full NMS. This highlights the importance of coordinating the control actions from controllable network elements. However, a small improvement in the total harvested energy can be achieved by controlling the power factor of DG plants simultaneously with the OLTC for this network. This is because the maximum voltage rise that could occur before control is 1.09 p.u. which is within the voltage regulation capability of the OLTC (i.e., $\tau_l^{(+)}$=1.1 p.u.).

To compare the volume of curtailment obtained in the full NMS with that used in the planning approach presented in Section 4.9.1, the studied horizon in the full NMS is extended to one month, as adopted in the planning approach. It is found that the total volume of curtailment is 5.1%. This is higher than the figure adopted (2%) in the planning approach and is due to the approximations adopted in the planning approach, which maps the wind power and loads into ranges. Therefore, potential curtailment that could exist for time steps are neglected in the planning approach. Also, the planning approach does not provide realistic modelling of the control aspects. This result highlights the need to develop more advanced planning approaches in order to determine the hosting capacity of distribution networks considering the real-time operational aspects, so that the maximum DG capacity can be adequately sized.

4.9.5 Effects of Thresholds

To effectively manage power flows within limits and avoid any overloading that could result from changes in wind power throughout the control cycle (from that observed at the decision making time) in the full NMS scheme, conservative thermal thresholds have to be adopted in the formulation of the deterministic NMS approach. This is similar to what is being adopted in practice where conservative thresholds are used to cater for the worst case scenario of wind power increase and demand reduction during the control cycle [11]. The following summarizes the modifications in the NMS.

Indeed, the NMS optimisation is triggered earlier, once the power flow at any branch (transformer or line) exceeds predetermined thresholds. More conservative set points are found by the AC OPF to maintain power flows throughout the lines and transformers at levels below the defined threshold compared to the use of seasonal thermal ratings. Therefore, the relative effect of wind power changes throughout the control cycle would result in a smaller magnitude of thermal congestion compared to the potential issues that could be found before adopting thresholds. In order to do so, the thermal constraints in, Equation (4.16) in the AC OPF is changed as follows.

$$\left(f_l^{(1,2),P}\right)^2 + \left(f_l^{(1,2),Q}\right)^2 \leq (\gamma f_l^+)^2 \quad \forall l \in L \tag{4.24}$$

The full NMS scheme for the multiple DG plants presented in Section 4.9.4 is adopted to demonstrate the benefits and the effects of using thresholds considering the same volume of controllable DG plants of 53 MW to the network (with capacities of 5, 17, 22 and 9 MW at buses 201, 205, 206 and 210, respectively). The thermal threshold is only used and it is set to 90% ($\gamma = 0.9$).

Fig. 4.16 shows the usage of line 200-210 and the optimal DG settings produced by the NMS. Compared to the approach without thresholds, it is clear that congestion issues have reduced dramatically in frequency (from 233 to 31 minutes for the first day of February) and in magnitude (during minute 16, the overload reduced from 12% to 1%).

The operation of the NMS is performed for the first week of February 2010, considering the 1-min resolution data. The results presented in Table 4.3 show that the power flow throughout the lines 200-201 and 200-210 are effectively managed below their thermal capacities. Overloading only occurs for 0.4% of the week compared to 7.2% before the adoption of thresholds. Also, the maximum overload is reduced significantly from 1.186 p.u.to 1.1 p.u. However, this is at the expense of the volume of curtailment. Indeed, energy curtailment increases from 10.2% to 17% when thresholds are adopted.

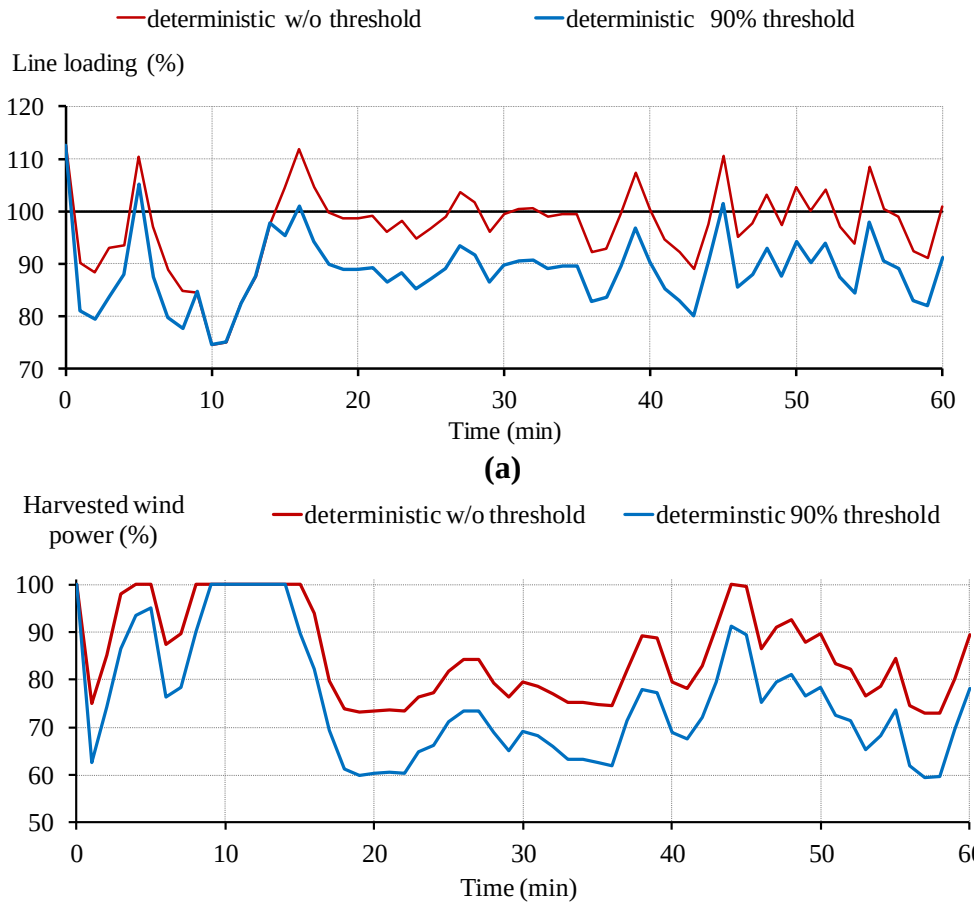

Fig. 4.16 Full NMS before and after using 90% thermal thresholds: (a) loading of line 200-201 and (b) harvested wind power from all the controllable DG

Table 4.3: Effects of thermal thresholds on the Performance of Full NMS

Thermal thresholds	Performance metrics			
	Total Duration of Overloads for line 200-201 (min)	Longest Overload >15% for line 200-201 (min, avg overload)	EN50160 compliance of bus 205 (%)	Curtailed Energy (%)
100%	727	1 ; 18.6%	96.5 (yes)	10.2
90%	42	-	98.0 (yes)	17.0

It is important to highlight the fact that the performance of the NMS depends on the selected threshold. Lower values manage network constraints effectively, but at the

expense of the volume of energy curtailment. The selection of the most adequate threshold can be defined after assessing the performance of the NMS for different threshold values, as this depends on the particular characteristics of the network and the wind resource.

4.10 Summary of Chapter 4

This chapter presents AC OPF-based NMS to minimise DG curtailment whilst actively managing technical network constraints (i.e., voltage rise and thermal overloads) in real-time operation. This is achieved through the optimal coordination of DG reactive power, voltage control devices and using DG curtailment as a last resort. The proposed NMS is applied to the 33 kV UK network for one week using wind and load profiles with 1-min resolution.

The following presents the key contributions of this work which have not yet been adequately addressed in the literature:

- Simultaneous management of voltage and thermal constraints.
- Realistic (minute resolution) modelling of network elements/participants, in particular considering on-load tap changers and DG power factor (in addition to curtailment).
- A methodology that allows detailed investigation of the benefits and impacts of adopting different ANM schemes (key metrics: voltage compliance with the EN50160 standard, congestion, the capacity factor of wind farms).
- The adaptation and expansion of a full deterministic AC OPF into a system used for realistic operational purposes.

In addition to the above contributions, the following summarises additional key points:

- Actively managing network constraints allows the connection of 53 MW of renewable DG, which is 135% above the existing capacity of firm generation.

- Controlling DG power factor and OLTC allows the solving of voltage issues which in turn increases the energy harvested from wind power plants compared to only using generation curtailment.

- The adoption of a 1-min control cycle allows solving of network issues and the effective management of network constraints (i.e., constraint violations with a maximum duration of one minute). However, this is at the expense of control actions from DG plants and OLTCs.

- To effectively manage power flows within limits in the deterministic NMS and avoid any overloading that could result from the changes in wind power throughout the control cycle (from that observed at the decision making time), conservative thresholds (e.g., a threshold of 90% of thermal capacity) have to be adopted. However, this will increase the volume of energy curtailment.

- The results also highlight the need to develop more advanced planning approaches in order to determine the hosting capacity of distribution networks considering the real-time operational aspects, so that the maximum DG capacity can be adequately sized.

Chapter 5: Advanced Network Management Systems – A Risk-Based Approach

5.1 Introduction

This chapter extends the deterministic NMS discussed in Chapter 4 to a risk-based NMS that allows the adoption of multi-minute control cycles in order that the volume of actions from on-load tap changers (OLTCs) and distributed generation (DG) plants can be reduced whilst effectively catering for the effects of wind power uncertainties. The AC OPF used in the deterministic NMS is adapted and expanded to produce a risk-based AC OPF that caters for wind power uncertainties (wind power changes during the control cycle), particularly during multi-minute control cycles, to reduce the volume of control actions. A risk level is used to determine the extent to which congestion and voltage rises could exist during a control cycle, so that the optimal set points can be obtained to both minimise DG curtailment and reduce/avoid operational problems (i.e., risk of thermal overloading and voltage rise).

First, this chapter presents the architecture of the risk-based NMS and the formulation of the optimisation engine. Then, the methodology adopted to handle uncertainties due to wind power is provided. The results from the application of the risk-based NMS on the 33 kV network (presented in Chapter 4) are presented and discussed. This includes the operational aspects and comparisons with the deterministic approach using different control cycles (1, 5 and 15 minutes). The performance metrics presented in Chapter 4

(voltage compliance with the EN50160 standard, congestion and volume of curtailment from wind farms) are used to perform the comparison between the risk-based and the deterministic NMS. To show the benefits of increasing the control cycle, the volume of control actions from OLTCs and DG plants are also quantified and compared.

5.2 Risk-Based NMS Architecture and Operation: Overview

In the deterministic approach presented in Chapter 4, short control cycles are required (e.g., one minute) to closely follow the network behavior and quickly solve voltage rise and congestion issues due to the high variability of the wind resource. However, frequent adjustments of the set points of the active elements will be needed which in turn may affect the lifespan of these expensive assets (e.g., OLTC movements, finite cycles of charge/discharge for electrical storage devices). Also, the control cycles are limited by the time requirements of the data acquisition processes, the optimisation engine and the communication channels. Therefore, this chapter aims to provide an advanced NMS that allows the control cycle to be extended from one minute (as used in Chapter 4) to multi-minute control cycles.

In the deterministic approach, the set points are identified to solve only the issues at the start of the control cycle. These set points may not be appropriate throughout the entire cycle (e.g., due to wind gusts) and hence may lead to a violation of constraints. To cater for this, it is necessary to deploy predictive decision-making algorithms within the NMS to account for possible changes in network conditions (i.e., due to wind power) within the control cycle. The optimisation engine extends the deterministic approach by considering optimal set points that solve not only the network issues seen at the start of the control cycle but throughout it, hence catering for the stochastic nature of wind. This facilitates the adoption of multi-minute (instead of multi-second) control cycles, allowing a significant reduction in the volume of required control actions.

The intensity and probability of changes in wind power outputs are obtained by analysing historical data. This is used to find the K likely scenarios of wind power changes (more

details can be found in Section 5.4). This can be illustrated in the scenario tree presented in Fig. 5.1 for the no-transition scenario ($k=0$), scenarios of positive wind power transitions ($k>0$), i.e., increase from the observed value, and scenarios of negative wind power transitions ($k<0$), i.e., decrease from the observed value.

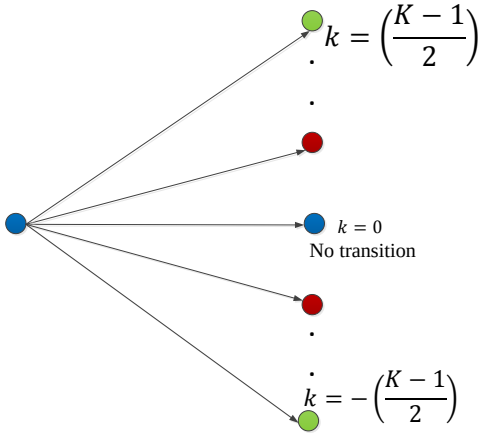

Fig. 5.1 Potential transition scenario tree of wind throughout a control cycle

Once the corresponding scenario tree is established, the various scenarios are considered by the optimisation engine as K simultaneous AC OPF problems linked by probabilistic and non-probabilistic constraints. Considering all the scenarios at once makes it possible to identify set points that satisfy all of them. This approach is known as Chance-Constrained Programming [122] which is an approach within Stochastic Programming. It should be noted that the risk-based OPF is adopted in the literature to minimise the cost of preventative and corrective control actions in transmission networks after relaxing security constraints (N-1 security constraint). The uncertainty refers to the circuit outages [123-124].

The non-probabilistic constraints aim to maintain voltages and power flows within limits to eliminate the issues that triggered the controller (at the start of the control cycle). The probabilistic constraints use the probabilities of the K scenarios to 'weigh' the voltage excess or thermal overloads for a given element. This overall value, which caters for all scenarios leading to issues, is then compared with a predefined risk level. Indeed, with the

probabilistic constraints, the OPF allows voltages to rise above the statutory limit and power flows through lines or transformers are also allowed to exceed their thermal capacities. However, the intensity of voltage excursions and congestion is controlled using the pre-defined risk level. In practice, the most adequate risk level will only be defined after assessing the performance of the NMS with different values as this depends on the particular characteristics of the network and the wind resource.

5.3 NMS Optimisation Engine

Similar to the deterministic NMS, at the start of each control cycle, the state of loads, firm/controllable generators and network elements (i.e., tap positions of OLTCs) for a given instant are sent from OpenDSS (in practice, the SCADA system) to the AC OPF-based NMS optimisation engine. To run the AC OPF, in addition to the states above, an identical network representation is considered (i.e., topology, impedances, nominal capacity of loads and generators, etc.).

The objective used in the deterministic approach is adopted here and the AC OPF formulation is given below; as a proxy to minimising DG curtailment, it maximises the total active power that could be injected by the controllable wind farms (set *N* indexed by *n*).

$$max \quad \sum_{n \in N} SP_n \left(\frac{p_n}{SP_n^0} \right) \tag{5.1}$$

where SP_n represents the new set point for the corresponding control cycle, p_n is the active power output and SP_n^0 is the original set point for the last control cycle.

With this objective function, the OPF will find the most adequate set point (via Equation (5.2)) that harvests as much as possible the available wind resource (active power injection is divided by the set point used throughout the last control cycle). In practice, the available wind resource can be obtained by either directly measuring the wind power

output or indirectly using wind speed measurements and the power characteristics of the wind turbines.

$$0 \leq SP_n \leq 1 \quad \forall n \in N \tag{5.2}$$

The optimisation will be carried out in a framework that considers the information available at the decision making time and the K scenarios (indexed by k) throughout the control cycle. Each scenario, obtained from a statistical analysis of historical wind data, has a probability and a magnitude of the potential wind power change (more details in Section 5.4). These *K* changes (relative to nominal capacity) are denoted by $\omega_{g,k}$ and $\omega_{n,k}$, for firm generation (set G indexed by g) and controllable DG plants (set *N* indexed by *n*), respectively, and with a probability $Pr(k)$.

The objective is also subject to a range of constraints including those related to the general AC OPF constraints (i.e., Kirchhoff's voltage law and power balance), the non-probabilistic constraints for the *k*=0 scenario and the probabilistic constraints for all the scenarios. These constraints will be presented in the following subsections.

5.3.1 General AC OPF Constraints

Active, $f_{l,k}^{(1,2),(P)}$, and reactive power, $f_{l,k}^{(1,2),(Q)}$, injections at the start and end buses (denoted as 1 and 2) for each line and each transformer are calculated according to the standard Kirchhoff voltage law expressions, as presented below. The flows are found for all the scenarios of wind power changes ($k \in K$). In contrast, the deterministic approach only considers the wind power scenario observed at the start of the control cycle (no change) (k=0).

$$f_{l,k}^{(1,2),(P)} = f_{l,k,KVL}^{(1,2),(P)}(\boldsymbol{V}, \boldsymbol{\delta}) \quad \forall l \in L, \forall k \in K \tag{5.3}$$

$$f_{l,k}^{(1,2),(Q)} = f_{l,k,KVL}^{(1,2),(Q)}(\boldsymbol{V}, \boldsymbol{\delta}) \quad \forall l \in L, \forall k \in K \tag{5.4}$$

where $f_{l,k,KVL}^{(1,2),(P)}(\boldsymbol{V},\boldsymbol{\delta})$ and $f_{l,k,KVL}^{(1,2),(Q)}(\boldsymbol{V},\boldsymbol{\delta})$ are the standard KVL expressions at each possible scenario (more details are available in Section 4.5.1).

Also, the import/export real and reactive powers $(p_{x,k}, q_{x,k})$ at the interface with the upstream grid x (X, set of external connections) are found for all the K scenarios and their values should be within limits $\left(p_x^{(-,+)}, q_x^{(-,+)}\right)$. The modelling adopted to control the tap ratio τ_l for the OLTCs and the corresponding integer tap position m_l is the same as used in the deterministic approach. More details can be found in section 4.5.2.

The formulation in the deterministic approach to control the power factor of the controllable DG plants is adopted here. Indeed, the controllable DG units can operate at different power factor $\emptyset_n$, making reactive power "dispatchable" [13] within the MVA capability of the DG plants S_n^{rated}, while the firm generation is operating at fixed power factor angle $\emptyset_g$. More details are available in section 4.5.3. It should be noted that all the set points ($SP_n, \tau_l, \emptyset_n$) found by the optimisation engine are unique; in other words, they are not functions of k.

KCL describes the balance of real and reactive power at each bus (set *B* indexed *b*), and for each scenario k, according to Equations (5.5) and (5.6), respectively. Here, the potential wind power changes, $\omega_{g,k}$ and $\omega_{n,k}$, are incorporated in the balance equations by multiplying the corresponding nominal capacities of the DG plants (p_g^{rated} and p_n^{rated}). These wind power changes are applied to both firm and controllable DG plants.

$$\sum_{n\in N|\beta_{n=b}} SP_n\left(\left(\frac{p_n}{SP_n^0}\right)+\ \omega_{n,k}p_n^{rated}\right)+\sum_{g\in G|\beta_{g=b}}\left(p_g+\ \omega_{g,k}p_g^{rated}\right) + \sum_{x\in X|\beta_{x=b}} p_{x,k} = d_b^P + \sum_{l\in L|\beta_l^{(1,2)}=b} f_{l,k}^{(1,2)(P)} \tag{5.5}$$

$$\sum_{n\in N|\beta_{n=b}} SP_n\left(\left(\frac{p_n}{SP_n^0}\right)+\ \omega_{n,k}p_n^{rated}\right)tan(\emptyset_n) + \sum_{g\in G|\beta_{g=b}}\left(p_g+\ \omega_{g,k}p_g^{rated}\right)\ tan(\emptyset_g) + \sum_{x\in X|\beta_{x=b}} q_{x,k}\ = d_b^Q + \sum_{l\in L|\beta_l^{(1,2)}=b} f_{l,k}^{(1,2),(Q)} \quad (5.6)$$

where β_u maps the location of each network element ($u \subset \{n, g, x, l\}$) to its associated bus and $d_b^{(P,Q)}$ are the active and reactive demand at the same bus.

5.3.2 Non-Probabilistic Constraints (Scenario *k*=0)

Even if wind power changes are likely throughout the control cycle, it is crucial to ensure that the voltage and/or congestion issues seen at the start of the cycle are effectively eliminated. To implement this, the corresponding wind power output (scenario *k*=0) has to be considered in a deterministic fashion (as discussed in Chapter 4).

Thus, the voltage magnitude at bus b (V_b) should be within the statutory limits $V_b^{(-,+)}$ and the apparent start/end power flows through lines and transformers should be limited to their corresponding thermal capacity f_l^+.

$$V_b^- \le V_{b,k=0} \le V_b^+ \quad \forall b \in B \quad (5.7)$$

$$\left(f_{l,k=0}^{(1,2),P}\right)^2 + \left(f_{l,k=0}^{(1,2),Q}\right)^2 \le (f_l^+)^2 \quad \forall l \in L \quad (5.8)$$

5.3.3 Probabilistic Constraints (All Scenarios)

While it is crucial to solve the network issues seen at the start of the control cycle, it is also essential to incorporate the effects of potential changes in wind power output (during the control cycle). Consequently, in addition to the previous constraints, probabilistic

inequality constraints are incorporated to tackle the uncertainties brought about by wind power.

With the probabilistic constraints, the OPF allows voltages to rise above the statutory limit and power flows through lines or transformers are also allowed to exceed their thermal capacities. However, the intensity of voltage excursions and congestion is controlled using a pre-defined risk level ε, as given in Equation (5.9) for voltage excursions and in Equation (5.10) for thermal violations:

$$\sum_{k\in K} \Delta_{b,k}^{V}\ Pr(k) \leq \varepsilon \qquad \forall b \in B \tag{5.9}$$

$$\sum_{k\in K} \Delta_{l,k}^{S}\ Pr(k) \leq \varepsilon \qquad \forall l \in L \tag{5.10}$$

where $\Delta_{b,k}^{V}$ is voltage excursion at bus b in scenario k and $\Delta_{l,k}^{S}$ is the percentage of thermal violation for branch l in scenario k, where its calculation is given in (5.11).

$$\Delta_{l,k}^{S} = \begin{Bmatrix} 0\,, & f_{l,k}^{(1,2)} \leq f_l^{+} \\ \dfrac{f_{l,k}^{(1,2)} - f_l^{+}}{f_l^{+}}, & f_{l,k}^{(1,2)} > f_l^{+} \end{Bmatrix} \forall l \in L \tag{5.11}$$

Large values of ε (close or equal to 1) mean that constraints (5.9) and (5.10) will accept all types of voltage and congestion violations. This will make the non-probabilistic constraints (5.7) and (5.8) dominant, forcing the set points to only be optimised for scenario k=0. Therefore, irrespective of the adopted risk levels (ε), the risk-based approach can perform, at worst, as the deterministic approach. In contrast, zero risk level (ε=0) prevents thermal overloading and voltage rise issues for the scenario of maximum potential changes in wind power output (during the control cycle) even with low probability of occurrence. The extent to which the risk-based performance can be improved will depend on the selection of the risk level, as well as the characteristics of the network, demand and

wind resource. It should be highlighted that voltage excursions and congestion throughout the control cycle can be controlled using different values of risk level, i.e., a voltage risk level and thermal risk level. For simplicity, the same risk level for both congestion and voltage is used.

In order to protect the system from unexpected failure, emergency current ratings for lines and transformers (i.e., 1.30 p.u.) are assigned as a boundary for acceptable overloading levels regardless of the likelihood of occurrence. Thus, the OPF will prevent the congestion of any branch over its emergency current rating for all scenarios. Moreover, to avoid congestion beyond emergency limits, a further constraint is also included, as given in Equation (5.12).

$$\left(f_{l,k}^{(1,2),P}\right)^2 + \left(f_{l,k}^{(1,2),Q}\right)^2 \leq \left(f_l^{emergency}\right)^2 \quad \forall l \in L \tag{5.12}$$

In addition, due to the BS EN50160 standard [59] adopted in the UK, voltages can never exceed 10% of nominal.

$$V_{b,k} \leq 1.1 \quad \forall b \in B \tag{5.13}$$

5.4 Production of the Scenario Tree

Because of the short time horizon needed by the NMS (control cycles from 1 to 15 minutes), it is assumed that the availability of the wind resource remains constant (also known as persistence forecasting) [125]. However, the potential changes or errors, known here as *transitions*, need to be computed so that the corresponding uncertainties are taken account of.

This section presents the methodology used to produce the scenario tree of wind power changes and the corresponding probabilities and magnitudes. Because of the short time horizon needed by the NMS (control cycles from 1 to 15 minutes)

For this, 1-min resolution historical normalised wind power data is statistically analysed using different time periods, such as 1, 5 and 15 minutes. These time periods will correspond to the control cycles to be adopted by the NMS optimisation engine.

First, the 1-min resolution wind power profile is segmented by the length of the defined time period. The magnitudes (changes in normalised wind power) of the intra-segment transitions are then calculated. For instance, for a period of 5 minutes, segments will have 5 transitions: min 0 to min 1, min 0 to min 2, and so on. The corresponding magnitudes of these intra-segment transitions are then stored in a pool for the whole historical wind power profile.

The number of scenarios K has to be defined. However, this number has to be a trade-off between a better representation of potential wind power changes (more scenarios) and the corresponding computational burden. It also has to be an odd number in order to consider the scenario k=0.

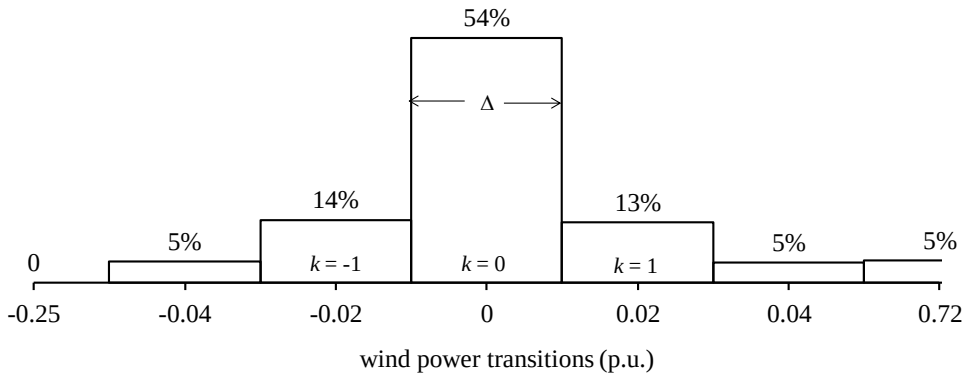

Fig. 5.2 Probability distribution of 1-min wind power data using a 5-min time period

The distribution produced by the pool of transitions is divided into K 'bins' as shown in Fig. 5.2. The mean value of each bin will correspond to the magnitude of the scenario. The size of each bin (Δ) has to be carefully determined to reduce errors due to approximation. Adopting large values leads to more transitions inside a single bin (e.g., scenario k=0), thus hiding actual changes.

In addition, the production of scenarios (intensity and probability) has to be undertaken according to the wind power output, to better represent the potential changes. For instance, the potential changes for wind power below 0.1 p.u. might not be the same as for when the power injections are as high as 0.8 p.u. Also, applying the same statistical uncertainty information (magnitude and probability of the persistence forecast errors) to any predicted wind power value may lead to scenarios which cannot physically occur, i.e. a negative-valued power output level or output beyond the wind farm capacity (e.g., a forecast error of +25% for a wind power of 0.9 p.u.). To tackle this issue, the 'binning' process is conducted considering different subsets of the pool of transitions. Each subset will contain only those transitions that depart from a given range of wind power output (e.g., 0.8p.u.-0.9 p.u.). Fig. 5.3 illustrates the process of obtaining the scenarios of wind power changes at the start of the control cycle.

To illustrate the process, the normalised wind power profile for a site in England is analysed. This data corresponds to February 2010 and has a 1-min resolution. The pool of transitions considers a control cycle of 5 minutes and ten different subsets for wind power output ranges at the start of each defined period [0-0.1], (0.1-0.2], …, (0.9-1] p.u. In this work, seven scenarios are considered: one without changes (k=0), three with positive changes (k=1, 2, 3) and three with negative changes (k=-1,-2,-3). Due to the characteristics of the historical data, Δ was considered to be 0.02 p.u. (or 2% of wind power change relative to nominal capacity). Thus, the bins are (-min. transition, -0.05), [-0.05, -0.03), [-0.03, -0.01), [-0.01, 0.01), [0.01, 0.03), [0.03, 0.05) and [0.05, max. transition). The minimum and maximum transition values will depend on the corresponding subset. The corresponding magnitudes for the scenarios are the middle of each bin.

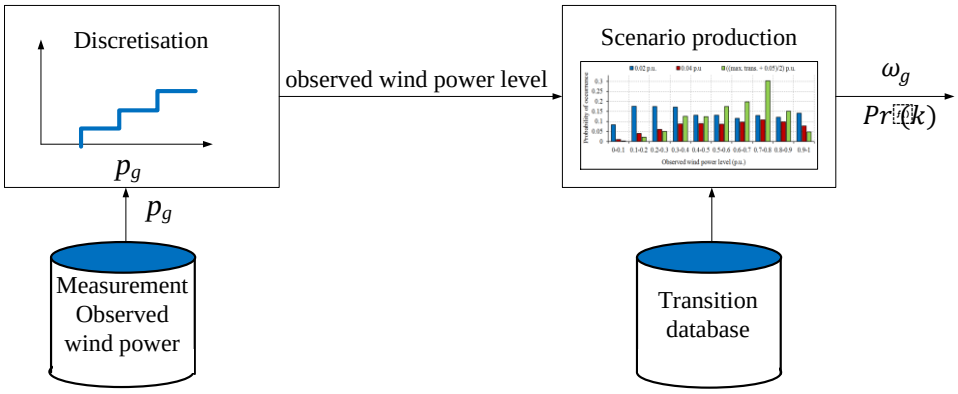

Fig. 5.3 Block diagram of the scenario production at each control cycle

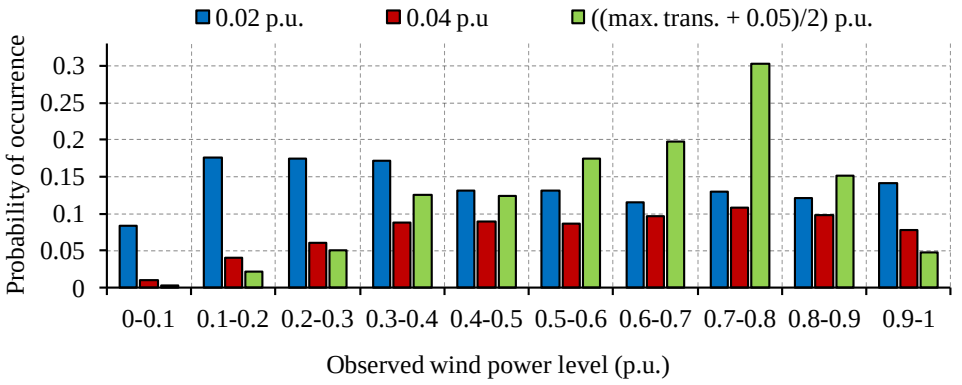

(a)

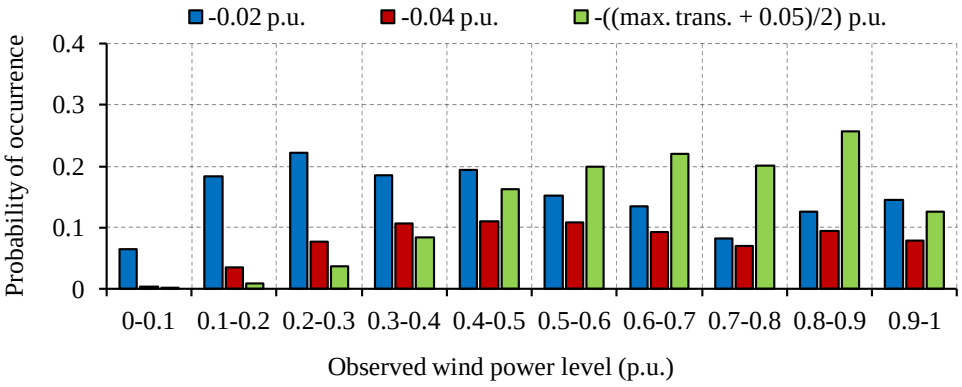

(b)

Fig. 5.4 Probability density function using a 5-min time period for (a) the positive wind power transitions and (b) the negative wind power transitions

The resulting probability density function (pdf) for the positive transitions per wind power range at the start of the control cycle is shown in Fig. 5.4 (a). This pdf (similar to the negative transitions at Fig. 5.4 (b)) clearly highlights the importance of the differentiation

per wind power range. Hence, at each control cycle, the NMS optimisation engine obtains the possible wind power surplus transitions. For instance, if the wind power at the start of the control cycle lies in the range [0.8-0.9) p.u., then the optimisation engine considers that the available wind power may increase during the next control cycle by 0.02, 0.04 and 0.10 p.u. with occurrence probabilities of 12%, 10% and 15%, respectively.

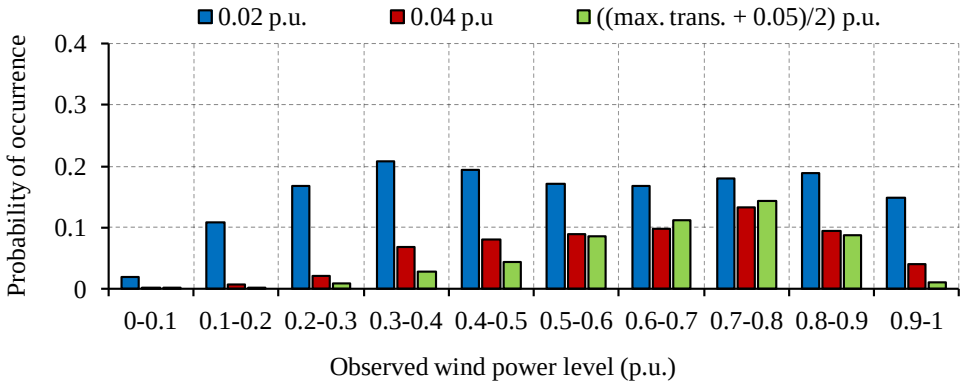

Fig. 5.5 Probability density function for the positive wind power transitions using a 1-min period

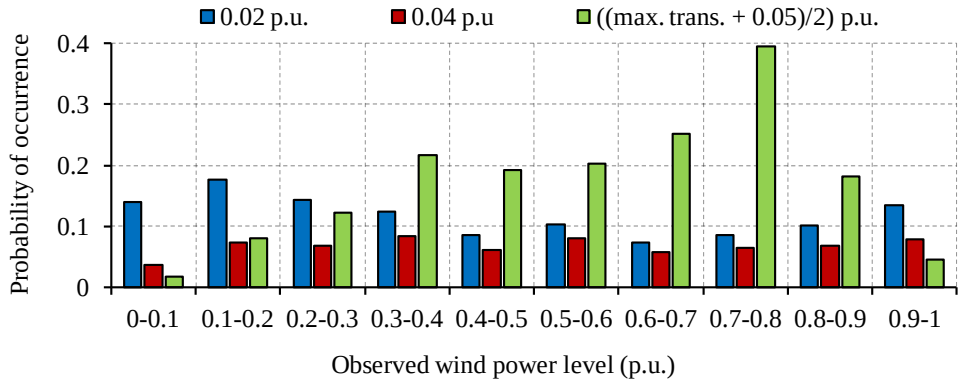

Fig. 5.6 Probability density function for the positive wind power transitions using a 15-min period

To show the effect of the control cycle, the probability density functions for the positive transitions per wind power range at the start of the control cycle are produced for control cycles of 1 minute and 15 minutes, as presented in Fig. 5.5 and Fig. 5.6, respectively. It can be seen that, as the control cycle increases from 1 minute to 15 minutes, the frequency of positive wind power transitions per wind range is increased. For instance, if the wind

power at the start of the control cycle of 1-min lies in the range [0.8-0.9) p.u., then the probabilities that the wind power may increase in the next control cycle by 0.02, 0.04 and 0.10 p.u. are 19%, 10% and 9%, respectively. In contrast, for a control cycle of 15 minutes, the probabilities that the wind power may increase in the next control cycle by the same intensity are 10%, 8% and 19%, respectively. This highlights the challenges of managing network constraints in the deterministic approach for a multi-minute control cycle.

In this work, it is assumed that all the wind farms are driven by the same wind profile since all the DG plants are located in a small geographical area. However, it should be noted that, although the scenario generation is based on a single wind profile, the modelling of the NMS optimisation is generic to different wind profiles.

5.5 Simple Case Study: Congestion and Voltage Management

The NMS is applied to a UK 33 kV network in the north-west of England, as presented in Chapter 4. A single line representation of the network is given in Fig. 5.7. To demonstrate the real-time operation of the NMS controller in managing congestion and maintaining voltage within statutory limits ($\pm$6% of nominal), controllable DG is connected at buses 205 and 206 with capacities of 20 MW and 15 MW, respectively; this creates significant congestion at line 204-205 (thermal capacity of 23 MVA) and voltage rise at bus 205. The new controllable DG units are operating with unity power factor. To illustrate the risk-based NMS approach, first the simpler deterministic NMS (optimal decision making based on measurements taken at the start of the control cycle) will be presented. The analysed period is 60 minutes with a 5-min control cycle (sufficient to assess the multi-minute control cycle performance).

The set points produced by the AC OPF, for both deterministic and risk-based approaches, are applied simultaneously but considering a response of one minute to mimic the corresponding mechanical and communication delays of the controllable devices.

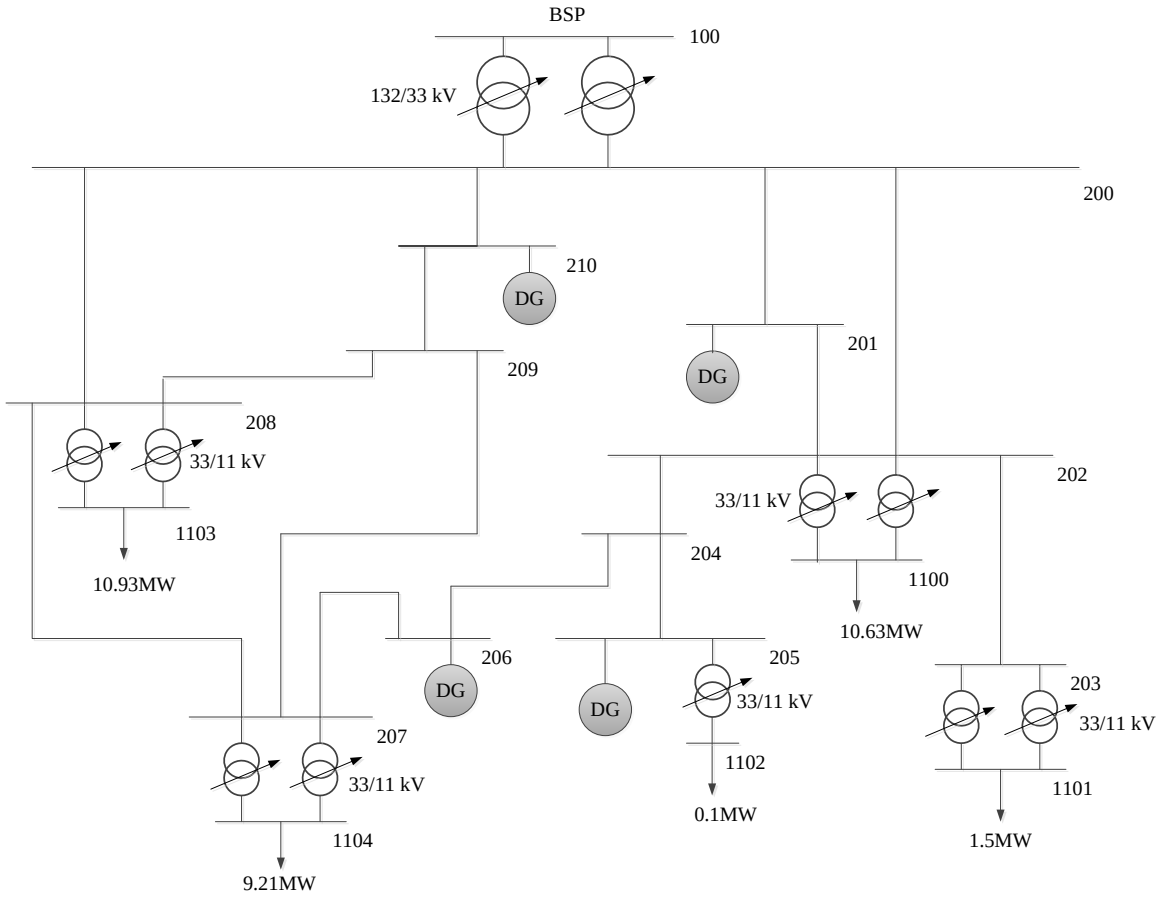

Fig. 5.7 A 33 kV UK network in the north-west of England

5.5.1 Deterministic Approach

In the deterministic approach, optimal set points are identified to solve network issues seen at the start of the control cycle but are adopted throughout the same cycle. To avoid potential issues (such as wind gusts), multi-second control cycles can be adopted (as shown in [18, 20, 26]). However, this very short control cycle would increase control actions, accelerating the aging of elements such as OLTCs and even the wind turbines (due to pitch angle control). In addition, delays due to the mechanical response of elements as well as communication delays limit the practical length of the control cycle. Based on this, the shortest control cycle considered in this work is 1 minute.

First, a deterministic curtailment-only NMS scheme is applied. Fig. 5.8 shows the 1-min

resolution loading of line 204-205, the voltage profile at bus 205 and the set point of the wind farm at bus 205. The other controllable DG unit (206) is not curtailed by the NMS during this period. At the start of the simulation, the controller is activated to simultaneously solve congestion (an excess of 17%) and voltage rise (1.07 p.u.).

Based on the optimisation engine, the NMS actions the wind farm at bus 205 to change its set point (SP_{DG_205}) from the initial 100% (1.00 p.u.) to 63%. This setting is retained throughout the control cycle. At minute 5 (the next control cycle), there is no constraint violation. However, given that curtailment has been applied to the wind farm, the NMS triggers the optimisation to find a new set point that increases the harvesting. The set point is improved at minute 6 to 97%.

To explore the benefits of additional flexibility, the OLTC at the BSP is controlled. As can be seen in Fig. 5.9, during the first three control cycles the tap ratio increases (i.e., secondary voltage decreases) to minimise curtailment whilst maintaining the voltage at bus 205 within the statutory limits. In addition, when voltage is the main issue, the DG set point tends to be much higher compared to the curtailment-only scheme, e.g. at minute 30 the set point is improved from 53% to 68%.

Although the deterministic approach does improve network performance, the voltage rise issues are not managed effectively in the curtailment-only scheme and congestion exists for many minutes for both schemes. This is because the optimal settings solve the network issues at the start of the 5-min control cycle but disregard the potential wind power changes within the cycle. For instance, in Fig. 5.9 the set point at minute 15 is reduced to 91% to tackle congestion. At the time of effective control action at minute 16, the wind resource increases throughout the control cycle and the line is overloaded again by 21%. The above illustrates the need to incorporate the potential wind power changes into the NMS optimisation engine to hedge against undesirable scenarios that may lead to the violation of network constraints.

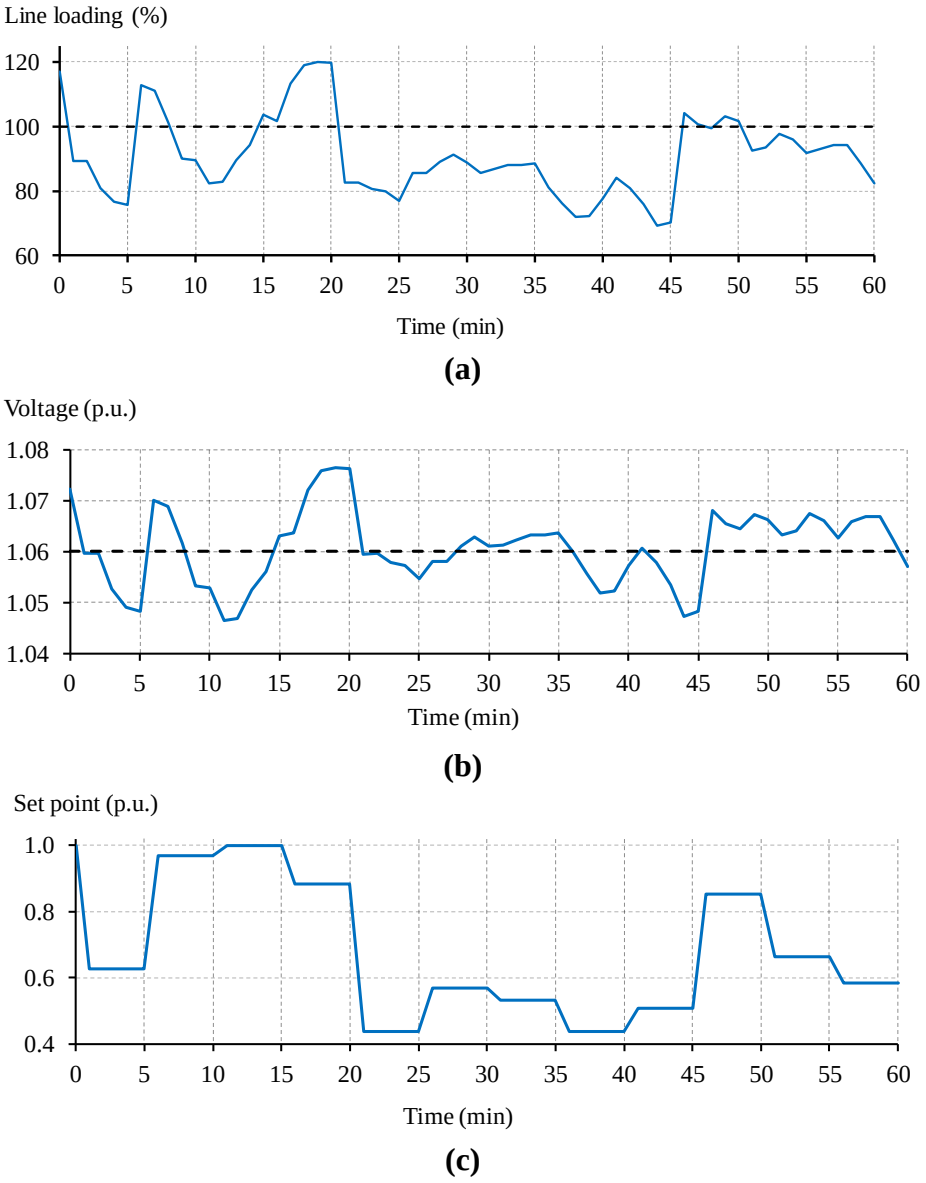

Fig. 5.8 Deterministic curtailment-only NMS using a 5-min control cycle (a) loading of line 204-205 (%) (b) voltage at bus 205 p.u and (c) set point for the wind farm at bus 205 p.u.

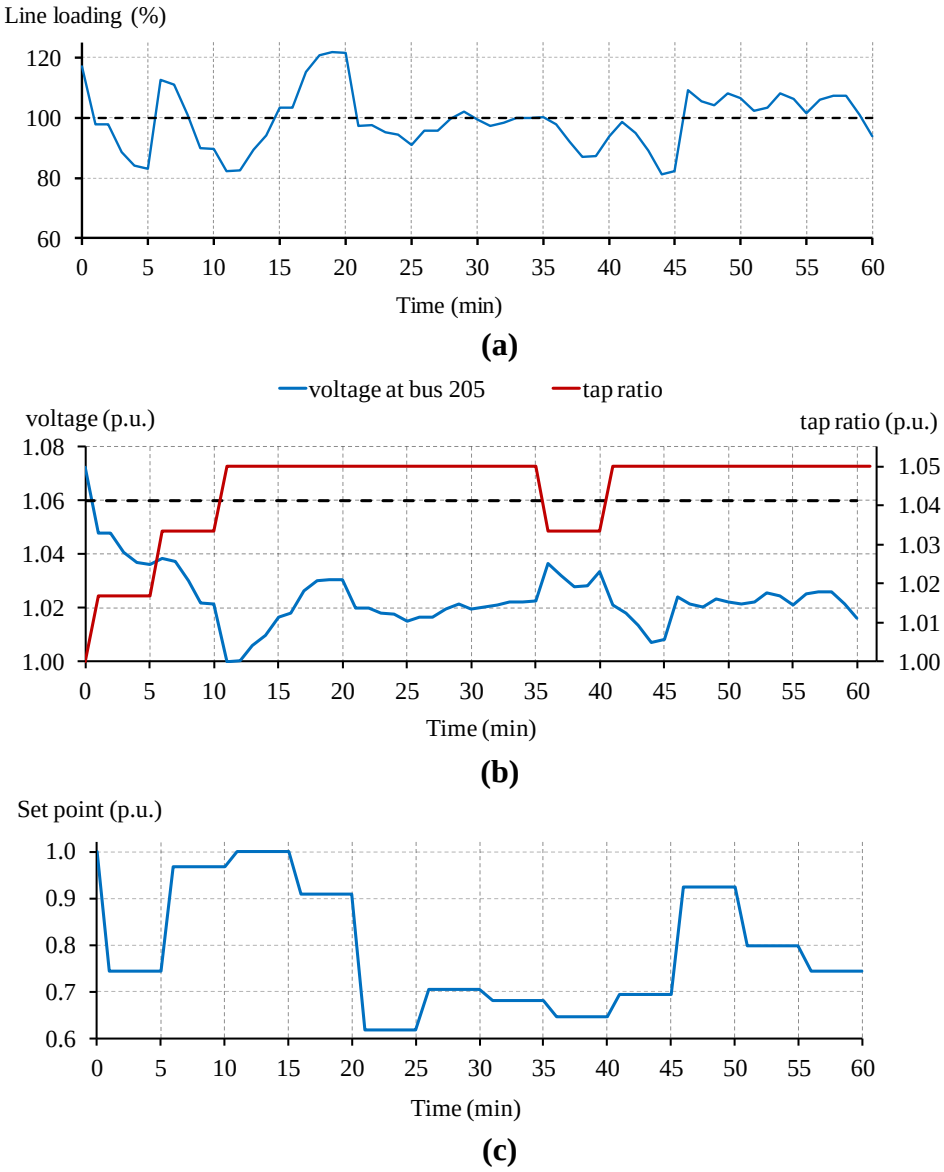

Fig. 5.9 Deterministic curtailment and OLTC NMS using a 5-min control cycle (a) loading of line 204-205 (%) (b) voltage at bus 205 p.u. and tap ratio and (c) set points for the wind farm at bus 205 p.u.

5.5.2 Risk-Based Approach

In order to use the risk-based NMS, first a risk level has to be adopted. This value has to be found on a case-by-case basis after performing multiple analyses. Here, for simplicity, a value of 0.5% (0.005) is adopted. As mentioned previously, seven scenarios of wind power changes are considered.

The intensity and probability of the seven wind power changes will be updated for each control cycle based on the statistical analysis of historical data. To illustrate this, all corresponding intensities and probabilities of scenarios at minute 15 (the start of the fourth control cycle) are shown in Table 5.1. Based on the scenarios at the start of each control cycle, the optimisation engine will find the best set points to minimise curtailment whilst managing network constraints within the specified risk level (ε).

Table 5.1: Wind Power Scenarios at Minute 15

k	-3	-2	-1	0	1	2	3
ω_k	0.4	0.04	0.02	0	0.02	0.04	0.15
Pr(k)	20.1	7	8.2	10.6	13.0	10.8	30.3

Considering both curtailment and OLTC, Fig. 5.10 shows scenarios of thermal overloading at line 204-205 (the other scenarios do not lead to overloads). The resulting risk for a given control cycle (i.e., the sum of overloads multiplied by the corresponding probability of the scenario) must be lower than the specific risk level. For instance, for the fourth control cycle, congestion only occurs with scenario k=3, exceeding the limit by 1.65%. This, multiplied by its probability (30.3%), results in an overall risk below 0.005. It should be noted that, when the wind power value is close to unity (e.g., in the fifth control cycle), thermal overloading for all scenarios is almost eliminated.

Fig. 5.11 shows the usage of line 204-205 and the optimal DG settings produced by the risk-based NMS. Compared to the deterministic approach, it is clear that congestion issues have been reduced dramatically in frequency (from 26 to 5 minutes) and in magnitude. For the latter, during the fourth cycle, the overload reduced from 21% to 4%. This was achieved by considering that the potential wind power increase of 0.15 p.u. (of nominal capacity) had a 30.3% chance of occurring. As for voltages, although issues were also solved deterministically, the number of tap changes reduced slightly (two tap changes).

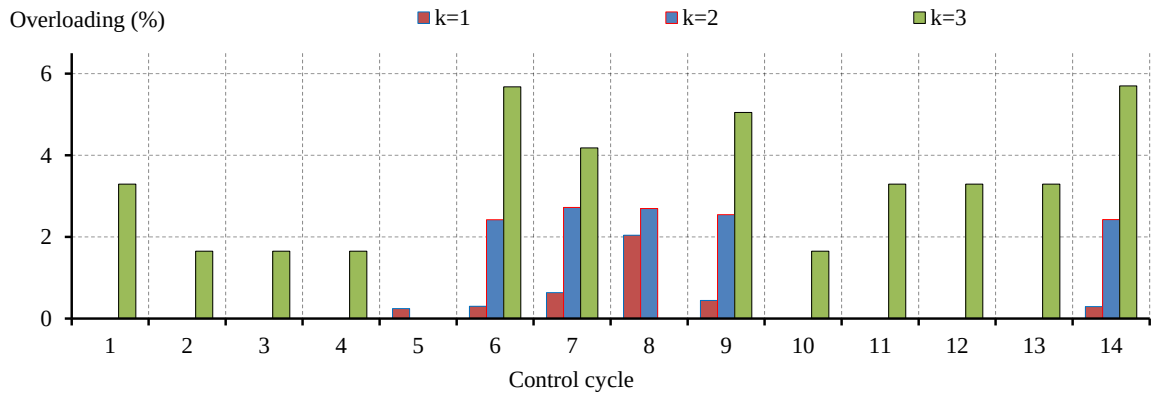

Fig. 5.10 Thermal overloading for line 204-205 (%) for curtailment and OLTC NMS using a 5-min control cycle

In this case, using a 5-min control cycle, the risk-based approach also allows a reduction in the volume of control actions from the DG plant at bus 205. The total variation (TV) of the DG set point, defined as the sum of absolute changes in the set points [126], is reduced by a third when compared to the deterministic approach (from 1.5 to 1.0 p.u.). In a multi-minute framework, the risk-based approach provides effective management of network constraints compared to the deterministic approach (i.e., conservative set points) and using smaller volumes of control actions. However, this improvement in the management and the control actions is at the expense in the increase of curtailment. As shown in Fig. 5.11, the DG set point for the risk-based approach is in general below that of the deterministic approach.

It is important to highlight that the performance of the risk-based NMS depends on the specified risk level. Lower values will force the probabilistic constraints to be more restrictive of congestion and voltage rises in all scenarios. Higher values, however, will relax the probabilistic constraints, potentially resulting in increased congestion and voltage rises that at worst (i.e., $\varepsilon = 1.0$) are equal to the deterministic approach.

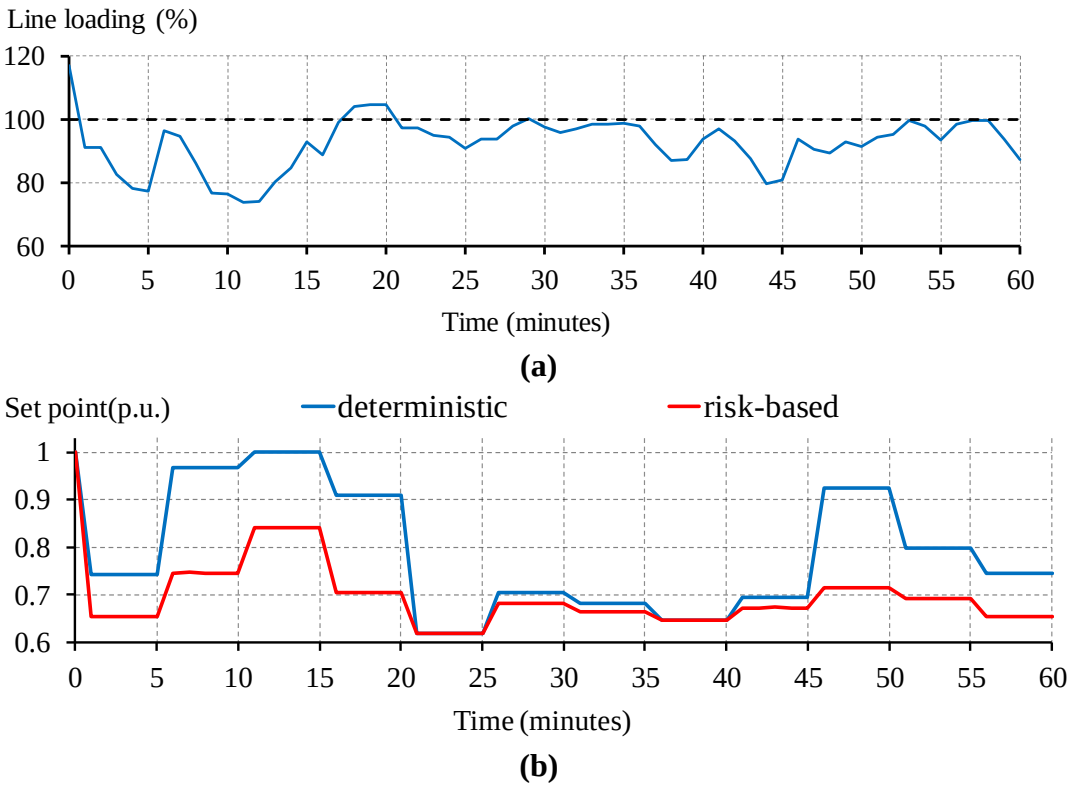

Fig. 5.11 Curtailment and OLTC NMS using a 5-min control cycle (a) loading of line 204-205 p.u. using a risk-based approach (ε=0.005) and (b) deterministic and risk-based set points for the wind farm at bus 205 p.u.

5.6 Full Case Study

This section demonstrates the performance of the NMS optimisation engine, considering the usage of different control cycle lengths, ANM schemes and risk levels (ε). Moreover, to produce a more complex environment, the network previously used will now be studied, considering a significantly higher wind penetration.

The full case study used in Section 4.9 to demonstrate the operation of the deterministic NMS is also used in this section considering the same capacities of DG plants. As discussed in Section 4.9, the multi-period AC OPF planning tool developed in [13] shows that an extra 53 MW (a 135% increase in DG capacity) could be connected (5, 17, 22 and 9 MW at buses 201, 205, 206 and 210, respectively). The connection of this capacity without control would not be possible in practice since it overloads lines 200-201, 204-205 and

200-210 beyond 25% of their thermal capacities. In addition, the voltage at bus 205 would exceed the upper limit for more than a quarter of the time. Similar to the previous section, 1-min resolution simulations for the first week of February 2010 are carried out, applying different control solutions to this new generation portfolio (53 MW of controllable DG units). All the generators are capable of operating with power factor between 0.95 inductive and capacitive according to UK requirements [121].

5.6.1 Performance Assessment

The metrics adopted in Chapter 4 are applied to assess performance during the analysed period. Briefly, to assess the effectiveness of the approach in terms of managing congestion, two metrics are used: total duration of overloads (in minutes); and the longest duration and the corresponding average magnitude of overloads larger than 15%. For voltages, the BS EN50160 [59] standard (95% of 10-min voltage magnitudes must be within $\pm$6% of nominal) is used to appraise the NMS performance against voltage rise problems. Further, the curtailed energy is also computed.

Two metrics are used to quantify the volume of control actions from the OLTCs and the DG plants: (1) the number of BSP tap changes and (2) the total variation of the DG set points, calculated as the sum of absolute changes [126]. The use of these metrics could indicate how control would affect the lifespan of the controllable elements.

Table 5.2 compares the performance of the deterministic and the risk-based approaches (with different risk levels) for the full NMS schemes (with OLTC and power factor control). Three control cycle lengths are investigated: 1, 5 and 15 minutes. Results for thermal overloads and voltages are presented for line 200-201 and bus 205, respectively, as they were the most affected. Adopting shorter control cycles allows more frequent monitoring of the network status and closer following of the variability of wind resource. This results in better management of congestion and voltages. For instance, in the deterministic approach using a 1-min control cycle, the longest overload (average of 19%) lasts for only 1 minute. These figures rise to 24%, lasting for 12 minutes, using a 15-min

control cycle. However, this improvement is at the expense of the control actions: the number of BSP tap changes and TV are, respectively, 10 and 5 times greater for a 1-min cycle.

The risk-based NMS always manages congestion and voltage excursions better than the deterministic approach. This effective network management allows the adoption of multi-minute control cycles to reduce the volume of control actions. For example, in the full NMS scheme, the effectiveness of the risk-based approach to manage congestion using a 5-min control cycle and a 0.005 risk-level is similar to the effectiveness of the 1-min control cycle of the deterministic approach. Consequently, it allows the adoption of a 5-min control cycle which in turn dramatically reduces the number of tap changes and the TV of DG plants by 80% and 62%, respectively. The risk level also has a significant influence on performance. The full NMS scheme with $\varepsilon = 0.005$ manages to significantly reduce congestion issues for all control cycles when compared to the deterministic approach. Tighter risk levels result in fewer and smaller congestion issues and control actions, but increases the curtailed energy.

Table 5.2: Deterministic and Risk-Based Full NMS (Curtailment + OLTC + PF control) Performance Metrics

Control Cycle	NMS Approach		Performance metrics					
			Total Duration of Overloads for 200-201 (min)	Longest Overload >15% for 200-201 (min, avg overload)	EN50160 Compliance of Bus 205 (%)	BSP Tap Changes	TV for all DG	Curtailed Energy (%)
15-min	Deterministic		938 min	12 min, 24%	95 (yes)	33	13	10.3
	Risk-Based (**ε**)	0.005	569 min	5 min, 20%	96 (yes)	29	10	13.5
		0.001	235 min	5 min, 20%	97 (yes)	15	9.5	14.8
		0	160 min	5 min, 20%	98 (yes)	15	9.3	15.4
5-min	Deterministic		903 min	4 min, 23%	96 (yes)	89	32	10.1
	Risk-Based (**ε**)	0.005	444 min	2 min, 18%	96 (yes)	59	26	13.3
		0.001	143 min	2 min, 16%	96 (yes)	43	24	14.6
		0	76 min	2 min, 16%	98 (yes)	33	23	15.3
1-min	Deterministic		727 min	1 min, 19%	96 (yes)	305	68	10.2
	Risk-Based (**ε**)	0.005	383 min	None	97 (yes)	300	66	11.8
		0.001	88 min	None	97 (yes)	101	65	13.4
		0	28 min	None	98 (yes)	69	57	14.2

5.6.2 Risk-Based vs Deterministic With Conservative Thresholds

The conclusions drawn from Section 4.9.5 are that the adoption of a conservative thermal threshold (below 100%) in the deterministic approach also allows the effective management of power flows within limits and avoids any overloading issues that could result from changes in wind power throughout the control cycle (from that observed at the decision making time). However, this is at the expense of the volume of curtailment. Therefore, this section aims to compare the deterministic approach (by incorporating thermal thresholds presented in Section 4.9.5) with the risk-based approach in terms of network management and volume of curtailment.

In order to do so, both control approaches are demonstrated using the 33 kV network considering multiple DG plants. Also, the full NMS scheme of controlling OLTC, DG power factor and generation curtailment as a last resort is adopted for both control approaches, considering a control cycle of 1 minute. A thermal threshold of 90% is adopted in the deterministic approach (γ=0.9), while a zero risk level ($\varepsilon = 0$) is used in the risk-based approach.

Fig. 5.12 shows the usage of line 200-201 and the overall harvested wind power from all the controllable DG plants (proxy for presenting unique set points for all the DG plants) obtained from both control approaches for the first hour on 1st February 2010. It can be seen from the figure that the power flows are managed below thermal capacity (effective management) for both control approaches. However, the risk-based approach provides greater harvested wind power for most of the time and, therefore, better line usage in comparison to the deterministic approach using a 90% thermal threshold. For example, from minute 18 to minute 22, the risk-based approach gives a higher harvested wind power of 73% compared to 60% in the deterministic approach using thermal thresholds whilst effectively solving congestion (no thermal violations).

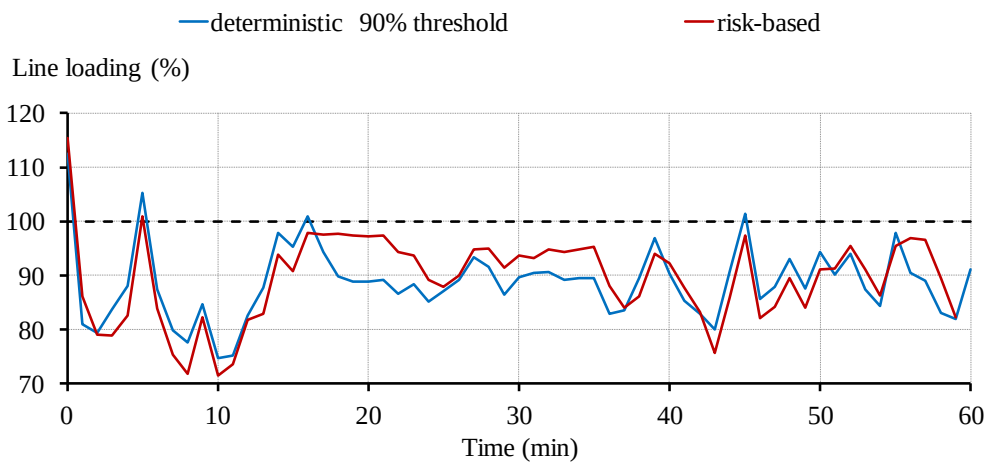

(a)

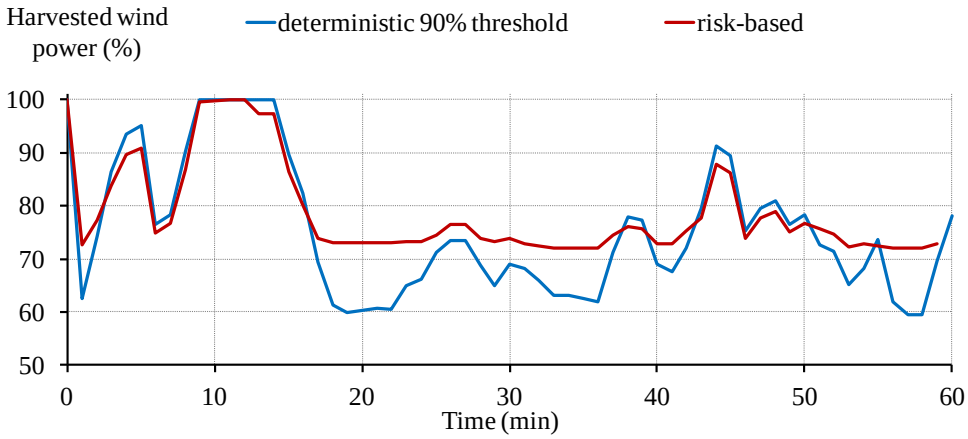

(b)

Fig. 5.12 Full NMS using a 1-min control cycle using the deterministic approach with threshold (γ=0.9) and the risk-based approach (ε=0) (a) loading of line 200-201 and (b) harvested wind power from all controllable DG in (%)

Indeed, the set points in the risk-based approach using a zero risk level are determined according to the scenario of maximum wind power transition, so that even if this scenario occurs, the obtained set points will maintain the voltages and power flows within limits. However, the maximum wind power transition depends on the level of the observed wind

power. It can be seen from the wind power change scenarios presented in Fig. 5.5 (for a control cycle of 1-min) that the wind power at minute 18 is 1 p.u. (rated output), meaning that there is no possible wind power increase from the observed value during the control cycle. Therefore, the decision to make the power flows throughout the lines below 100% of thermal capacity is only based on the observed values (no scenarios of wind power changes). In contrast, considering a 90% threshold in the deterministic approach, the set points are found to keep power flows below the thermal threshold (90% of thermal capacity), neglecting the wind power levels. Therefore, higher levels of unnecessary curtailment may be applied.

The comparison is extended for the first week of February 2010 and considering the 1-min control cycle. The results show that the power flow throughout the lines 200-210 and 200-201 are effectively managed for both control approaches. Indeed, overloading only occurs for 0.4% and 0.2% during the analysed week for the risk based (zero risk level) and the deterministic approach (90% threshold), respectively. However, the volume of energy curtailment in the risk-based approach using a zero risk-level is 14.2%, which is much lower than that obtained with the deterministic approach using thermal thresholds (17%). Also, it should be highlighted that larger thermal thresholds will be needed for longer control cycles to avoid congestion that could result from the changes in wind power. This in turn would result in a much larger volume of curtailment than the risk-based approach using zero risk level.

Also, it should be highlighted that the settings of voltage thresholds are more challenging than the settings of thermal thresholds since large search spaces have to be trialed before determining the best values. In contrast, in the risk-based approach, a zero risk level can simply be adopted. However, the production scenarios required in the risk-based approach make it more complex than the deterministic approach using thresholds.

5.7 Summary of Chapter 5

This chapter demonstrates the effectiveness of using a risk-based AC OPF as the decision making engine of an advanced distribution Network Management System (NMS) aimed at maximising the harvesting of wind energy whilst tackling congestion and voltage issues, as well as the effects of wind uncertainty. The approach allows the adoption of multi-minute control cycles, thus reducing the volume of control actions from OLTCs and DG plants. The framework allows a detailed investigation of the benefits and impacts of adopting different control cycles, quantifying in particular the compliance of voltages with the EN50160 standard, congestion levels, capacity factor of wind farms and, crucially, volume of control actions. High-resolution operational aspects were implemented to optimally control OLTCs, DG power factor and DG curtailment (as a last resort) in such a way that the influence of control cycles and different risk levels on the overall performance of the NMS were investigated and compared against a simpler deterministic approach.

The approach is applied to a UK 33 kV network, considering high penetration of wind power capacity. The following summarises the key points in this chapter:

- In the deterministic approach, adopting shorter control cycles allows more frequent monitoring of the network status and a close following of the variability of the wind resource. This results in better management of congestion and voltages.

- In the deterministic approach, the improvement resulting from adopting shorter control cycles to manage network constraints is at the expense of the volume of control actions from the OLTCs and the DG plants.

- The development of a risk-based NMS approach that decreases the effects of wind power uncertainties, particularly during longer control cycles, resulting in a better performance than a deterministic approach and less control actions, given that the

variability of wind power is considered at the decision making time.

- The risk-based approach allows the adoption of longer control cycles which in turn reduces dramatically the number of tap changes and the volume of control actions from DG plants.

- Tighter risk levels were found to improve the overall performance of the NMS optimisation (in terms of congestion and voltages) even with longer control cycles. However, this increases significantly the volume of curtailment.

- To provide a robust quantification of wind power transitions in the risk-based approach, the historical assessment should be applied over a significant period. In this work, 1-min resolution data for one month was used. This analysis may be further improved by adopting a sliding window, i.e. updating the historic data periodically (e.g., each day or week) to consider the new wind power measurements.

- Long-term use of the NMS requires the risk level to be defined periodically, i.e. monthly or seasonally, to consider the corresponding changes in demand and wind generation.

- The work could become an important tool in allowing distribution network operators to understand the benefits and challenges of departing from deterministic multi-second-based control cycles into risk-based longer ones.

- The risk-based approach is also compared with the deterministic approach, which considers thermal thresholds below 100%. The results show that similar network management is achieved by both control approaches. However, the risk-based approach provides higher levels of harvested energy.

Chapter 6: Optimal Sizing of Energy Storage in Network Management Systems

6.1 Introduction

Electrical energy storage is considered to be a key technology in future network management systems, which will allow greater energy harvesting from renewable DG. Due to the relatively high cost of storage facilities compared to other control solutions, this chapter will focus on the sizing of energy storage facilities.

This chapter presents a planning framework through which to find minimum storage sizes (power and energy) at multiple locations in distribution networks, in order to reduce curtailment from renewable DG whilst managing congestion and voltages. The framework incorporates high granularity control aspects to enable enhanced accuracy in the sizing of storage facilities. Congestion and voltages are managed through the optimal control of storage (active and reactive power), on-load tap changers (OLTCs), DG power factor and DG curtailment as a last resort.

First, an overview and the formulation of the proposed planning framework is presented. The storage planning framework is applied to the 33 kV network presented in Chapter 4. The control aspects will be demonstrated first using a single storage facility to show the benefits of storage in managing congestion and voltages. Also, the importance of

modelling high granularity control aspects in the storage planning framework is investigated. Then, the optimal size of storage is found. In addition, the planning framework is demonstrated for multiple storage facilities. The benefits of coordination with other controllable control solutions (OLTCs, storage and DG power factor controls) to reduce the required size of storage facilities are also shown. Finally, a comparison is provided between the planning framework and other storage sizing approaches for multiple storage facilities.

6.2 Storage Sizing Framework

To assess the potential benefits of storage facilities in the reduction of wind power curtailment (resulting from the management of congestion or voltage issues), an adequate horizon has to be considered. Furthermore, given that the ability of storage to charge/discharge energy depends on previous control actions, it is necessary to consider the time-series nature of load and generation present in the studied network. Hence, the complexity of finding optimal storage sizes for a given horizon increases with the granularity of the time-series data. The framework with which to find the minimum storage size (power and energy) for a *desired curtailment level* (% of the capacity factor) is presented in Fig. 6.1.

The adoption of two stages, planning and control, allows a reduction of the computational burden that would otherwise be created by incorporating high granularity intervals into the first stage. Each of the stages and the iterative procedure are described below.

It is important to highlight that the scope of this Chapter is to provide an approach able to incorporate real-time control aspects to size storage facilities in future Network Management Systems (NMS). Due to the availability of high granularity time series data of wind and load profiles, one week planning horizon is only adopted. Further work can be carried out based on the developed approach to consider long economic planning horizon

(i.e., at least one year) so that the economics issues related to the integration of storage can be properly addressed (More details in Section 7.5).

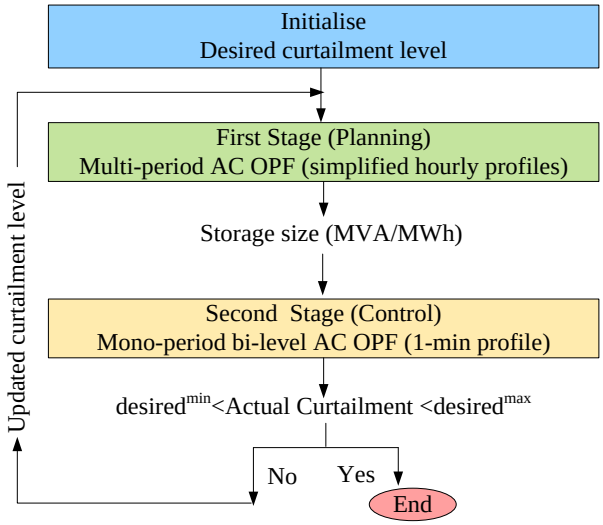

Fig. 6.1 Two-stage storage sizing framework

6.2.1 First Stage (Planning)

The multi-period AC OPF in [12] is modified by forcing the adoption of the time-series nature of the demand and generation, and also by incorporating inter-temporal constraints needed to adequately model the operation of storage facilities. By minimising the total cost of storage, this OPF finds the minimum sizes (MVA, MWh) able to reduce curtailment to below a desired level. This is undertaken by considering all of the time steps (i.e., multiple periods) within the studied horizon simultaneously.

The OPF also embeds ANM schemes which provide further flexibility to manage congestion and voltage constraints, potentially allowing the use of smaller storage sizes. This includes the control of tap positions of OLTCs as well as the power factor of DG plants and storage facilities.

This first stage considers hourly time-series data as a trade-off between the scale of the

problem and the high granularity representation of the operational aspects. However, this granularity might result in over- or under-sized storage facilities, given that intra-hourly fluctuations are neglected. For instance, the storage requirements for a congestion issue due to a 60-min average generation can be significantly different from those resulting from 15 or 1 minute values where sudden gusts of wind can occur. Consequently, to check the effectiveness of the storage sizes found during the first stage in achieving the desired curtailment, a second stage is introduced during which the optimal control is applied adopting a high granularity control environment.

6.2.2 Second Stage (Control)

The second stage examines the *actual curtailment* level to be achieved by the storage sizes determined in the first stage. This is accomplished by considering 1-min control cycles. As shown in Fig. 6.2, at the start of each control cycle, the states of loads, generation, storage devices and OLTCs are sent to the decision-making algorithm to find the best set points of controllable elements to allow minimisation of generation curtailment (Level 1). To guarantee that the storage devices only store the excess of generation determined in Level 1, Level 2 is introduced. For those control cycles where there is no need for curtailment, Level 2 also determines the adequate level of discharge. Following Level 2, the final optimal set points for all the controllable elements are issued.

The decision-making algorithm is formulated as a mono-period bi-level AC OPF. It is mono-period because it only deals with a single network state (single time step). It is bi-level because the optimisation carried out in *Level 2* requires the curtailment determined by the optimisation in *Level 1*. The volume of curtailment resulting from each control cycle is aggregated throughout the studied horizon to determine the *actual curtailment* level achieved by the corresponding storage sizes.

Since the control stage is used for planning purposes, an ideal control action is adopted (i.e., the time delay between decisions and actions is neglected). This allows elimination of

the potential noise created by the changes in demand and generation from one minute to another, resulting in a much cleaner quantification of the benefits of storage facilities in the context of renewable DG curtailment minimisation.

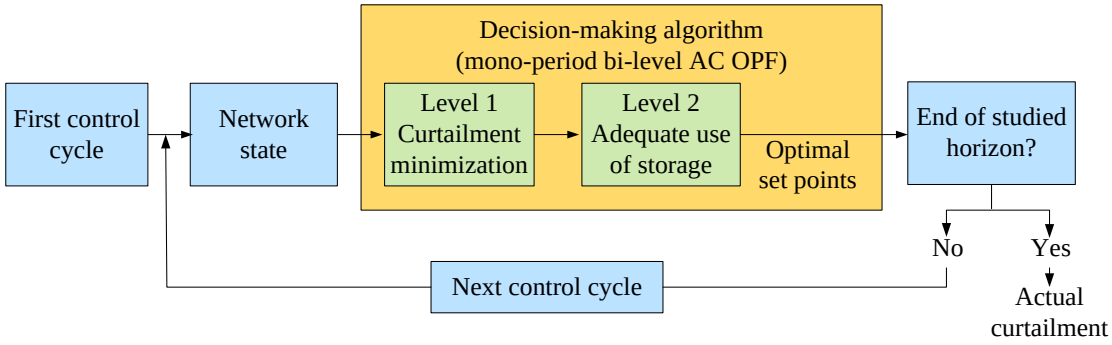

Fig. 6.2 Second stage (control) framework

6.2.3 Iterative Procedure

If the *actual curtailment* level obtained in the second stage is outside the defined tolerance (i.e., $desired^{min}$ and $desired^{max}$, see Fig. 6.1), new storage sizes are required. For this, the first stage is given an *updated curtailment level* which is calculated by adjusting the previous curtailment level (e.g., by 1%) up or down according to the binding tolerance (more details will follow in section 6.3). This process is iteratively applied until the difference between the *actual curtailment* in the second stage and the desired curtailment falls within the tolerance.

6.3 Problem Formulation

This section presents the formulations of the framework aimed at finding the minimum energy capacity E_{st}^{rated} (MWh) and apparent power rating S_{st}^{rated} (MVA) of storage facilities (set *ST* indexed by *st*) required to achieve the *desired curtailment level*, $\lambda_{curt}^{desired}$. The section is divided into planning and control stages, and the iterative procedure.

6.3.1 Planning Stage "Multi-Period AC Optimal Power Flow"

The multi-period AC OPF with inter-temporal constraints considers for each period (set *T* indexed by *t*) the hourly average of the high granularity wind and demand profiles. To determine the minimum size of storage facilities, for both energy and power, the objective function is formulated to minimise a proxy of the overall capital cost. This allows the realistic relating of energy capacities and power ratings in a single equation, as shown in Equation (6.1).

$$min \sum_{st \in ST} C_E \, E_{st}^{rated} + C_S \, S_{st}^{rated} \tag{6.1}$$

The weighting coefficients C_E and C_S are the costs of the energy capacity and the apparent power rating, respectively. Here, the proportion between these weighting coefficients is used instead of their actual values. In particular, the cost of the energy capacity is considered to be one and a half times that of the apparent power rating, i.e., C_E=1 and C_S=0.67, corresponding to a Lithium-Ion battery [80].

This objective is subject to a range of constraints including those relating to storage facilities, controllable DG plants and OLTCs, voltage and thermal limits, as well as the traditional AC OPF constraints (i.e., Kirchhoff's voltage law and power balance).

Storage Facilities

Storage facilities are controlled to discharge (i.e., inject) or charge (i.e., absorb) active power, $p_{st,t}$, at each time step within the converter apparent power rating, S_{st}^{rated}. Positive values of $p_{st,t}$ are considered for the injection of power.

$$-S_{st}^{rated} \leq p_{st,t} \leq S_{st}^{rated} \qquad \forall \, st, t \tag{6.2}$$

It is important to highlight that this approach of adopting a single variable to model power

injection/absorption is an improvement on previous studies [28-30, 108] where two variables have been used to represent charging and discharging. The approach is more general and scalable, and does not require further constraints to prevent simultaneous charging and discharging.

The energy losses that result from energy and power conversion have to be accounted for during charging and discharging. Therefore, the change in the stored energy, $\Delta E_{st,t}^{stor}$, at each time step and the corresponding stored energy, $E_{st,t}^{stor}$, can be represented by Equations (6.3) and (6.4), respectively.

$$\Delta E_{st,t}^{stor} = \begin{cases} -\frac{p_{st,t}\,\Delta t}{\eta_{st}^{dis}}, & p_{st,t} \geq 0 \\ -p_{st,t}\,\eta_{st}^{ch}\Delta t, & p_{st,t} < 0 \end{cases} \qquad \forall\, st, t \tag{6.3}$$

$$E_{st,t}^{stor} = E_{st}^{(0)} + \sum_{t=1}^{t} \Delta E_{st,t}^{stor} \qquad \forall\, st, t \tag{6.4}$$

where η_{st}^{ch} and η_{st}^{dis} are the charging and discharging efficiencies, respectively. Δt is 1 hour and $E_{st}^{(0)}$ is the initial stored energy at the beginning of the planning horizon.

To preserve the cycle life of the battery storage facilities, the stored energy is not allowed to fall below a particular percentage of the capacity (e.g., 20%) [80]. This is defined here as the maximum Depth of Discharge (DoD^{max}). Therefore, the stored energy is controlled between a minimum level and its rated capacity.

$$(1 - DoD^{max})E_{st}^{rated} \leq E_{st,t}^{stor} \leq E_{st}^{rated}\ ;\ \forall\, st, t \tag{6.5}$$

Finally, the power factor angle, $\emptyset_{st,t}$, of each storage facility is also controlled to inject or absorb reactive power within the corresponding apparent power rating and reactive power capability, $\emptyset_{st}^{(+,-)}$. As shown in Fig. 6.3, the storage facility can simultaneously inject or

absorb reactive power during charging and discharging processes.

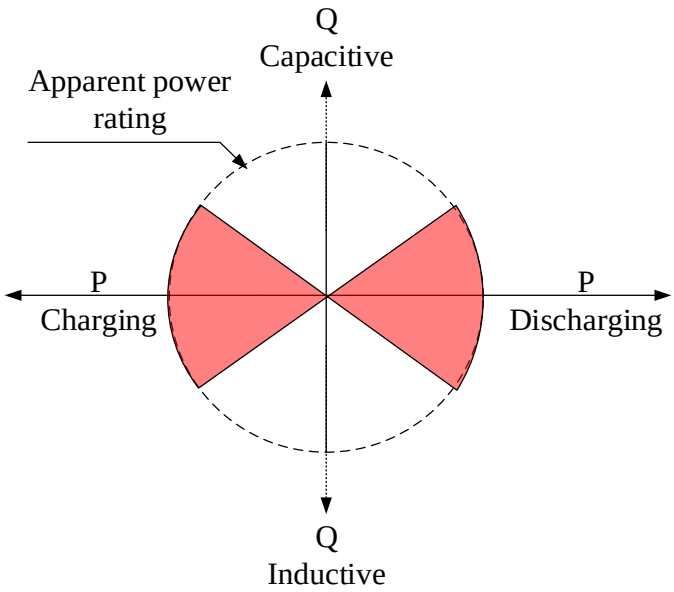

Fig. 6.3 Active and reactive power cabability of storage facilities

The shaded area is the operating zone of the storage facility determined by the apparent power rating of the storage facility S_{st}^{rated} and the reactive power capability $\emptyset_{st}^{(+,-)}$. For example, at the second quadrant (within the shaded area), the storage facility can charge active power whilst injecting reactive power. Some technologies of storage facilities allow decoupling of the active and reactive power output so that the reactive power can be injected or absorbed with zero active power output. Therefore, the storage facility can operate at any point in the four quadrants and within the apparent power rating (full circle). To model such extended reactive power capability, the constraint in Equation (6.7) is relaxed. However, due to the non-linear nature of the problem and to avoid trapping in local solutions, Equation (6.6) can be represented using a set of linear equations [127]. It is assumed in this work that the active and reactive power of storage facilities are coupled.

$$\left(p_{st,t}\right)^2 + \left(p_{st,t}\ tan\left(\emptyset_{st,t}\right)\right)^2 \leq \left(S_{st}^{rated}\right)^2 ;\ \forall\ st, t \tag{6.6}$$

$$\emptyset_{st}^{-} \leq \emptyset_{st,t} \leq \emptyset_{st}^{+} \; ; \; \forall \; st, t \tag{6.7}$$

Controllable DG Plants (Curtailment)

The controllable DG plants (set *N* indexed by *n*) can be subjected to curtailment in order to keep voltage and thermal constraints within limits. The power output, $p_{n,t}$, at each time step is limited by the available wind power resource that is the product of the DG power rating, p_n^{rated}, and the normalised wind power pattern, Γ_t, for the same period. This is presented in Equation (6.8). The curtailed power, $p_{n,t}^{curt}$, is formulated in Equation (6.9).

$$p_{n,t} \leq p_n^{rated} \, \Gamma_t \; ; \; \forall \, n, t \tag{6.8}$$

$$p_{n,t} = \; p_n^{rated} \, \Gamma_t - \; p_{n,t}^{curt} \; ; \; \forall \, n, t \tag{6.9}$$

However, the total volume of curtailment for all DG plants will be limited to the *curtailment level*, λ_{curt}^{v} (at iteration v). This is a percentage of the total available wind energy resource that could be harvested across the planning horizon.

$$\sum_{n \in N, t \in T} p_{n,t}^{curt} \leq \lambda_{curt}^{v} \sum_{n \in N, t \in T} p_n^{rated} \, \Gamma_t \tag{6.10}$$

Furthermore, the controllable DG plants can operate at different power factor angles, $\emptyset_{n,t}$. This makes reactive power "*dispatchable*" within the MVA capability, S_n^{rated}, of the corresponding DG plant, $\emptyset_n^{(-,+)}$.

$$\left(p_{n,t}\right)^2 + \left(p_{n,t} \; tan\left(\emptyset_{n,t}\right)\right)^2 \leq \; (S_n^{rated})^2 \; ; \forall \, n, t \tag{6.11}$$

$$\emptyset_n^{-} \leq \emptyset_{n,t} \leq \emptyset_n^{+} \; ; \; \forall \, n, t \tag{6.12}$$

On-Load Tap Changers

The tap ratio, $\tau_{l,t}$, for OLTC-fitted transformers (represented within the set *L* indexed by *l*) can be controlled at each time step considering its capabilities $\tau_l^{(-,+)}$.

$$\tau_l^- \leq \tau_{l,t} \leq \tau_l^+; \ \forall \ l,t \tag{6.13}$$

General AC OPF Constraints

Active, $f_{l,t}^{(1,2),(P)}$, and reactive power, $f_{l,t}^{(1,2),(Q)}$, injections at the start and end buses (denoted 1 and 2) for each line and each transformer are calculated according to the standard Kirchhoff's voltage law expressions as presented below [12].

$$f_{l,t}^{(1,2),(P)} = f_{l,t,KVL}^{(1,2),(P)}(\boldsymbol{V}, \boldsymbol{\delta}); \ \forall \ l,t \tag{6.14}$$

$$f_{l,t}^{(1,2),(Q)} = f_{l,t,KVL}^{(1,2),(Q)}(\boldsymbol{V}, \boldsymbol{\delta}); \ \forall \ l,t \tag{6.15}$$

If the transformers are equipped with OLTCs, the corresponding terms in Equations (6.14) and (6.15) for voltage at the start bus of the line will be divided by the tap ratio $\tau_{l,t}$.

The distribution network is supplied by at least one point interfacing with the upstream grid. It is assumed that this point x (X, set of external connections) can import/export real and reactive power $(p_{x,t}, q_{x,t})$ within limits $\left(p_x^{(-,+)}, q_x^{(-,+)}\right)$. One of these external connections is taken as the slack bus with voltage angle, $\delta_{slack,k}$, equal to zero.

The balance of real and reactive power at each bus (set *B* indexed *b*), and for each time step, is formulated according to Equations (6.16) and (6.17), respectively. The modelling considers firm generation (set *G* indexed by *g*), whose power output, $p_{g,t}$, is not controllable. Firm generation are assumed to have fixed power factor, $\emptyset_g$.

$$\sum_{n\in N|\beta_{n=b}} p_{n,t} + \sum_{g\in G|\beta_{g=b}} p_{g,t} + \sum_{x\in X|\beta_{x=b}} p_{x,t} + \sum_{st\in ST|\beta_{st=b}} p_{st,t} = d_{b,t}^{P} + \sum_{l\in L|\beta_{l}^{(1,2)}=b} f_{l,t}^{(1,2),(P)};\ \forall\, l,t \tag{6.16}$$

$$\sum_{n\in N|\beta_{n=b}} p_{n,t}\, tan(\emptyset_{n,t}) + \sum_{g\in G|\beta_{g=b}} p_{g,t}\ tan(\emptyset_{g}) + \sum_{x\in X|\beta_{x=b}} q_{x,t} + \sum_{st\in ST|\beta_{st=b}} p_{st,t}\ tan(\emptyset_{st,t}) = d_{b,t}^{Q} + \sum_{l\in L|\beta_{l}^{(1,2)}=b} f_{l,t}^{(1,2),(Q)};\ \forall\, l,t \tag{6.17}$$

where β_u maps the location of each network element ($u \subset \{st, n, g, x, l\}$) to its associated bus, and $d_{b,t}^{(P,Q)}$ are the active and reactive demand at the same bus. It should be mentioned that the active $p_{st,t}$ and reactive power $q_{x,t}$ of storage is the new element in the real and reactive power balance equations in (6.16) and (6.17) compared to the balance equations in the OPF presented in Chapter 4 ((4.14) and (4.15)).

The voltage magnitude at bus b ($V_{b,t}$) should be within the statutory limits, $V_b^{(-,+)}$, and the apparent start/end power flows through lines and transformers should be limited to their corresponding thermal capacity f_l^+.s

$$V_b^- \le V_{b,t} \le V_b^+;\ \forall\, b,t \tag{6.18}$$

$$\left(f_{l,t}^{(1,2),P}\right)^2 + \left(f_{l,t}^{(1,2),Q}\right)^2 \le (f_l^+)^2;\ \forall\, l,t \tag{6.19}$$

6.3.2 Control Stage "Mono-Period Bi-Level AC OPF"

This stage finds the *actual curtailment level*, λ_{curt}^{actual}, that could be achieved by the storage sizes obtained in the first stage (S_{st}^{rated}, E_{st}^{rated}) considering 1-min control cycles. The optimisation carried out at Level 1 maximises the total active power of the controllable DG plants, p_n, whose maximum values are restricted by the available wind power resource, p_n^+, at that control cycle. By maximising the harvesting of DG plants, the minimum volume of curtailment is ensured for the corresponding control cycle.

$$max \sum_{n \in N} p_n \tag{6.20}$$

$$p_n \leq p_n^+ \tag{6.21}$$

This objective function is also subject to those constraints in the first stage related to the storage facilities (Equations (6.2), (6.5)-(6.7)), the controllable DG units (Equations (6.11)-(6.12)), the controllable OLTCs (Equation (6.13)) and the general AC OPF constraints (Equations (6.14)-(6.19)). These constraints are adapted to consider a single time period.

In addition, for each control cycle, Tc, the energy stored at the previous control cycle, E_{st}^{Tc-1}, is used as an initial condition to find the new store level, E_{st}^{Tc}, as given in Equation (6.22).

$$E_{st}^{Tc} = \begin{Bmatrix} E_{st}^{Tc-1} - \dfrac{p_{st}\,\Delta T_c}{\eta_{st}^{dis}}, & p_{st} \geq 0 \\ E_{st}^{Tc-1} - p_{st,t}\,\eta_{st}^{ch}\,\Delta T_c, & p_{st} < 0 \end{Bmatrix};\ \forall\ st \tag{6.22}$$

where ΔT_c is 1/60 hour (i.e., a 1-min control cycle). It is worth to note that the ramp rate of storage facilities is not considered in this work. To cater for this, further constraint has to be incorporated in the formulation of the control stage such that the maximum change (upwards/downwards) in the power output of a storage facility between two consecutive

control cycles is below a defined limit determined in respect to the storage technology.

Once the maximum active power of controllable DG is identified, the volume of curtailment E_{curt} can be determined.

$$E_{curt} = \sum_{n \in N} (p_n^+ - p_n)\ \Delta T_c \tag{6.23}$$

This volume of curtailment is then used by the optimisation at Level 2 to ensure that the storage facilities are adequately used for the corresponding control cycle. To do so, Level 2 minimises the stored energy (Equation (6.24)), subject to all constraints at Level 1 plus one further constraint, Equation (6.25). The latter guarantees that curtailment will not go beyond that previously calculated (E_{curt}).

$$min \sum_{st \in ST} E_{st}^{Tc} \tag{6.24}$$

$$\sum_{n \in N} (p_n^+ - p_n)\ \Delta T_c \leq E_{curt} \tag{6.25}$$

The output of Level 2 corresponds to the final set points for all controllable elements within the analysed control cycle. It should also be highlighted that the $E_{curt}^{(1)}$ (calculated at the first level) has to be increased by a very small number in the order of 10^{-5} to cater for the tolerance value of the solver, without affecting the curtailed energy obtained at the first level.

At the end of the studied horizon, the actual curtailment level, λ_{curt}^{actual}, can be calculated by adding up the curtailment volumes of each cycle, E_{curt}, and dividing the total by the horizon's available wind energy resource.

6.3.3 Iterative Procedure

Further iterations may be needed to produce new sizes of storage facilities until the difference between the *actual curtailment level* and the *desired curtailment level* becomes smaller than the defined tolerance, γ.

$$\left|\lambda_{curt}^{actual} - \lambda_{curt}^{desired}\right| \leq \gamma \tag{6.26}$$

The curtailment level, λ_{curt}^{v}, used by the first stage is given by Equation (6.27) in each iteration v. For the first iteration ($v = 1$), this curtailment level is set to the *desired curtailment level*, $\lambda_{curt}^{desired}$. Then, in the subsequent iterations ($v > 1$) it will be reduced or increased by a defined step μ^{v} (e.g., 1%) from its previous value, λ_{curt}^{v-1}.

$$\lambda_{curt}^{v} = \begin{cases} \lambda_{curt}^{desired} & v = 1 \\ \lambda_{curt}^{v-1} \pm \mu^{v} & v > 1 \end{cases} \tag{6.27}$$

It is important to highlight that the setting of the step μ^{v} throughout the iterations depends on the sign of the difference between actual curtailment and desired curtailment. If there is no change in the sign between two successive iterations, then μ^{v} is held (1% is adopted in this work). Otherwise, if there is a change in the sign, μ^{v} will be halved from its previous value. Note that λ_{curt}^{v} is only used to force the planning stage to improve the storage sizes. Ultimately, a value of λ_{curt}^{actual} close to the desired value is the target of the iterative procedure.

6.4 Case Studies: Description and Modelling

The storage sizing framework is applied to the same UK 33 kV network used in previous chapters. A single-line representation of the network is given in Fig. 6.4 [128]. Minute-by-minute wind profiles for the first week of February 2010 are adopted for all the DG plants.

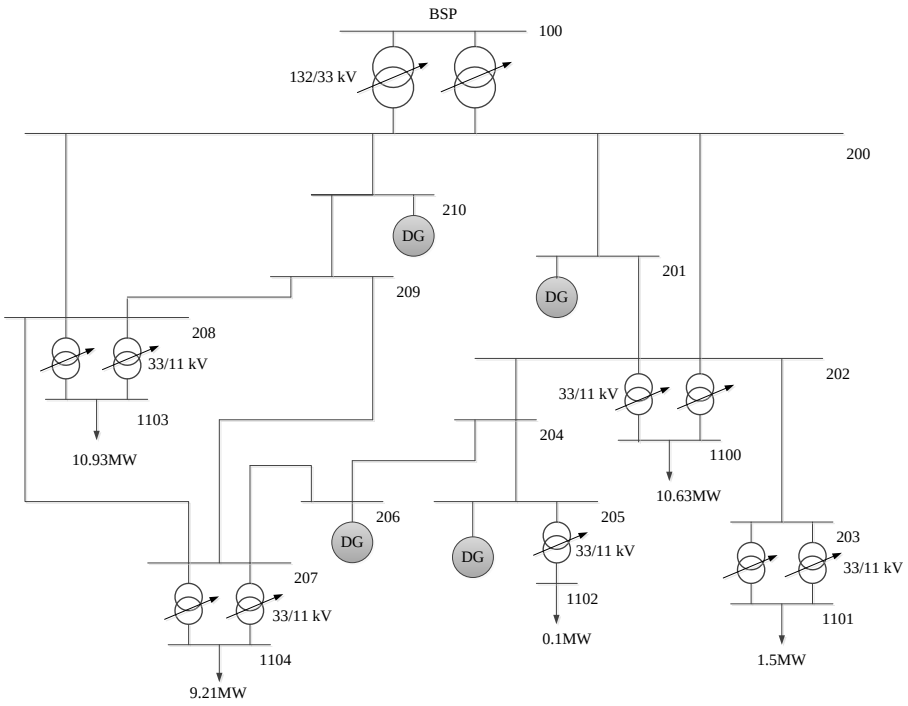

Fig. 6.4 A 33 kV network in the north-west of England

The sizing approach will first be demonstrated for a single storage facility for two case studies and for a one-day planning horizon. A storage facility is used to show a reduction in the curtailment required to solve congestion issues, before a new case study is presented to show the benefits of storage in managing both congestion and voltage rise issues. Finally, the approach will be investigated in a more complex environment considering multiple storage facilities and multiple DG plants. The planning horizon is also extended to one week. The modelling language AIMMS [118] is used to formulate and solve the multi-period AC OPF (planning stage) as well as the mono-period bi-level AC OPF (control stage).

6.5 Case Study 1: Sizing and Control of a Single Storage Facility – Congestion Management

In this section, the benefits of optimally operating storage facilities in the context of

curtailment reduction are demonstrated, using a single storage facility at bus 201 to manage congestion issues in line 200-201 due to two new DG plants. The effects of data granularity on storage sizing are also investigated. Finally, the two-stage approach is demonstrated by finding the optimal size of storage at bus 201.

In this section, a new 9 MW wind power plant is connected as firm generation (uncontrollable) to bus 201. This corresponds to the maximum capacity that can be connected to this location without overloading line 200-201 (20 MVA). Furthermore, a 6 MW controllable DG plant is connected to bus 201. By controlling the active power of the 6 MW DG plant, it is possible to mitigate the overloads through line 200-201. To illustrate the volume of curtailment required to do so, the minute-by-minute wind profile corresponding to 1st February 2010 is adopted for all DG plants. The Level 1 mono-period AC OPF is used to calculate the curtailment needed to avoid congestion at each minute. The resulting curtailment is 51 MWh, i.e. 42% of the available wind energy resource (121.7 MWh), and the maximum power curtailed is 5.9 MW.

6.5.1 Operation of a Predetermined Storage Size

This section demonstrates the operation of the bi-level mono-period AC OPF to optimally control the operation of a predetermined size of storage facility (charging, discharging and idling) at bus 201 and the 6 MW DG plant using a realistic control cycle length of 1 minute. A lithium-ion storage facility will be used, given the required fast response. It is considered to have round trip efficiency of 85%, i.e. charging (η_{st}^{ch}) and discharging (η_{st}^{dis}) efficiencies of 92%. The maximum depth of discharge (DoD^{max}) is adopted as 80% of the energy capacity [80].

To demonstrate the benefits of the approach, and in particular the control aspects, an initial arbitrary size of 4 MVA and 12 MWh is considered for the battery at bus 201. To illustrate the optimal operation of storage, the power flow through line 200-201 that would occur

without controlling the 6 MW DG plant and the storage facility is presented in Fig. 6.5 (a). The power flow through line 200-201 resulting from controlling the storage and the DG power output is presented in Fig. 6.5(b). The percentage of harvested wind power (red line) is presented in Fig. 6.5 (c). The wind power harvested using the "curtailment-only" scheme (black line) is also presented to show the benefits of storage in the reduction of curtailment. The stored energy found by the optimisation in each control cycle (i.e., resulting in no congestion issue) is presented in Fig. 6.5 (d).

At the beginning of the day, from 0:00 to 1:40, due to the excess generation, the storage is required to deal with the congestion of line 200-201. However, throughout this period, the excess power is greater than the storage rating (4 MVA), resulting in curtailment (harvested energy below 100%). For those periods where the excess generation is less than 4 MVA, such as 4:00 to 10:00, the storage is capable of managing the congestion issue without the need for curtailment. To ensure storage capacity is available for future congestion events, discharging has to be applied when there is enough headroom in line 200-201. For instance, from 1:40 to 3:00, although there are periods with excess generation, there are also those with sufficient headroom to allow discharging. This process lasts until the stored energy reaches the minimum of 2.4 MWh according to the adopted maximum depth of discharge (DoD^{max}) of 80% (i.e., 0.2×12 MWh). In addition, the storage goes into idling mode when there is no need for charging (e.g., from 9:00 to 10:00) or no possibility of discharging (e.g., from 19:00 to 21:00). Indeed, once the stored energy reaches the storage capacity (12 MWh), curtailment will be the only solution to managing congestion. It can be seen from Fig. 6.5 (b) that the power flow through line 200-201 is managed below its thermal capacity. Also, the line usage increased during the discharging process compared to the power flow that would occur without controlling, as shown in Fig. 6.5 (b). It should be noted that the time delay between decision and action is not considered.

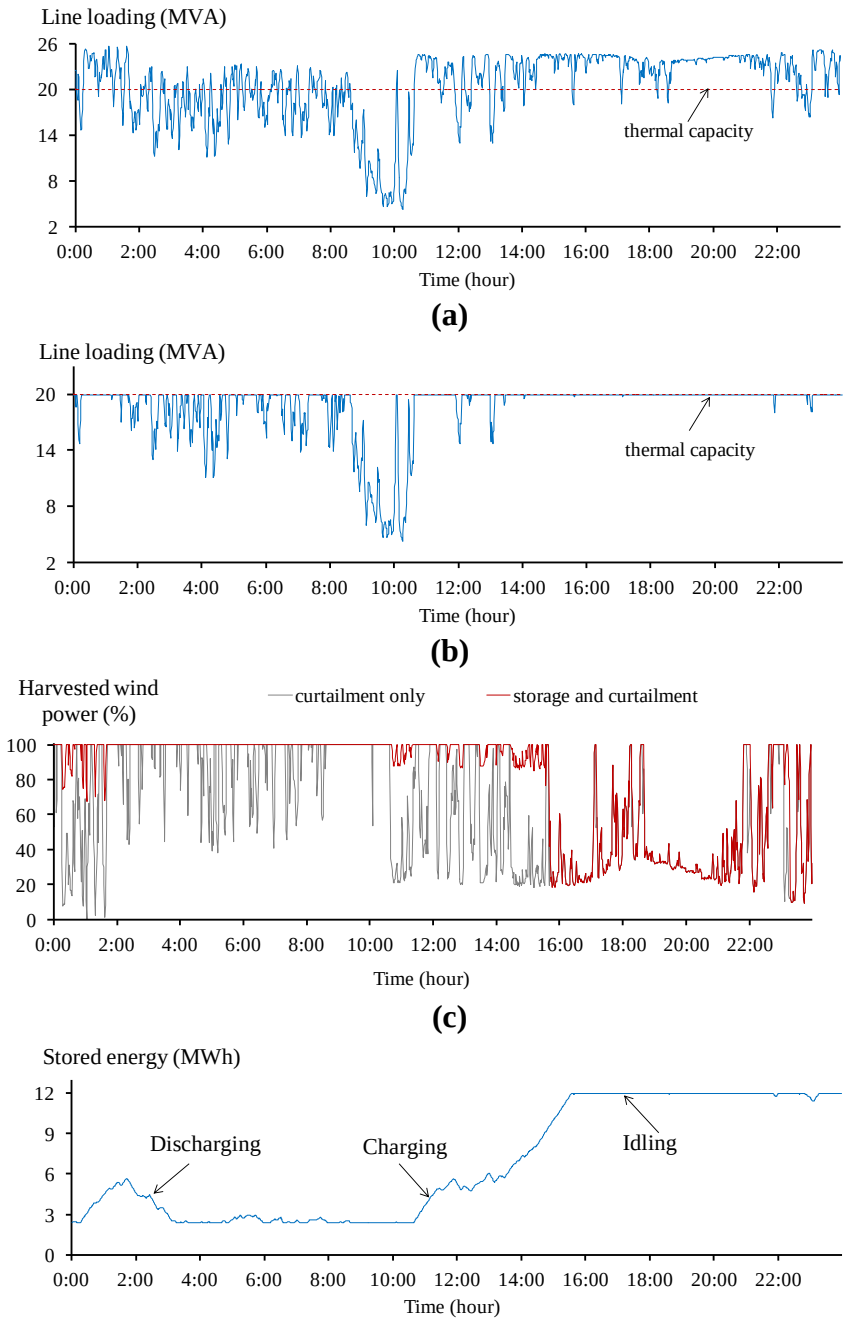

Fig. 6.5 (a) line 200-201 loading (MVA) without control (b) line 200-201 loading (MVA) after control, (c) harvested wind power from the 6MW DG plant (in %) (d) stored energy (MWh) for the 4 MVA-12 MWh storage facility

The resulting curtailment level upon utilising the optimal operation of storage and the 6 MW DG plant is 24% (29.2 MWh). This represents a significant reduction from the 42% found by applying a curtailment-only scheme (21.8 MWh). In contrast, the energy losses in storage due to charging and discharging cycles is 2.6 MWh (1.8 MWh during charging and 0.8 MWh during discharging), which in turn reduces the actual volume of exported energy from 21.8 MWh to 19.2 MWh. Therefore, the net export energy from DG plants for each 1 MWh of energy storage capacity is 1.6 MWh.

In addition, the amount of exported energy highlights the importance of utilising discharging periods to facilitate the adoption of smaller energy capacity and thus better utilization of the installed capacity compared to the storage sizing approach presented in [30] which neglects discharging periods and selects the storage energy capacity as the volume of curtailment.

6.5.2 Effects of Data Granularity on Storage Sizing

The ability to find the actual curtailment level using a control cycle of 1-min allows investigation of the extent that storage sizing approaches need to embed high granularity control aspects, in addition to determining errors in the size of storage facilities where only simplified hourly profiles are adopted. In order to do this, the mono-period bi-level AC OPF is used to investigate the effects of data granularity on storage sizing by assessing the volume of curtailment (% of available wind resource) for hourly and 1-min time resolution profiles and considering a number of storage sizes. This is of particular importance given that most studies found in the literature adopt hourly data [27, 30-32]. A comparison is carried out considering 1-min and 60-min resolution profiles as well as different sizes for a storage facility located at bus 201. The required level of curtailment is used as the performance metric. The 60-min wind and load profiles are obtained by averaging the 1-min profiles previously used. The adopted profiles are presented in Fig. 6.6.

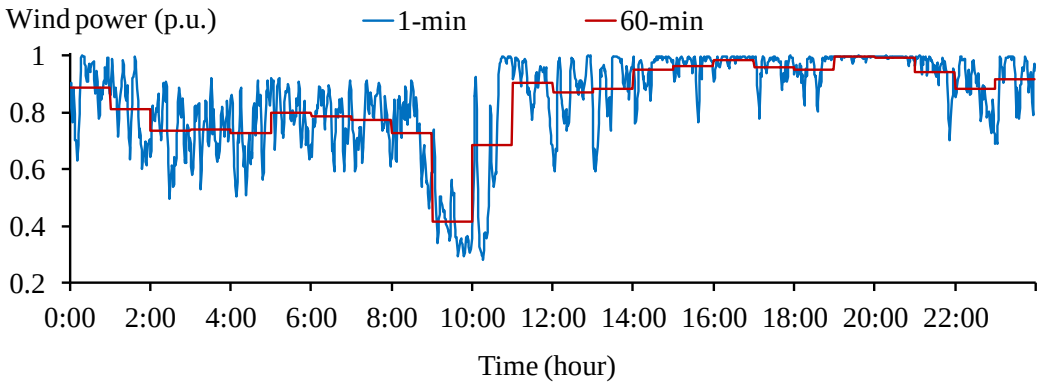

Fig. 6.6 1-min and 60-min wind power profiles (p.u.) for 1st February 2010

Table 6.1: Curtailment for Different Sizes of Storage and Data Granularity

Storage size		Curtailment (%)		
MVA	MWh	60-min	1-min	Error
-	-	33	42	9.0
1	3	29.8	35.8	6.0
2	6	26.8	30.9	4.1
3	9	24.5	27.1	2.6
4	12	22.3	24.1	1.8
5	15	20.2	21.4	1.2
6	18	18.1	18.9	0.8

Six sizes for the storage facility are analysed. Power ratings from 1 MW to 6 MW (maximum curtailment required) are selected in steps of 1 MW. For illustration purposes, the corresponding energy capacity is considered to be three times the power rating.

The curtailment levels for each storage size and data granularity case are presented in Table 6.1. It can be seen that curtailment is always underestimated using hourly profiles, given that issues will need to be solved at shorter intervals. This also can have a significant impact when deciding upon the most cost-effective storage size. For example, using hourly profiles, a storage facility of 2 MVA and 6 MWh seems to be capable of limiting curtailment to 27%. However, the more accurate 1-min case shows that 27% can only be achieved with a 3 MVA and 9 MWh storage facilities.

The curtailment achieved when adopting hourly profiles is due to the fact that the intra-hour fluctuations and the corresponding congestion issues are neglected. This can be observed from the optimal operation of the 2 MVA and 6 MWh storage and the 6 MW controllable DG plant presented in Fig. 6.7. For example, for the hourly profile between 2:00 and 11:00 there is no congestion issue and therefore the storage is in idling mode and the DG unit is not curtailed. However, due to the wind variability (see Fig. 6.6), curtailment and storage of energy are in reality needed for the same period when using 1-min resolution profiles.

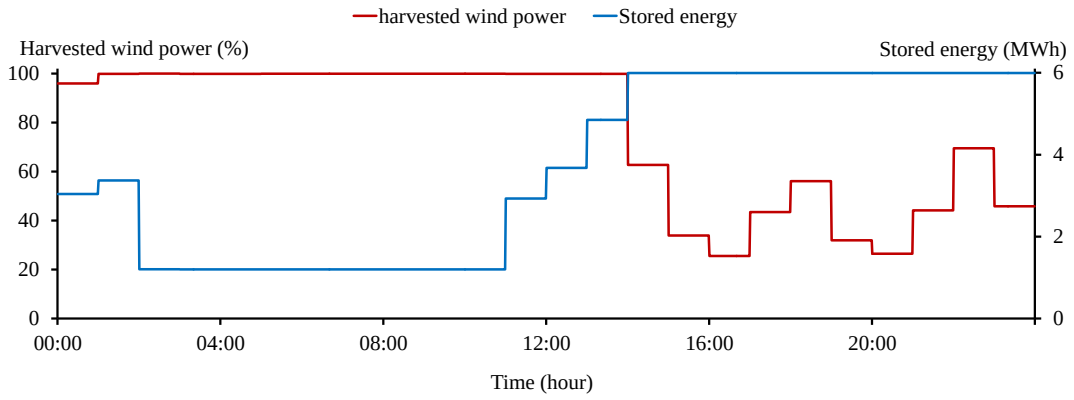

(a)

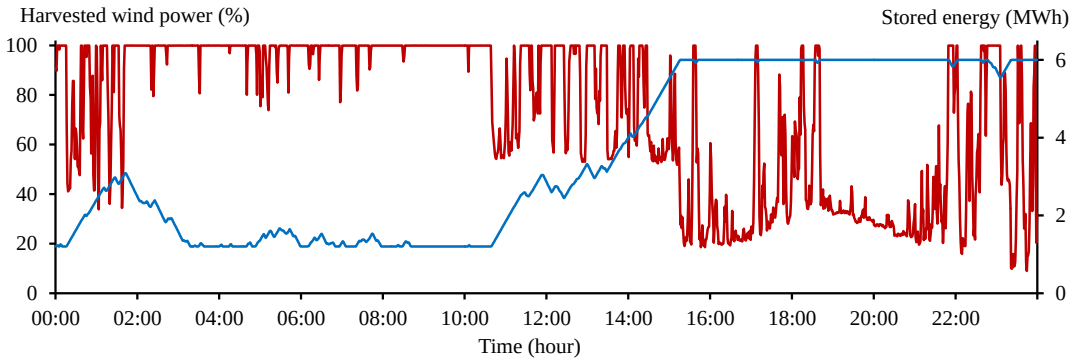

(b)

Fig. 6.7 Harvested wind power from the 6 MW DG plant (in %) and stored energy (MWh) for the 2 MVA 6 MWh storage facility for 1st February 2010: (a) 60-min and (b) 1-min resolution profiles

It is interesting to note that the difference in curtailment reduces for larger storage sizes (Table 6.1). Therefore, the use of simplified hourly profiles may be considered adequate when sizing storage in cases where significant reductions of curtailment are required. Nonetheless, it is still important to realistically model control aspects to truly quantify the curtailment level to be achieved.

6.5.3 Optimal Size of Storage "Two-Stage Iterative Framework"

To find the storage size at bus 201 using the two-stage sizing framework (see Fig. 6.1), a *desired curtailment* level needs to be defined. A value of 21% is used to halve the curtailment that would otherwise be required. The tolerance is set to +/- 1% (i.e., the final *actual curtailment* level must be between 20% and 22%), representing the evolution of the sizing of the storage facility resulting from the iterative process including the corresponding *actual curtailment*. After the first iteration, a storage size of 2.7 MVA and 12.6 MWh is suggested by the first stage (planning) in order to achieve the 21% *desired curtailment*. However, the second stage (control) reveals an *actual curtailment* of 24.9%, which is much larger than desired. Thus, an *updated curtailment level* of 20% is triggered. This iterative procedure stops at the fourth iteration, resulting in a storage size of 2.7 MVA and 16.9 MWh, which corresponds to an *actual curtailment* level of 21.6% (i.e., within the It can be seen that the energy capacity of the storage facility obtained by the first stage increases throughout the iterations to cater for the error in the curtailment, whilst the power rating is held. This is due to the adopted hourly resolution profiles at this stage underestimating the curtailed power required to manage congestion.

Also, it is important to highlight that the trial and error approach presented in Table 6.1 might produce adequate values for a single storage facility. For example, a storage facility of 5 MVA and 15 MWh could be considered feasible in achieving a *desired curtailment* level of 21%, considering 1-min resolution profiles and with an overall cost using Equation (6.1) of 1.9% less than that obtained with the approach. However, the complexity

introduced in considering multiple sites is likely to render the approach unfeasible.

tolerance) as presented in Table 6.2.

Table 6.2: Iterative Storage Sizing at Bus 201 for 21% *Desired Curtailment*

Iteration	First Stage Desired curtailment (%)	Storage size (MVA/MWh)	Second Stage Actual curtailment (%)
1	21	2.7/12.6	24.9
2	20	2.7/13.8	24.0
3	19	2.7/15.7	22.7
4	18	2.7/16.9	21.6

6.6 Case Study 2: Sizing and Control of a Single Storage Facility – Voltage and Congestion Management

Here, the storage sizing framework is implemented for a new case study, to solve both congestion and voltage rise issues. The benefit of controlling the power factor of storage facilities to reduce the required size of storage facility is demonstrated. Similar to the previous section, the effects of data granularity are presented. Finally, the storage sizing framework approach is utilised to find the optimal storage size.

To create a case study in which voltage excursion drives curtailment from additional DG plants, new 14 MW and 18 MW DG plants are connected to the 33 kV network at bus 205 and 206, respectively. Also, the target voltage for the OLTC at the BSP in the 33 kV network is set to 1.02 p.u. The connection of this additional generation capacity increases the voltage at bus 205 to in excess of the upper statutory limit (1.06 p.u.), and particularly to 1.1 p.u. during periods of maximum generation and minimum demand. Also, the power flow throughout line 204-205 exceeds its thermal capacity (23 MVA) by 4.7%.

The control stage (*Level* 1) is used to find the required curtailment from the additional 14 MW and 18 MW DG plants to effectively manage voltage issues at bus 205 and

congestion throughout line 204-205. By using *Level* 1 of the mono-period AC OPF, the total volume of curtailment from each DG plant can be calculated for each minute within the analysed day (1st Feb.).

The resulting curtailment from the controllable DG at bus 205 is 121.2 MWh (mainly to solve voltage rise issues), while the other controllable DG (206) is not curtailed during the analysed day. This volume of curtailment accounts for 18% of the total available wind resource (649 MWh) at the two sites. The maximum power curtailed in order to manage network constraints from the controllable DG at bus 205 is 14 MW.

Therefore, to reduce the overall volume of curtailment, a storage facility is placed at bus 205. The control stage will first be presented by only controlling the active power of the storage facility in addition to generation curtailment using a realistic control cycle length of 1 minute. Then, the coordinated control actions between the active and reactive power output of the storage facility and generation curtailment will be presented.

6.6.1 Operation of a Predetermined Storage Size with Unity Power Factor

To clearly illustrate the benefits of controlling the power factor of storage facilities by the adoption of reduced energy capacity, the apparent power capacity of the storage facility is selected as 15 MVA, which is just higher than the maximum curtailed power allowed to avoid the curtailment that could result when the excess power is larger than the storage rating. Therefore, if there is a reserve in the store, the storage can charge excess power generation at all time periods.

In addition, the energy capacity is selected arbitrarily at 45 MWh. Characteristics typical of the storage discussed in Section 6.5 are adopted. Charging and discharging efficiency parameters are both set to 92%, and the minimum stored energy (E_{st}^{min}) is assigned 20% of the energy capacity.

Here, the active power output of the storage and the DG plant are actively managed every 1-min. The corresponding set point for the DG plant is compared to the curtailment-only scheme over the course of the day. To illustrate the optimal operation of storage, the power flow through line 204-205 and the voltage profile at bus 205 that would occur where there was no control over the controllable DG plants and the storage facility are presented.

To illustrate the optimal operation of storage, the voltage at bus 205 that would occur before control is presented in Fig. 6.8 (a) and the voltage resulting from controlling the storage and the DG power output is presented in Fig. 6.8 (b). Also, the percentage of wind power harvested using the "curtailment-only" scheme (black line) and after controlling the storage power output (red line) is presented in Fig. 6.8 (c) for the DG plant at bus 205. The level of stored energy in MWh achieved as a result of optimisation in each control cycle (i.e., resulting in no constraint issue) is shown in in Fig. 6.8 (d).

It can be seen that, for the majority of the time between 00:00-08:30, the storage facility is controlled to charge excess generation (i.e., stored energy is increasing) to keep voltages and power flow within limits, which results in 100% harvested wind power and no need for curtailment. This represents a significant improvement in terms of harvested wind power compared to low-energy harvesting in the curtailment-only scheme, particularly during the first two hours of the analysed day.

During the time intervals when the DG plants can export the available wind power without breaching thermal and voltage limits in the curtailment-only scheme (i.e., no curtailment), the storage facility is controlled to discharge the stored energy to create a reserve in the store, which in turn allows the charging of excess generation in the upcoming time intervals. The discharging process continues until the stored energy reaches the minimum store level of 9 MWh (20% of the energy capacity). This can be seen between 08:30-11:00. It should be noted that the output power of the storage facility during the discharging process increases the voltage at bus 205 to the limit, as shown in Fig. 6.8 (b). Once the

stored energy reaches the storage energy capacity (45 MWh), generation curtailment becomes the only solution to manage network constraints. This can be seen between 16:30-24:00 when the storage goes into idling mode and the levels of harvested wind power before and after storage are the same.

The curtailment level that results from using the optimal operation of storage and the two controllable DG plants is 5.9% (38.35 MWh). This is a significant reduction from the 18% (121.2 MWh) that results from applying only curtailment. In contrast, the energy loss in storage due to power conversion processes is 9.2 MWh, consisting of 6.3 MWh and 2.9 MWh during charging and discharging modes, respectively. The energy losses in storage reduce the actual volume of exported energy from 83.8 MWh to 74.6 MWh. Therefore, the net export energy from DG plants for each 1 MWh of energy storage capacity is 1.7 MWh. This figure of exported energy is slightly higher than that stated in Section 6.5.2 due to the use of storage to manage both thermal and voltage constraints.

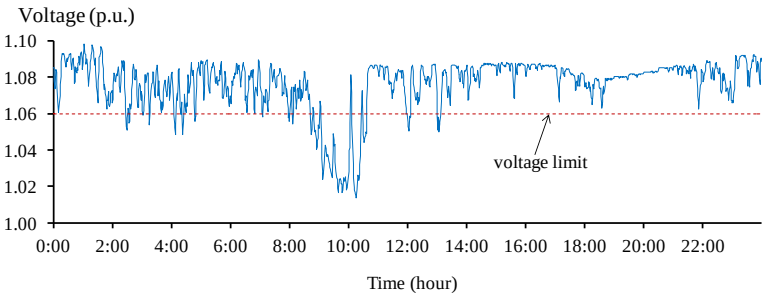

(a)

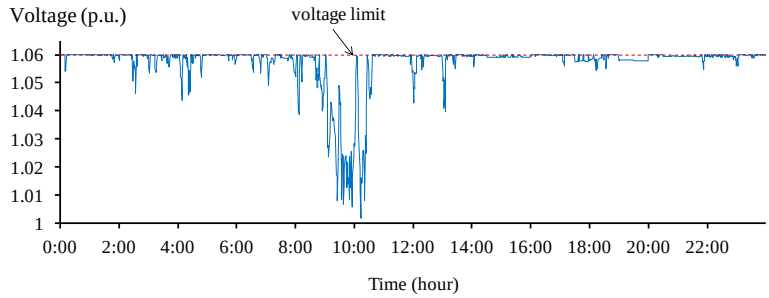

(b)

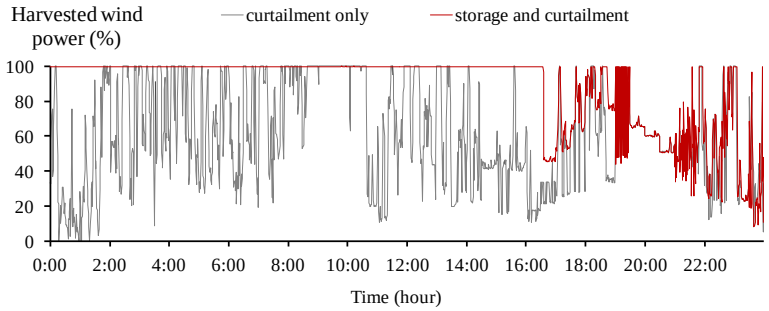

(c)

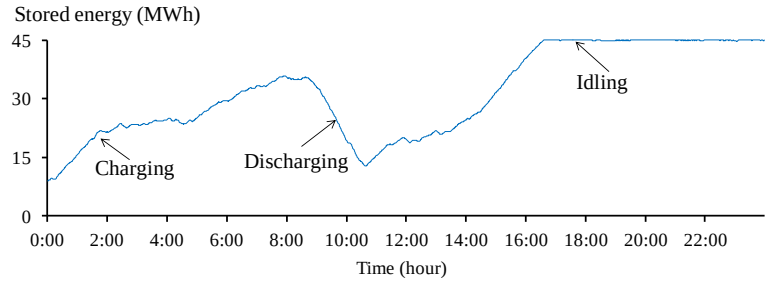

(d)

Fig. 6.8 (a) Voltage profile at bus 205 (p.u.) without control (b) Voltage profile at bus 205 (p.u.) after control, (c) harvested wind power (%) (d) stored energy (MWh) for the 15 MVA-45 MWh storage facility

6.6.2 Operation of a Predetermined Storage Size with Controllable Power Factor

This section illustrates the benefits of controlling the storage power factor within 0.95 inductive and capacitive. Increased energy harvesting can be yielded by controlling the storage power factor. Indeed, voltage rise issues (most critical in this case study) can be solved by controlling the storage to consume reactive power. The consumption of reactive power can reduce the volume of charged energy required to manage constraints which in turn facilitates the adoption of reduced energy capacity. Fig. 6.9 presents the percentage of wind power harvested using the "curtailment-only" scheme (black line) and after controlling the storage active and reactive power output (red line), the stored energy (in MWh) and the reactive power output of storage achieved by optimisation in each control cycle. It can be seen that the harvested wind power is almost at unity (i.e., 100%) during the analysed day. Indeed, voltage rise issues can be solved by controlling the storage to consume reactive power. This can be seen between 00:00-08:30 when the stored energy is only increased to 15 MWh compared to 34 MWh at the unity power factor which may allow the adoption of smaller energy capacities. In addition, the stored energy reaches the energy capacity by the end of the day while stored energy reaches the capacity earlier (at 16:30) by controlling only the active power of the storage facility. This highlights the importance of controlling the power factor to adopt smaller energy capacities.

Also, the use of inductive reactive power allows the volume of discharged energy during discharge modes to be maximised, which in turn increases the reserve in the store from which to charge excess generation (leading to network issues) during the next time intervals (e.g., after two hours).

The overall volume of curtailment is reduced significantly from 18.8% (121.2 MWh) in the curtailment-only scheme to a negligible 0.6 MWh by controlling both the active and reactive power of the storage facility. The corresponding energy loss in storage during charging and discharging cycles is 6.9 MWh, and therefore the actual volume of the

exported energy to the network is 114.7 MWh. Thus, each 1 MWh of storage leads to an increase in exported energy of 2.6 MWh which is an improvement on controlling only the active power of the storage facility (1.7 MWh).

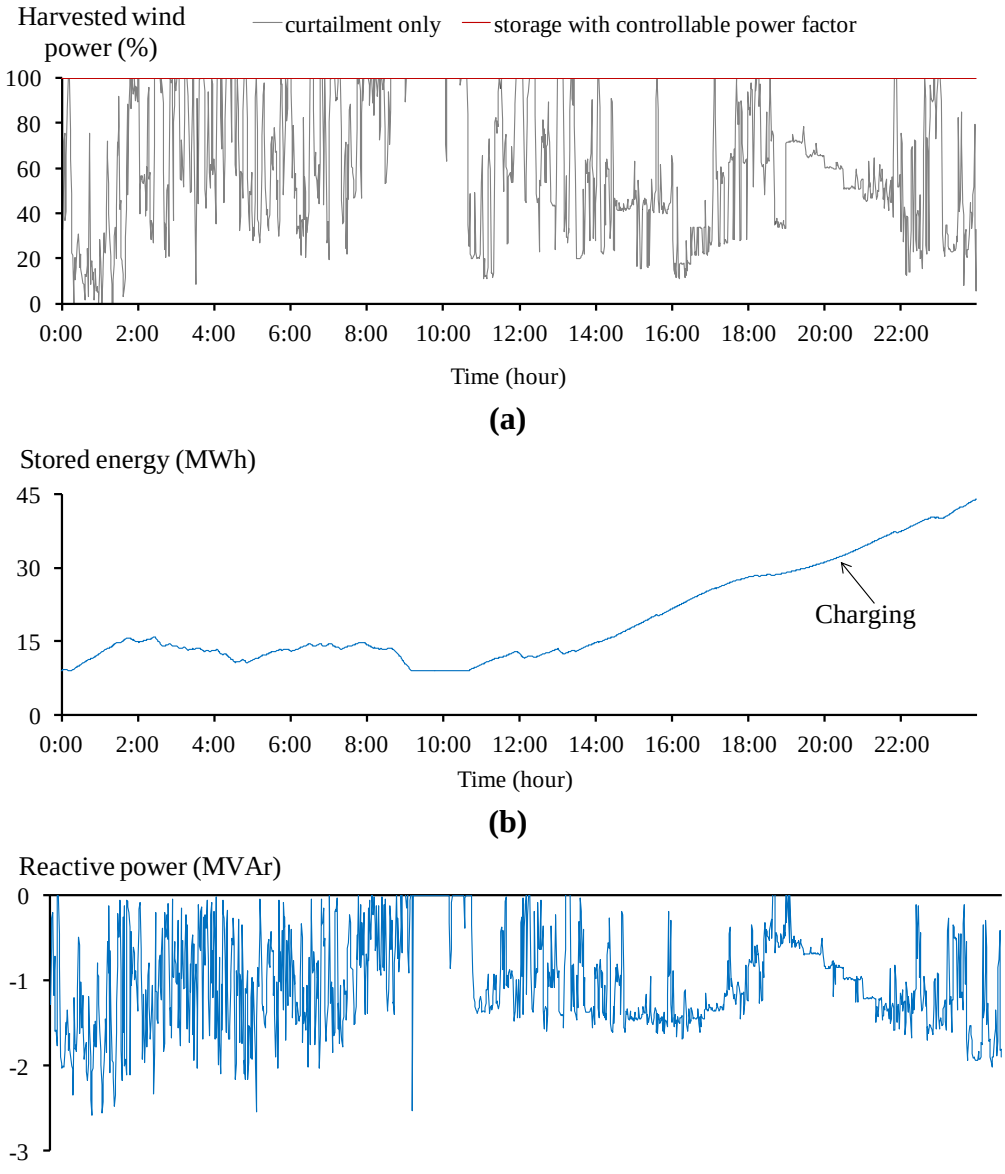

Fig. 6.9 (a) Harvested wind power for the 14, 18MW DG plant (in %) and (b) stored energy (MWh) for the 15MVA-45MWh storage facility using 0.95 PF at bus 205 and (c) reactive power (MVar) for the corresponding storage facility – 1st February 2010

6.6.3 Effects of Data Granularity on Storage Sizing

The effects of data granularity on the volume of curtailment and storage sizing are also investigated for this case study, considering storage at the unity power factor. The comparison is carried out considering 1-min and 60-min resolution profiles as well as different sizes for a storage facility located at bus 205, as previously presented in Section 6.5.

Six sizes for the storage facility are analysed. The power rating is selected from 1 MW to 15 MW in steps of 3 MW (maximum curtailment required). For illustration purposes, the corresponding energy capacity is considered arbitrarily to be three times the power rating. The curtailment levels for each storage size and data granularity case are presented in Table 6.3.

The results confirm the conclusions of Section 6.5.3 whereby curtailment is always underestimated using hourly profiles, which in turn affects decision making in relation to the optimum size of a storage facility. For example, using hourly profiles, a storage facility of 3 MVA and 9 MWh seems to be capable of limiting curtailment to 11%. However, the more accurate 1-min case shows a higher volume of curtailment of 13.1% which in turn requires adjusting the size of the storage facility to 6 MVA and 18 MWh. This highlights the importance of the control stage in accurately sizing the storage.

Also, the results clearly show (as previously concluded) that the difference in curtailment reduces as the storage size increases. Therefore, the use of simplified hourly profiles may be considered adequate when sizing storage in cases where significant reductions of curtailment are required. Nonetheless, it is still important to realistically model control aspects in order to truly quantify the curtailment level to be achieved and assess the potential benefits of storage in reducing curtailment. For example, the reduction in curtailment for a storage size of 15 MVA, 45 MWh is 8.5% (13.8% to 5.3%) considering hourly resolution profiles, while it is actually 13% (18.8% to 5.9%) using the 1-min

profiles.

Table 6.3: Curtailment for Different Sizes of Storage and Data Granularity

Storage size		Curtailment (%)		
MVA	MWh	60-min	1-min	Error
-	-	13.8	18.8	5.0
1	3	12.7	15.5	2.8
3	9	10.9	13.1	2.1
6	18	8.1	10.8	2.7
9	27	7.0	8.8	1.8
12	36	6.3	7.2	0.9
15	45	5.3	5.9	0.6

6.6.4 Size of Storage "Two-Stage Iterative Framework"

The optimal storage size at bus 205 is found using the storage sizing framework to achieve a desired curtailment level of 9% which is half the curtailment that could result from the curtailment-only scheme (before storage). The optimal size is found for both storage with a unity power factor and storage with a controllable power factor. The tolerance is set to +/- 1% (i.e., the final actual curtailment level must be within 8% and 10%). The final storage sizes obtained from the iterative process after three iterations are presented in Table 6.4. It can be noticed that controlling the power factor of storage allows a reduction in both the apparent power rating and energy capacity of the required storage facility of approximately 50%. This highlights the importance of using the reactive power capability of storage facilities to reduce the adopted size of a storage facility.

Also, the sizing approach provides increased accuracy and a smaller size of storage facility compared to results achieved using a trial and error approach. For example, using the two-stage storage sizing approach, the size of storage facility required to achieve the desired curtailment level, considering the unity power factor, is 8.7 MVA and 21.2 MWh. In contrast, and according to Table 6.3, the size of storage facility that can be considered

feasible to achieve a curtailment level close to the desired one (9%) and within the defined tolerance (of 1%) is 9 MVA and 27 MWh, which is greater in size than that provided by the storage sizing approach.

Table 6.4: Iterative Storage Sizing at Bus 205 for 9% *Desired Curtailment*

Storage and Curtailment	Storage size (MVA)	Storage size (MWh)	Second Stage Actual curtailment (%)
Unity PF	8.7	21.2	9.5
+/-0.95PFc	4	9	8.9

6.7 Case Study: Multiple Storage Facilities

This section investigates the two-stage sizing framework in a more complex environment, considering multiple storage facilities and adopting different Active Network Management (ANM) schemes to increase the flexibility in solving congestion and voltages issues. The potential benefits of incorporating further ANM schemes into the adoption of smaller storage capacities are also quantified. The studied horizon is extended for the first week of February 2010. The capacities of firm wind generation in the UK 33 kV network (Fig. 6.4) are increased by 16 MW to achieve the maximum capacity that can be connected without voltage or congestion issues. This corresponds to 6, 2 and 8 MW connected at buses 201, 205 and 210, respectively.

A further 16 MW of total controllable wind farms are connected to the network. To demonstrate the benefits of implementing optimal storage sizing in combination with power factor control, as well as other ANM schemes, the controllable DG units are located in such a way that voltage issues also become more critical (3, 10 and 3 MW at buses 201, 205 and 210, respectively). All of the controllable generators are capable of operating with power factor between 0.95 inductive and capacitive according to UK requirements [121].

Similar to Section 6.6.5, the Level 1 mono-period AC OPF is used to calculate the curtailment that would be needed if no other solution was available. The resulting

curtailment is 113.8 MWh (i.e., 11.1% of the available wind resource for the studied week). The curtailment levels for the controllable DG at buses 201, 205 and 210 are 18.5%, 11.1% and 3.8%, respectively. To reduce curtailment, three storage facilities are placed at the same locations as the controllable DG plants. The optimal storage sizes found by the approach are presented in Table 6.5 for 5% and 0% *desired curtailment* levels and considering different ANM schemes. A tolerance of +/- 1% is used which defines the stopping criteria of the iterative process. For 0% *desired curtailment* levels, the final *actual curtailment* level must be below 1%.

To quantify the benefit of adopting different ANM schemes in reducing the size of storage facilities, the overall capital cost is also presented (in p.u.) according to the proxy adopted in Equation (6.1). For 5% *desired curtailment* and considering storage with a unity power factor, no storage facility is placed at bus 210; this is due to the small volume of curtailment from the DG connected to this bus compared to the other DG sites. However, for 0% *desired curtailment*, the storage facilities are placed at all the potential locations to effectively avoid curtailment. The storage at bus 205 has the largest power rating and energy capacity available, to solve voltage issues at this bus in addition to congestion at lines 200-201 and 200-210. Furthermore, the total storage energy capacity required at 0% *desired curtailment* is approximately 57% of the total volume of curtailment, demonstrating the importance of discharging in adopting smaller energy capacities.

The reactive power capability of storage facilities enables the solution of voltage rise issues by the consumption of reactive power using reduced charging power which in turn reduces the overall sizes of storage facilities, in particular the energy capacities. For 5% *desired curtailment*, the capital cost is reduced by 27% and 38% by maintaining the power factor of storage between +/-0.975 and +/- 0.95, respectively. For 0% *desired curtailment*, smaller cost reductions of 13% and 16% are obtained for storage power factor control between +/-0.975 and +/- 0.95, respectively.

In addition, active management of the OLTC at the BSP and the DG power factor provide flexibility with which to solve voltage issues which in turn reduces dramatically the overall capital cost of storage facilities (e.g., 83% and 42% for *desired* curtailment of 5% and 0%, respectively) compared to only using storage with unity power factor. Furthermore, there is no storage facility placed at bus 205 as voltage issues are solved mainly by the OLTC. It can also be seen that using the reactive capability of storage simultaneously with the OLTC and DG power factor does not provide further cost reduction.

The marginal benefits achieved by increasing the energy capacity of a storage facility to increase the harvested energy decrease at larger energy capacities. For example, 28 MWh (unity power factor) is required to reduce curtailment by 6% compared to an extra 40 MWh for a further reduction of 5%.

It is also important to highlight that the number of charge/discharge cycles for the analysed week is less than five for all the ANM schemes, which in turn will not affect the lifespan of storage that corresponds to 4000 cycles over ten years (7.7 cycles/week) [80]. In practice, a more conservative approach may be needed to avoid ageing storage by imposing more limitations on the minimum stored energy.

It is worth noting that three iterations are required to achieve 5% curtailment for all the ANM schemes, thus highlighting the need to validate the curtailment levels at high resolutions to accurately size storage facilities for a particular curtailment level. However, as the volume of the extracted energy is increased, the difference in the curtailment level between 60-min and 1-min becomes smaller, and thus less iteration is needed. In this respect, only one iteration is required at 0% desired curtailment.

The computational intensity of the proposed approach are mostly dependent on the planning horizon and the corresponding number of samples. The most demanding case explored in this work corresponds to a horizon of 1 week and 1-min resolution profiles (i.e., 10,080 time steps) and resulted in a simulation time of around 3 minutes for the first

stage (planning) and around 20 minutes for the second stage (control). This time is reduced by approximately 1/7 for the cases limited to one day (section VI). All the simulations presented in this and the previous sections here were carried out on a laptop with an Intel Core i7 2.2 GHz processor and 8 GB of RAM.

Table 6.5: Two Stage Storage Sizing (MVA/MWh)

Storage and Curtailment	Additional Flexibility	5% Desired Curtailment					0% Desired Curtailment				
		Storage size per bus MVA/MWh			Total MVA/MWh	Cost (p.u.)	Storage size per bus MVA/MWh			Total MVA/MWh	Cost (p.u.)
		201	205	210			201	205	210		
Unity PF	-	1.5/13.4	3.3/15.2	-	4.8/28.6	31.8	1.9/20.5	5.8/42.1	0.6/1.7	8.3/64.3	69.9
+/0.975PFc	-	1.8/6.3	3.1/13.5	-	4.9/19.8	23.1	2.0/24.6	3.8/26.7	1.1/4.8	6.9/56.1	60.7
+/0.95PFc	-	1.6/6.9	3.4/9.4	-	5.0/16.3	19.6	2.3/25.9	3.2/22.1	1.3/5.8	6.8/53.8	58.4
Unity PF	OLTC+ DG PF	1.1/4.9	-	-	1.1/4.9	5.6	2.8/28.5	-	1.8/9.4	4.6/37.9	41.0
+/0.975PFc	OLTC+ DG PF	1.1/4.8	-	-	1.1/4.8	5.5	2.8//28.3	-	1.8/9.4	4.6/37.7	40.8
+/0.95PFc	OLTC+ DG PF	1.2/4.7	-	-	1.2/4.7	5.5	2.8/28.3	-	1.8/9.4	4.6/37.7	40.8

6.8 Comparison with Other Storage Sizing Approach

To further highlight the benefits of adopting the proposed storage sizing approach to provide more accurate sizing of storage facilities compared to those proposed in the literature, the approach presented in [29] is adopted and developed. It uses the control scheme to size storage facilities for 0% desired curtailment, without the need for a trial and error approach. Basically, the power rating and energy capacity of the storage facility are initially set to relatively large values. Then, the optimum size of a storage facility is found from the maximum power output and energy store level achieved during the simulation period. However, it is important to note that the adopted control scheme in this approach does not provide a comprehensive and general formulation to control the storage facilities wherein all the storage facilities are required to have the same operation mode (charging and discharging). Also, the reactive power capability of storage facilities and DG plants are not explicitly formulated. In addition, this approach does not consider the minimum stored energy constraint and nor does it ensure that charging is limited so as to reduce curtailment. All of these gaps are covered in the proposed control stage in this work. Therefore, to cater for the above gaps in the control schemes used in [29], they are replaced by the proposed control stage in this work. This sizing approach will be called the "control-only storage sizing approach" in the following sections.

In the control-only storage sizing approach, the second control stage is used to find the minimum sizes of storage facilities for 0% desired curtailment, without the use of the first stage and the iterative process. To find the minimum size that could accommodate the total volume of curtailment, the power and energy constraints for all the storage facilities first have to be relaxed. Indeed, due to the design of the decision-making algorithm at the second control stage as bi-level, the store level and the power output during charging mode will only rise to the levels that prevent curtailment even if the energy and power constraints of storage are relaxed.

The apparent power ratings of all the energy storage facilities are set to large values higher than the maximum curtailed power across all the DG plants (before the connection of storage facilities). On the other hand, the energy capacities are also set to large values higher than the total volume of energy curtailment from all the DG plants considering the maximum depth of discharge (80%). For example, if it is assumed that the volume of curtailment is 100 MWh, the energy capacity of a storage facility will be set to 100/0.8= 125 MWh.

The application of the control stage for each minute within the planning horizon allows determination of the power and energy needs of each storage facility. The apparent power rating for a storage facility is its maximum apparent output power during the planning horizon. Based on the difference between that maximum store level E_{st}^{max} reached throughout the planning horizon and the minimum (i.e., 20% of the initially adopted value), the required storage capacity for each storage facility can be calculated by Equation (6.28).

$$E_{st}^{rated} = \frac{E_{st}^{max} - E_{st}^{min}}{DoD^{max}} \tag{6.28}$$

Case Study: Multiple Storage Facilities

Following the control-only storage sizing approach (adopted and developed from [29]), the control stage is used to find the minimum sizes of storage facilities that accommodate all volumes of curtailment (0% desired curtailment) during the analysed week for the case study of multiple storage facilities, considering a unity power factor for all storage facilities.

Since the maximum curtailed power required to manage constraints is about 10 MW, the power ratings for all the storage facilities are set to this value. The energy capacities of the storage facilities are set to 143 MWh in order to accommodate the total volume of energy

curtailment (113.8 MWh), taking into account 80% maximum depth of discharge.

Fig. 6.10 shows the stored energy of the storage facility at bus 201 for the first three days of February 2010 (the period that determines the size of storage facilities). It can be seen that, although the energy capacity is 143 MWh, the maximum store level throughout the week is increased to just 64 MWh. This highlights the benefits of adopting the bi-level optimisation approach, which limits charging for curtailment and also allows quick discharging when network constraints are not binding. In this respect, the required storage capacity to prevent curtailment is 44.2 MWh, based on Equation (6.28), and the corresponding apparent power rating is 9.98 MVA according to the maximum output of storage during the analysed period.

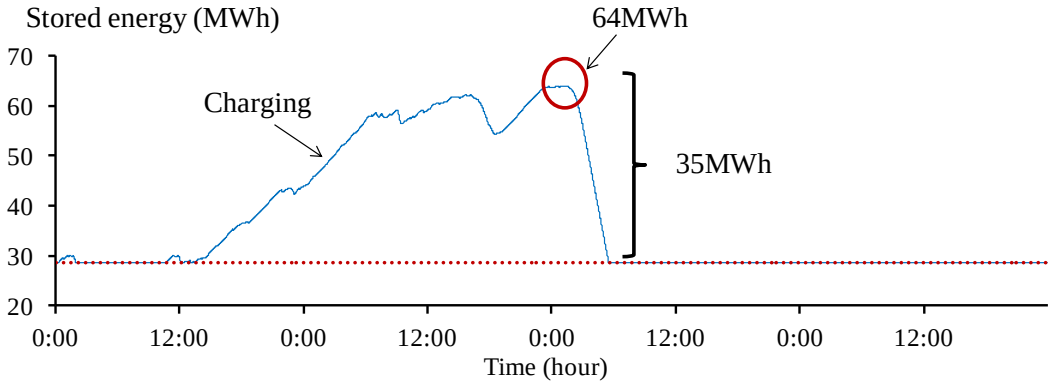

Fig. 6.10 Stored energy MWh considering storage with unity power factor during the first three days of February 2010

The resultant sizes of the storage facilities using the control-only storage sizing approach (adopted and developed from [29]) are presented in Table 6.6 and compared with those found using the proposed two-stage storage sizing approach.

It can be seen that the proposed two-stage storage sizing approach provides slightly smaller total energy capacities than the control-only storage sizing approach. In addition, much smaller power ratings of storage facilities can be obtained by the proposed two-stage

approach. The overestimation of power ratings in sizing the storage facilities using the control-only storage sizing approach is due to the adopted objective in the control stage to maximise the discharged power up to the available headroom in the network when it is technically possible. Thus, the power ratings of storage facilities are mainly determined according to the discharged power output.

Table 6.6: Sizes of Storage Facilities Using the Proposed Two Stage Sizing Algorithm and the Control-only Sizing Approach (adopted and developed from [29])

Storage Sizing Approach	0% Desired Curtailment				
	Storage size per bus MVA/MWh			Total MVA/MWh	Cost (p.u.)
	201	205	210		
Proposed two stage approach	1.9/20.5	5.8/42.1	0.6/1.7	8.3/64.3	69.9
Control-only Sizing Approach	9.98/44.2	9.98/9.7	9.98/13.2	29.9/67.1	87.2

In addition, the control-only storage sizing approach (adopted and developed from [29]) can only be used for a zero *desired curtailment* level. In contrast, the proposed two-stage storage sizing is general and is modelled to find the sizes of storage facilities for any *desired curtailment* level.

6.9 Summary of Chapter 6

This work presents a two-stage iterative framework to find the minimum size of multiple storage facilities (power and energy capacities) in order to reduce curtailment whilst managing congestion and voltages. The first stage uses a multi-period AC Optimal Power Flow (OPF) across the studied horizon to obtain initial storage sizes considering hourly wind and load profiles. The second stage adopts a high granularity minute-by-minute control driven by a mono-period bi-level AC OPF to tune the first-stage storage sizes according to the actual curtailment. Congestion and voltages are managed through the optimal control of storage (active and reactive power), on-load tap changers, DG power

factor and DG curtailment as a last resort.

The proposed approach is applied to the UK 33 kV network presented in Chapter 4, to which multiple wind farms and storage sites are added. One-min resolution wind and load profiles for the first week of February 2010 are used.

The following summarises the key points in this chapter:

- The planning stage (first stage) was effective in producing initial storage sizes by adopting hourly profiles and a multi-period AC Optimal Power Flow (OPF).

- From the control perspective (second stage), the results show the effectiveness of the proposed mono-period bi-level AC OPF in ensuring the adequate use of the charging, discharging and idling modes of the storage facilities to minimise curtailment.

- The benefits of incorporating further flexibility were also assessed. By using the reactive power capabilities of storage facilities, it is possible to reduce storage sizes particularly when voltage issues prevail. The combined active management of OLTCs and power factor of DG plants resulted in the most significant benefits in terms of the required storage sizes.

- The proposed two-stage storage sizing approach provides a more accurate and smaller size of storage facility compared to those found using a trial and error approach, as mostly adopted in the literature.

- The benefits of increasing the energy capacity of a storage facility in terms of harvested energy decreases at larger energy capacities.

- It is vital that high granularity data is used to truly quantify the curtailment level that could actually be achieved by a given storage facility. The use of simplistic

hourly profiles was found to underestimate storage sizes (for the adopted wind and load profiles).

- The proposed two-stage planning framework provides slightly smaller total energy capacities, and significantly smaller power ratings, than another storage sizing approach proposed in the literature (adopted and developed from [29]). Also, the proposed two-stage storage sizing approach is general and is modelled to find the sizes of storage facilities for any *desired curtailment* level.

Chapter 7: Conclusions and Future Work

7.1 Introduction

This chapter provides a summary of the thesis, conclusions and potential future work.

7.2 Thesis Summary

The transition towards a low-carbon energy system is placing considerable challenges on distribution network operators in terms of accommodating the increasing levels of renewable DG, particularly wind generation which has an important role to play in achieving the environmental and energy targets. To facilitate the connection of larger volumes of DG without the need for expensive network reinforcements, and with faster connections, Chapter 2 discusses the importance of moving away from passive connection approaches that provide firm DG connection (not controllable) based on the worst-case scenario (maximum generation and minimum demand) to an approach where DG plants and controllable network elements are actively managed in real time.

Following a thorough literature review on the ANM control schemes, it is highlighted in Chapter 3 that, once more DG plants and network elements are actively controlled using different control ANM schemes, they will be required to move to a more advanced distribution Network Management System (NMS). Controllable devices and network participants will then be actively and optimally managed in order to simultaneously manage congestion and voltages. In addition, to accelerate the transition towards low-carbon energy systems and provide positive business cases for DG developers, advanced

NMS should consider resorting to other methods than just DG curtailment for managing network constraints.

In this context, this thesis aims to provide a model for advanced distribution NMS that aim to minimise energy curtailment from DG plants whilst simultaneously managing voltage and thermal constraints in close to real-time through the optimal control of OLTCs, DG power factor, storage devices and generation curtailment as a last resort. This research also aims to provide solutions to the operational challenges introduced by the uncertainties in wind power (i.e., variability).

Due to the relatively high investment costs of energy storage facilities compared to other ANM control solutions, this thesis also aims to provide an adequate storage sizing framework to determine the power ratings and energy capacities of storage facilities in the context of active distribution networks.

To achieve the above objectives in this research, and to tackle the relevant gaps in the literature, the following sections summarise the work undertaken in Chapter 4, Chapter 5 and Chapter 6.

Chapter 4: Deterministic Distribution Network Management Systems

A comprehensive distribution NMS is proposed, which aims to minimise DG curtailment whilst simultaneously managing network voltage rises and congestion in close to real-time, considering the realistic modelling of control and adopting 1-min resolution time series data. The AC Optimal Power Flow (OPF), which has been used in the planning perspective in [12], is adapted and expanded for realistic operational purposes to produce the optimal set points for OLTCs, DG reactive power output and generation curtailment as a last resort. Also, the AC OPF is tailored to comply with the existing firm connection agreements. The performance of the deterministic-based NMS is evaluated through time-series analysis for one week using 1-min resolution data for both demand and generation in

terms of voltage compliance with the EN50160 standard, congestion, capacity factor of wind farms and, crucially, volume of control actions.

Chapter 5: Risk-Based Distribution Network Management Systems

The deterministic NMS is extended to a risk-based system to allow the adoption of multi-minute control cycles in order that the volume of actions from OLTCs and distributed generation plants can be reduced whilst effectively catering for the effects of wind power uncertainties. The AC OPF is extended to produce optimal set points for the active elements, to both minimise DG curtailment and reduce/avoid operational problems (i.e., the risk of thermal overloading and voltage rise) that may result from wind uncertainty. A risk level is used to determine the extent to which congestion and voltage rise could exist during a control cycle. The performance of the risk-based NMS controller is compared against the deterministic NMS controller for different control cycles.

Chapter 6: Optimal Sizing of Storage Facilities to reduce Generation Curtailment

A two-stage planning framework that incorporates real-time control aspects is proposed, aimed at determining minimum sizes (power ratings and energy capacities) of storage facilities at multiple locations, required to reduce curtailment from DG plants whilst managing voltages and congestion. The first stage uses a multi-period AC Optimal Power Flow across the studied horizon to consider simplified hourly wind and load profiles. By limiting the search space, this stage is capable of procuring initial storage sizes (power and energy). The second stage adopts a high granularity minute-by-minute control driven by a mono-period bi-level AC OPF. This control minimises the required curtailment using the first-stage storage sizes, so that the actual curtailment can be assessed over the studied horizon. This assessment is then used to tune the first-stage storage sizes accordingly. Congestion and voltages are managed through the intelligent control of storage (active and reactive power), OLTCs, DG power factor and DG curtailment as a last resort. One-min resolution wind and load profiles are also used.

7.3 Research Contributions and Achievements

Distribution Network Management Systems

An innovative and advanced distribution NMS is developed in this research which bridges the gaps in the literature. The key and the original contributions are summarized as follows:

- For the first time, a risk-based AC OPF decision-making algorithm is developed that allows the adoption of multi-minute control cycles in advanced NMS to reduce the volume of control actions by reducing the effect of wind power uncertainties and controlling the risk of overloading and voltage excursions throughout the control cycle.

- A methodology that allows an investigation in detail of the benefits and impacts of adopting different control cycles (key metrics: voltage compliance with BS EN50160 standard, congestion, capacity factor of wind farms and, crucially, volume of control actions). This provides DNOs with an important tool to understand benefits and challenges of departing from deterministic multi-second-based control cycles into risk-based longer cycles.

Optimal Sizing and Control of Storage Facilities

The proposed planning framework to size storage facilities is innovative and bridges the gaps in the literature. The key and the original contributions are summarized as follows:

- The development of an innovative planning framework for sizing storage facilities that embeds the high granularity modelling of control aspects to capture accurately the actual power and energy needs of storage facilities. The proposed framework allows determination of the minimum size (power and energy) of multiple storage

facilities without the need for a trial and error approach to explore large combinations of power ratings and energy capacities.

- The development of an innovative decision-making algorithm (AC OPF-based), adequate to optimally control in close to real-time the active and reactive power of storage facilities, OLTCs and DG power factor in addition to generation curtailment as a last resort.

The original contributions in this thesis presented lead to peer reviewed journal and conference papers listed in Appendix C.

7.4 Conclusions

Advanced Distribution Network Management Systems

This section presents the general conclusions reached as a result of the application of the deterministic and risk-based NMS approaches to 33 kV distribution networks (presented in Chapter 4) using minute by minute simulation for one week.

- The realistic modelling of control aspects allows an assessment of the effectiveness of the proposed NMS of managing network constraints for different control schemes and control cycles.

- In the deterministic approach, the adoption of shorter control cycles (e.g., 1 min) allows a close following of the variability of wind resource (particularly from firm generation) and better management of congestion and voltages. However, this improvement is at the expense of the volume of control actions: the number of tap changes and the total variation of the DG set points (the sum of absolute changes).

- The risk-based approach allows a departure from deterministic multi-second-based control cycles into longer control cycles, which in turn reduces dramatically the

volume of control actions from OLTCs and DG plants.

- Tighter risk levels improve the overall performance of the NMS optimisation (in terms of congestion and voltages) even with longer control cycles (e.g., 15 min). However, this increases the volume of curtailment.

- Conservative thresholds (90% of the thermal capacity) in the deterministic NMS effectively keep power flows within limits and avoid overloading due to changes in wind power throughout the control cycle. However, the harvested energy is below that acheivable using the risk-based approach using a zero risk level (i.e., dynamic thresholds) for the same control cycle, which also provides similar performance to manage network constraints.

- Controlling the DG power factor and OLTC allows voltage issues to be solved, which in turn leads to increased levels of energy harvested from wind power plants compared to only using generation curtailment.

Optimal Sizing of Storage Facilities to Reduce Generation Curtailment

This section presents the general conclusions gained from the application of the proposed two-stage storage sizing planning framework to the 33 kV network (presented in Chapter 6). It considers multiple wind farms and storage facilities using a 1-min resolution of wind and load data for one week.

- The use of simplistic hourly profiles underestimates storage sizes (for the adopted wind and load profiles) required to achieve a desired curtailment level. This in turn shows the importance of embedding high granularity data in the storage sizing framework in order to truly quantify the curtailment level that could actually be achieved by a given storage facility.

- By using the reactive power capabilities of storage facilities it is possible to reduce

storage sizes, particularly when voltage issues prevail. The combined active management of OLTCs and power factor of DG plants results in the most significant benefits in terms of the required storage sizes.

- The proposed two-stage storage sizing approach allows improving the accuracy to size storage facilities compared to the trial and error approaches mostly adopted in the literature.

- The proposed two-stage planning framework provides slightly smaller total energy capacities and significantly smaller power ratings than another storage sizing approach proposed in the literature at [29], which only uses the control stage to size the storage facilities.

7.5 Future Work

This section discusses potential future research work by extending the work carried out in this thesis.

Distribution State Estimation

As discussed earlier in Section 4.3.1, it is assumed that the measurements are perfectly received (i.e., without errors) and that the network is fully observable in the proposed NMS. However, this assumption is not accurate in practice, given the need for accurate information and a high level of observability to actively control active network elements. Therefore, the NMS should interface with a state estimator in order to extend the observability of the network using fewer monitoring points and to cope with errors in the measurements.

The formulation of the risk-based AC OPF can be further developed to consider errors in the measurements similar to the adopted methodology used to produce scenarios of wind power changes. This will require statistical analysis of the errors from the state estimation.

Commercial Arrangements

Commercial arrangements for controllable DG plants have not been considered (i.e., the AC OPF has purely considered the best technical solution). In practice, controllable DG plants agree with DNOs on specific commercial arrangements, such as the way that curtailment will be carried out. Although this has not been considered in this work (i.e., the optimal set points are found on technical grounds only), approaches such as Last In First Out (LIFO) or Pro Rata can be implemented [129], [130]. In addition, time of use network charges (positive/negative) can be adopted to increase the match between generation and demand so that network issues can be solved [131]. This will in turn encourage DG developers to adopt storage facilities to increase their revenues.

Wind Power Transitions

To provide a robust quantification of wind power transitions, the historical assessment should be applied over a significant time period. In this work, 1-min resolution data collected over one month was used. This analysis may be further improved by adopting a sliding window, i.e. by updating the historic data periodically (e.g., each day or week) to consider the new wind power measurements

Control of Storage Facilities Considering the Realistic Modelling of Control Aspects

The incorporation of storage facilities into the proposed NMS considering realistic control aspects will increase the challenge of handling the uncertainties introduced by the wind, given that a decision made for the current state might not necessarily be suitable for the next control cycle. For instance, if a discharge action is initiated and a sudden gust occurs, this may lead to an overload.

The mono-period bi-level AC OPF should be developed to cater for the risk of wind power changes, as has been developed in the risk-based NMS. Also, this may allow an increase in

the control cycle, which will reduce the volume of control actions from storage and, thus, preserve the life cycle of the storage facility.

Planning of Storage facilities

The focus of the planning framework presented in Chapter 6 is to provide an approach able to incorporate real-time control aspects to size storage facilities in future Network Management Systems (NMS). Due to the availability of high granularity time series data of wind and load profiles, one week planning horizon is only adopted.

To provide adequate assessment of the volume of curtailment from DG plants, long economic planning horizon is required (i.e., at least one year) so that the economics issues related to the integration of storage can be properly addressed. In order to do so and to cater for the computational burden, the first planning stage has to be modified by the adoption of representative days/weeks. In contrast, the second stage and the iterative process can be directly adopted without modifications.

In addition, further work can be carried out by considering other applications of storage facilities (in addition to curtailment minimisation) to increase the benefits from storage facilities, for examples peak shaving, price arbitrage, energy losses reduction.

Future Low Voltage NMS

The proposed NMS in this work can be extended and adapted to actively manage network constraints in future low voltage distribution networks so that larger volumes of small scale domestic PV systems can be connected without the need to trigger network reinforcements. This involves the expansion of the AC OPF into three-phase unbalanced AC OPF required to model low voltage networks. The full AC unbalanced OPF can produce set points during each control cycle of the controllable PV systems (active power and reactive power output) and the tap position in distribution substations as demonstrated in Fig. 7.1. The use

of centralised LV NMS will require extensive levels of load and generation monitoring, which may not be available in the near future at this voltage level. However, the use of the OPF-based control approach (all controllable network elements are optimally managed) can provide theoretical bounds on the benefits of actively managing network constraints.

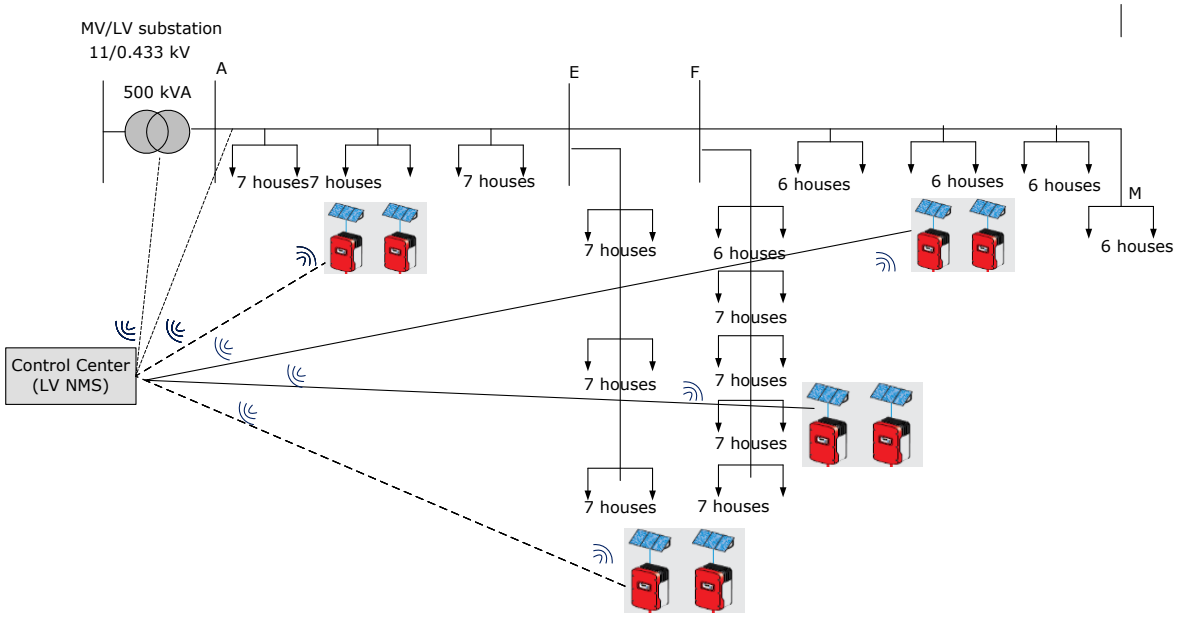

Fig. 7.1 Future LV NMS

Hierarchical Distributed NMS

The adoption of a single control centre to optimally control active elements in large geographical areas of distribution networks may not be an economical and reliable solution, particularly due to the extra expenses in relation to the data acquisition process and communications. Also, the computational burden required to model the networks in the optimisation engine will increase significantly.

Therefore, this requires in practice a transition towards hierarchal distributed control schemes in a smart grid environment. Fig. 7.2 is an example of such a system and illustrates the interactions and flows of control signals between NMS at different voltage

levels. Although this design can meet wide system objectives, its practical implementation may face a number of challenges that need to be tackled in future research. The challenges include, for example, the network areas controlled by each NMS, selection of control cycles, decision-making algorithms (rule-based/optimisation-based) and interactions between voltage levels.

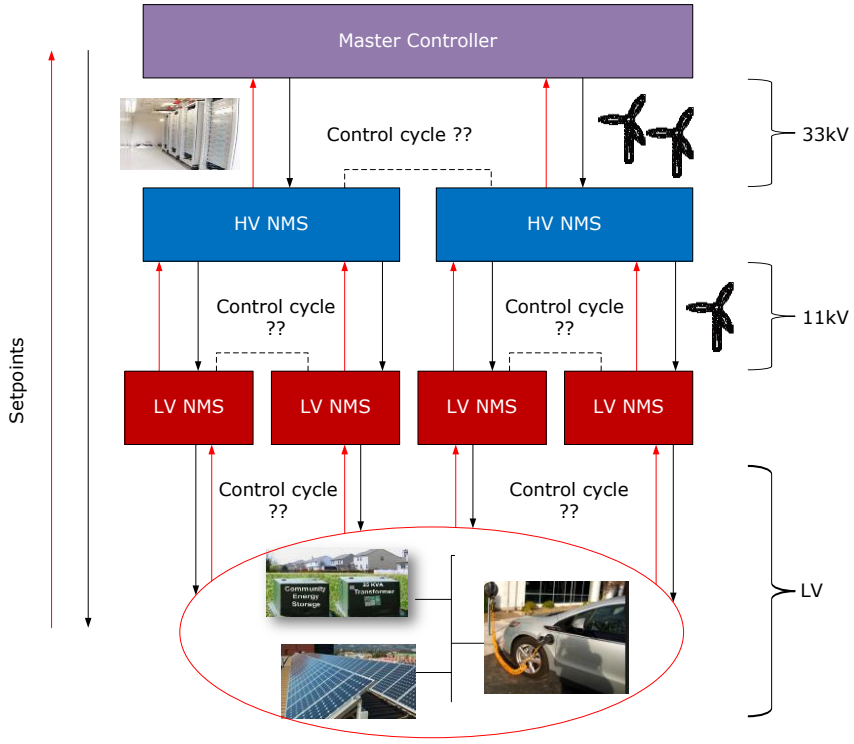

Fig. 7.2 Hierarchal Distributed Control NMS

References

[1] United Nations Framework Convention on Climate Change - UNFCCC. (2006, Aug.). Kyoto protocol - 1997. [Online]. Available: http://unfccc.int/essential_background/kyoto_protocol/items/1678.php

[2] Climate Change Act. "Climate Change Act 2008," 2008. [Online]. Available: http://www.legislation.gov.uk/ukpga/2008/27/contents

[3] Department of Energy and Climate Change (DECC), "*2050 Pathways analysis*," Jul. 2010.

[4] "Renewable energy roadmap," *Department of Energy and Climate Change (DECC)*, 2011.

[5] "UK Future Energy Scenarios," *National Grid*,, 2014.

[6] Office of Gas and Electricity Markets (Ofgem). Renewables Obligation (RO). [Online]. Available: https://www.ofgem.gov.uk/environmental-programmes/renewables-obligation-ro

[7] Office of Gas and Electricity Markets (Ofgem). Feed-in-Tariff (FIT) scheme. [Online]. Available: https://www.ofgem.gov.uk/environmental-programmes/feed-tariff-fit-scheme

[8] N. Jenkins, R. Allan, P. Crossley, D. Kirschen, and G. Strbac, *Embedded generation*. London: Institution of Electrical Engineers, 2000.

[9] G. W. Ault, R. A. F. Currie, and J. R. McDonald, "Active power flow management solutions for maximising DG connection capacity," *in Proc. 2006 IEEE/PES General Meeting*, pp. 5.

[10] A. Collinson, F. Dai, A. Beddoes, and J. Crabtree, "Solutions for the Connection and Operation of Distributed Generation," Report to UK Departement of Trade and Industry (DTI), *EA Technology*, 2003.

[11] R. A. F. Currie, G. W. Ault, C. E. T. Foote, and J. R. McDonald, "Active power-flow management utilising operating margins for the increased connection of distributed generation," *IET Proceedings Generation, Transmission & Distribution*, vol. 1, no. 1, pp. 197-202, Jan. 2007.

[12] L. F. Ochoa, C. Dent, and G. P. Harrison, "Distribution network capacity assessment: variable DG and active networks," *IEEE Transactions on Power Systems*, vol. 25, no. 1, pp. 87-95, Feb. 2010.

[13] L. F. Ochoa, A. Keane, and G. P. Harrison, "Minimizing the reactive support for distributed generation: Enhanced passive operation and smart distribution networks," *IEEE Trans. on Power Systems*, vol. 26, no. 4, pp. 2134-2142, Nov. 2011.

[14] T. Sansawatt, L. F. Ochoa, and G. P. Harrison, "Smart decentralized control of DG for voltage and thermal constraint management," *IEEE Trans. on Power Systems*, vol. 27, no. 3, pp. 1637 - 1645, 2012.

[15] J. P. Barton and D. G. Infield, "Energy storage and its use with intermittent renewable energy," *IEEE Transactions on Energy Conversion* vol. 19, no. 2, pp. 441 - 448, 2004.

[16] N. Wade, P. Taylor, P. Lang, and J. Svensson, "Energy storage for power flow management and voltage control on an 11kV UK distribution network," in *International Conference on Electricity Distribution (CIRED)*, 2009, pp. 1-4.

[17] E. M. Davidson, S. McArthur, C. Yuen, and M. Larsson, "AuRA-NMS: Towards the delivery of smarter distribution networks through the application of multi-agent systems technology," *in Proc. 2008 IEEE/PES General Meeting*, pp. 6.

[18] M. J. Dolan, E.M.Davidson, G. W. Ault, K.R.W.Bell, and S. D. J. McArthur, " Distribution Power Flow Management Utilizing an Online Constraint Programming Method," *IEEE Transactions on Smart Grid*, vol. 4, no. 2, pp. 798 - 805, 2013.

[19] T. Xu, N. S. Wade, E. M. Davidson, P. C. Taylor, S. D. J. McArthur, and W. G. Garlick., "Case-Based Reasoning for Coordinated Voltage Control on Distribution Networks," *Electric Power Systems Research* vol. 81, no. 12, pp. 2088-2098, December 2011 2011.

[20] M. J. Dolan, E. M. Davidson, I. Kockar, G. W. Ault, and S. D. J. McArthur, "Distribution Power Flow Management Utilizing an Online Optimal Power Flow Technique," *IEEE Transactions on Power Systems*, vol. 27, no. 2, pp. 790-799, 2012.

[21] F. Pilo, G. Pisano, and G. G. Soma, "Optimal Coordination of Energy Resources With a Two-Stage Online Active Management " *IEEE Transactions on Industrial Electronics*, vol. 58, no. 10, pp. 4526 - 4537, 2011.

[22] H. Zechun and L. Fu-Rong, "Cost-benefit analyses of active distribution network management, part I : Annual benefit analysis," *IEEE Transactions on Smart Grid,*, vol. 3, no. 3, pp. 1067-1074, 2012.

[23] "Grid 2020: Towards a Policy of Renewable and Distributed Energy Resources," *The Ressnick Stustaiability Institute, ,* 2012.

[24] P. P. Varaiya, F. F. Wu, and J. W. Bialek, "Smart operation of smart grid: Risk-limiting dispatch," *Proceedings of the IEEE*, vol. 99, no. 1, pp. 40-57, Jan. 2011.

[25] P. Daly, M. Power, A. Keane, and D. Flynn, "Operational security at high penetrations of stochastic, non-synchronous generation," in *International Universities Power Engineering Conference (UPEC)*, 2013.

[26] M. J. Dolan, E. M. Davidson, I. Kockar, G. W. Ault, and S. D. J. McArthur, "Reducing Distributed Generator Curtailment Through Active Power Flow Management," *IEEE Transactions on Smart Grid*, vol. 5, no. 1, pp. 149 - 157 2014.

[27] N. Etherden and M. H. J. Bollen, "Dimensioning of energy storage for increased integration of wind power " *IEEE Transactions on Sustainable Energy*, vol. 4, no. 3, pp. 546 - 553 2013.

[28] S. Gill, I. Kockar, and G. W. Ault, "Dynamic optimal power flow for active distribution networks," *IEEE Transactions on Power Systems*, vol. 29, no. 1, pp. 121 - 131 2014.

[29] S. Carr, G. C. Premier, A. J. Guwy, R. M. Dinsdale, and J. Maddy, "Energy storage for active network management on electricity distribution networks with wind power," *IET Renewable Power Generation*, vol. 8, no. 3, pp. 249-259, Apr. 2014.

[30] Y. M. Atwa and E. F. El-Saadany, "Optimal allocation of ESS in distribution systems with a high penetration of wind energy," *IEEE Transactions on Power Systems*, vol. 25, no. 4, pp. 1815-1822, 2010.

[31] M. Nick, R. Cherkaoui, and M. Paolone, "Optimal allocation of dispersed energy storage systems in active distribution networks for energy balance and grid support," *IEEE Transactions on Power Systems*, vol. pp, no. 99, 2014.

[32] G. Carpinelli, G. Celli, S. Mocci, F. Mottola, F. Pilo, and D. Proto, "Optimal integration of distributed energy storage devices in smart grids," *IEEE Transactions on Smart Grid*, vol. 4, no. 2, pp. 985 - 995, 2013.

[33] J. A. Martinez, F. de Leon, A. Mehrizi-Sani, M. H. Nehrir, C. Wang, and V. Dinavahi, "Tools for analysis and design of distributed resources - Part II: Tools for planning, analysis and design of distribution networks with distributed resources," *IEEE Transactions on Power Delivery*, vol. 26, no. 3, pp. 1653-1662, 2011.

[34] L. Alexio, G. Celli, E. Ghiani, J. Myrzik, L. F. Ochoa, and F. Pilo, "A general framework for active distribution network planning," in *CIGRE Symposium* 2013, pp. 1-8.

[35] Y. V. Makarov, P. Du, M. C. W. Kintner-Meyer, C. Jin, and H. F. Illian, "Sizing energy storage to accommodate high penetration of variable energy resources," *IEEE Transactions on Sustainable Energy* vol. 3, no. 1, pp. 34-40, 2012.

[36] L. F. Ochoa and G. P. Harrison, "Using AC optimal power flow for DG planning and optimisation," *in Proc. 2010 IEEE/PES General Meeting*, pp. 7.

[37] C. Dent, L. F. Ochoa, G. P. Harrison, and J. W. Bialek, "Efficient Secure AC OPF for Network Generation Capacity Assessment," *IEEE Trans. on Power Systems*, vol. 25, no. 1, pp. 575-583, Feb. 2010.

[38] F. Gonzalez-Longatt and C. Fortoul, "Review of Distributed Generation Concept: Attempt of Unification," *in Proc. 2005 International Conference on Renewable Energies and Power Quality (ICREPQ)*, pp. 16-18.

[39] T. Ackermann, G. Andersson, and L. Söder, "Distributed generation: a definition," *Electric Power Systems Research*, vol. 57, pp. 195–204, 2001.

[40] D. Sharma and R. Bartels, "Distributed electricity generation in competitive energy markets: a case study in Australia," *The Energy Journal*, pp. 17-39, 1997.

[41] J. Cardell and R. Tabors, "Operation and control in a competitive market: distributed generation in a restructured industry," *The Energy Journal*, pp. 111-136, 1997.

[42] O. Malík and P. Havel, "Active Demand-Side Management System to Facilitate Integration of RES in Low-Voltage Distribution Networks," *IEEE Trans on Sustainable Energy*, vol. 5, no. 2, pp. 673-681, 2014.

[43] L. Canbing, T. Shengwei, C. Yijia, X. Yajing, L. Yong, L. Junxiong, and R. Zhang, "A New Stepwise Power Tariff Model and Its Application for Residential Consumers in Regulated Electricity Markets," *IEEE Trans on Power Systems*, vol. 28, no. 1, pp. 300 - 308, 2013.

[44] M. A. El-Sharkawi, *Electric Energy - An Introduction (3rd Edition)*: Taylor & Francis.

[45] N. Jenkins, J. B. Ekanayake, and G. Strbac, *Distributed Generation*: Institution of Engineering and Technology, 2010.

[46] J. Aho, A. Buckspan, J. Laks, P. Fleming, Y. Jeong, F. Dunne, M. Churchfield, L. Pao, and K. Johnson, "A tutorial of wind turbine control for supporting grid frequency through active power control," *in Proc. 2012 American Control Conference (ACC), 2012*, pp. 3120-3131.

[47] "Electrical Data V90 - 3.0 MW 60 Hz Variable Speed Turbine," Item no. 950027.R1., 2005.

[48] S. Rehman and N. M. Al-Abbadi, "Wind shear coefficient, turbulence intensity and wind power potential assessment for Dhulom, Saudi Arabia," *Renewable Energy*, vol. 33, no. 12, pp. 2653–2660, 2008.

[49] M. L. Ray, A. l. Rogers, and J. G. McGowan, "Analysis of wind shear models and trends in different terrain," *in Proc. 2006 American Wind Energy Association Wind power*

[50] G. Sinden, "Wind power and the UK wind resource," Report to UK department of Trade and Industry (DTI), 2005.

[51] G. Sinden, "Characteristics of the UK wind resource: Long-term patterns and relationship to electricity demand," *Energy Policy*, vol. 35, no. 1, pp. 112-127, 2007.

[52] G. M. Masters, *Renewable and efficient electric power systems*: John Wiley & Sons, 2013.

[53] "Guide to interpreting I-V curve measurements of PV arrays," *Solmetric PVA-600 PV Analyzer, ,* 2011.

[54] G. Simmonds, *Regulation of the UK electricity industry*: University of Bath School of Management, 2002.

[55] E. Lakervi and E. J. Holmes, *Electricity distribution network design*. London: Peter Peregrines Ltd., 1995.

[56] Office of Gas and Electricity Markets (Ofgem). Distribution networks. [Online]. Available: https://www.ofgem.gov.uk/electricity/distribution-networks

[57] G. W. Ault and J. R. McDonald, "Planning for distributed generation within distribution networks in restructured electricity markets," *IEEE Power Engineering Review*, vol. 20, no. 2, pp. 52-54, Feb. 2000.

[58] L. F. Ochoa, A. Padilha-Feltrin, and G. P. Harrison, "Evaluating distributed time-varying generation through a multiobjective index," *IEEE Trans. on Power Delivery*, vol. 23, no. 2, pp. 1132-1138, Apr. 2008.

[59] UK Department of Trade and Industry,, "*The electricity supply, quality and continuity regulations 2002*," Sep. 2002.

[60] S. N. Liew and G. Strbac, "Maximising penetration of wind generation in existing distribution networks," *IEE Proceedings Generation, Transmission & Distribution*, vol. 149, no. 3, pp. 256-262, May 2002.

[61] T. Haggis, "Network design manual," *E. on*, 2006.

[62] M. STOJANOVIC, D. TASIC, and A. RISTIC. (89, Cyclic Current Ratings of Single-Core XLPE Cables with Respect to Designed Life Time. [Online]. Available: http://red.pe.org.pl/articles/2013/5/29.pdf

[63] K. Jarrett, J. Hedgecock, R. Gregory, and T. Warham, "Technical guide to the connection of generation to the distribution network," Report to UK Department of Trade and Industry (DTI), 2004.

[64] PB Power, "Application of fault current limiters," Report to UK Department for Business, Enterprise & Regulatory Reform (BERR), 2007.

[65] S. M. Brahma and A. A. Girgis, "Development of adaptive protection scheme for distribution systems with high penetration of distributed generation," *Power Delivery, IEEE Transactions on*, vol. 19, no. 1, pp. 56-63, 2004.

[66] Union of the Electricity Industry–EURELECTRIC. (2013, Feb). Active Distribution System Management A key tool for the smooth integration of distributed generation. [Online]. Available:

http://www.eurelectric.org/media/74356/asm_full_report_discussion_paper_final-2013-030-0117-01-e.pdf

[67] Scottish and Southern Energy Power Distribution (SSEPD), 2012, Orkney Smart Grid. [Online]. Available: https://www.ssepd.co.uk/OrkneySmartGrid/

[68] K. L. Anaya and M. G. Pollitt, "Finding the Optimal Approach for Allocating and Realising Distribution System Capacity: Deciding between Interruptible Connections and Firm DG Connections," *Faculty of Economics, University of Cambridge*, 2013.

[69] "Strategy decision for the RIIO-ED1 electricity distribution price control. Outputs, incentives and innovation. Supplementary annex to RIIO-ED1 overview paper," *Office of Gas and Electricity Market (ofgem)*, 2013.

[70] "Strategy decision for the RIIO-ED1 electricity distribution price control. Uncertainty mechanisms. Supplementary annex to RIIO-ED1 overview paper," *Office of Gas and Electricity Market (ofgem)*, 2013.

[71] "A smart grid route map," *Electricity Networks Strategy Group*, , 2010.

[72] D. Roberts, "Network management systems for active distribution networks: a feasibility study," Report to UK Department of Trade and Industry (DTI), 2004.

[73] B. Hayes, I.Hernando-Gil, A.Collin, G.Harrison, and S.Djokić, "Optimal Power Flow for Maximizing Network Benefits From Demand-Side Management," *IEEE Trans on Power Systems*, vol. 29, no. 4, pp. 1739 - 1747, 2014.

[74] L. Bird, J. Cochran, and X. Wang, "Wind and solar energy curtailment: Experience and practices in the United States," *National Renewable Energy Laboratory (NREL)*, 2014.

[75] S. N. Liew and T. Moore, "Design and commissioning of active generator constraint for an offshore windfarm," in *International Conference on Electricity Distribution (CIRED)*. Turin, Italy, 2005, pp. 4.

[76] E. H. Camm, M. R. Behnke, O. Bolado, M. Bollen, M. Bradt, C. Brooks, W. Dilling, M. Edds, W. J. Hejdak, D. Houseman, S. Klein, F. Li, J. Li, P. Maibach, T. Nicolai, J. Patino, S. V. Pasupulati, N. Samaan, S. Saylors, T. Siebert, T. Smith, M. Starke, and R. Walling, "Characteristics of wind turbine generators for wind power plants," *in Proc. 2009 IEEE/PES General Meeting*, pp. 5.

[77] A. Ellis, R. Nelson, E. Von Engeln, R. Walling, J. MacDowell, L. Casey, E. Seymour, W. Peter, C. Barker, and B. Kirby, "Reactive power performance requirements for wind and solar plants," *in Proc. 2012 IEEE/PES General Meeting*, pp. 1-8.

[78] P. Lyons, N. Wade, T. Jiang, P. Taylor, F. Hashiesh, M. Michel, and D. Miller, "Design and analysis of electrical energy storage demonstration projects on UK distribution networks," *Applied Energy*, vol. 137, pp. 677-691, 2015.

[79] S. Eckroad and I. Gyuk, "EPRI-DOE handbook of energy storage for transmission & distribution applications,," *Electric Power Research Institute (EPRI)*, 2003.

[80] S. Schoenung, "Energy storage systems cost update," *Sandia National Laboratories*, Albuquerque, New Mexico, 2011.

[81] J. Eyer and G. Corey, "Energy storage for the electricity grid: Benefits and market potential assessment guide," *Sandia National Laboratories*, , 2010.

[82] J. McDowall, "Battery life considerations in energy storage applications and their effect on life cycle costing," *in Proc. 2001 Power Engineering Society Summer Meeting*, , vol. 1, pp. 452-455.

[83] G. Strbac, M. Aunedi, D. Pudjianto, P. Djapic, F. Teng, A. Sturt, D. Jackravut, R. Sansom, V. Yufit, and N. Brandon, "Strategic assessment of the role and value of energy storage systems in the UK low carbon energy future, ," *Report for Carbon Trust*, 2012.

[84] J. Kabouris and C. D. Vournas, "Application of interruptible contracts to increase wind-power penetration in congested areas," *IEEE Trans. on Power Systems*, vol. 19, no. 3, pp. 1642 - 1649, 2004.

[85] R. A. F. Currie, G. W. Ault, R. W. Fordyce, D. F. MacLeman, M. Smith, and J. R. McDonald, "Actively managing wind farm power output," *IEEE Trans. on Power Systems*, vol. 23, no. 3, pp. 1523-1524, Aug. 2008.

[86] E. M. Davidson, M. J. Dolan, S. D. J. McArthur, and G. W. Ault, "The use of constraint programming for the autonomous management of power flows," in *Intelligent System Applications to Power Systems*. Curitiba, 2009, pp. 1-7.

[87] E. M. Davidson, S. D. J. McArthur, M. J. Dolan, and J. R. McDonald, "Exploiting intelligent systems techniques within an autonomous regional active network management system," in *IEEE/ PES General Meeting*. Calgary, 2009, pp. 1-8.

[88] M. J. Dolan, E. M. Davidson, G. W. Ault, F. Coffele, I. Kockar, and J. McDonald, "Using Optimal Power Flow for Management of Power Flows in Active Distribution Networks with Thermal Constraints," in *Universities' Power Engineering Conference (UPEC)*. Glasgow, UK, 2009, pp. 1-4.

[89] J. Mutale, "Benefits of active management of distribution networks with distributed generation," in *IEEE PES Power Systems Conference and Exposition*. Atlanta, 2006, pp. 1-6.

[90] A. E. Kiprakis and A. R. Wallace, "Maximising energy capture from distributed generators in weak networks," *IEE Proceedings Generation, Transmission & Distribution*, vol. 151, no. 5, pp. 611-618, Sep. 2004.

[91] T. Sansawatt, J. O'Donnell, L. F. Ochoa, and G. P. Harrison, "Decentralised voltage control for active Distribution Networks," in *Universities Power Engineering Conference (UPEC)*. Glasgow, 2009, pp. 1-5.

[92] P. N. Vovos, A. E. Kiprakis, A. R. Wallace, and G. P. Harrison, "Centralized and distributed voltage control: Impact on distributed generation penetration," *IEEE Trans. on Power Systems*, vol. 22, no. 1, pp. 476-483, Feb. 2007.

[93] M. Fila, J. Hiscock, D. Reid, P. Lang, and G. A. Taylor, "Flexible voltage control in distribution networks with distributed generation - Modelling anlaysis and field trial comparison," in *nternational Conference on Electricity Distribution (CIRED)*. Prague, Czech Republic, 2009, pp. 1-4.

[94] M. Fila, G. A. Taylor, J. Hiscock, M. R. Irving, and P. Lang, "Flexible voltage control to support Distributed Generation in distribution networks," in *Universities Power Engineering Conference (UPEC)*. Padova, 2008, pp. 1-5.

[95] M. Fila, "Modelling, Evaluation and Demonstration of Novel Active Voltage Control Schemes to Accommodate Distributed Generation in Distribution Networks," PhD dissertation, Brunel Institute of Power Systems (BIPS), Brunel University, Uxbridge, UK, 2010.

[96] M. Hird, N. Jenkins, and P. Taylor, "An active 11 kV voltage controller: practical considerations," in *International Conference on Electricity Distribution (CIRED)*. Barcelona, 2003, pp. 1-4.

[97] H. Y. Li and H. Leite, "Increasing distributed generation using automatic voltage reference setting technique," in *IEEE/PES General Meeting* Pittsburgh, 2008, pp. 1-7.

[98] S. L. White, "Active local distribution network management for embedded generation - GEN AVC," Report to UK department of Trade and Industry (DTI), 2005.

[99] C. M. Hird, H. Leite, N. Jenkins, and H. Li, "Network voltage controller for distributed generation," *IEE Proceedings Generation, Transmission and Distribution*, vol. 151, no. 2, pp. 150 - 156, 2004.

[100] Q. Zhou and J. W. Bialek, "Generation curtailment to manage voltage constraints in distribution networks," *IET Proceedings Generation, Transmission & Distribution*, vol. 1, no. 3, pp. 492-498, 2007.

[101] G. Strbac, N. Jenkins, M. Hird, P. Djapic, and G. Nicholson, "Integration of operation of embedded generation and distribution networks," Report to UK Department of Trade and Industry (DTI), May 2002.

[102] P. C. Taylor, T. Xu, N. S. Wade, M. Prodanovic, R. Silversides, T. Green, E. M. Davidson, and S. McArthur, "Distributed voltage control in AuRA-NMS," in *IEEE/PES General Meeting*. Minneapolis, 2010, pp. 1-7.

[103] T. Boehme, G. P. Harrison, and A. R. Wallace, "Assessment of distribution network limits for non-firm connection of renewable generation," *IET Renewable Power Generation*, vol. 4, no. 1, pp. 64 - 74, 2010.

[104] J. Robertson, G. P. Harrison, and A. R. Wallace, "A receding-horizon OPF for active network management," in *International Conference on Electricity Distribution (CIRED)*, 2013, pp. 1-4.

[105] S. W. Alnaser and L. F. Ochoa, "Hybrid controller of energy storage and renewable DG for congestion management," *in Proc. 2012 IEEE/PES General Meeting 2012* pp. 1-8.

[106] N. S. Wade, P. C. Taylor, P. D. Lang, and P. R. Jones, "Evaluating the benefits of an electrical energy storage system in a future smart grid," *Energy policy* vol. 38, no. 11, pp. 7180–7188, 2010.

[107] A. Gabash and P. Li, "Active-Reactive Optimal Power Flow in Distribution Networks With Embedded Generation and Battery Storage," *IEEE Transactions on Power Systems*, vol. 27, no. 4, pp. 2026 - 2035 2012.

[108] A. Gabash and P. Li, "Flexible Optimal Operation of Battery Storage Systems for Energy Supply Networks," *IEEE Transactions on Power Systems*, vol. 28, no. 3, pp. 2788 - 2797, 2013

[109] E. Davidson, A. Keane, R. Currie, N. McNeill, D. MacLeman, and M. Lee, "Requirements-driven distribution state estimation," *in Proc. 2013 International Conference on Electricity Distribution (CIRED)*.

[110] A. Abur and A. G. Exposito, *Power system state estimation: theory and implementation*: CRC Press, 2004.

[111] A. K. Ghosh, D. L. Lubkeman, and R. H. Jones, "Load modeling for distribution circuit state estimation," *IEEE Trans. on Power Delivery*, vol. 12, no. 2, pp. 999-1005, 1997.

[112] J. Wu, Y. He, and N. Jenkins, "A robust state estimator for medium voltage distribution networks," *IEEE Trans. on Power Systems*, vol. 28, no. 2, pp. 1008-1016, 2013.

[113] A. Alimardani, S. Zadkhast, J. Jatskevich, and E. Vaahedi, "Using smart meters in state estimation of distribution networks," *in Proc. 2014 IEEE/PES General Meeting*, pp. 1-5.

[114] J. Ekanayake, N. Jenkins, K. Liyanage, J. Wu, and A. Yokoyama, *Smart Grid: Technology and Applications*: John Wiley & Sons, 2012.

[115] B. Hayes and M. Prodanovic, "State estimation techniques for electric power distribution systems," *in Proc. 2014 IEEE European Modelling Symposium*

[116] J. Lopes, N. Hatziargyriou, J. Mutale, P. Djapic, and N. Jenkins, "Integrating distributed generation into electric power systems: A review of drivers, challenges and opportunities," *Electric Power Systems Research*, vol. 77, no. 9, pp. 1189-1203, 2007.

[117] R. Dugan and T. E. McDermott, "An open source platform for collaborating on smart grid research," in *IEEE/PES General Meeting 2011*, 2011, pp. 1 - 7.

[118] J. Bisschop and M. Roelofs, "AIMMS - The User's Guide," *Paragon Decision Technology*, 2006.

[119] IPSA Power. [Online]. Available: http://www.ipsa-power.com/software

[120] Elexon, " Load Profiles and Their Use in Electricity Settlement," 2013.

[121] National Grid, *The Grid Code*, Feb. 2010.

[122] A. Shapiro, D. Dentcheva, and A. P. Ruszczyńsk, *Lectures on stochastic programming : modeling and theor*: Philadelphia : Society for Industrial and Applied Mathematics : Mathematical Programming Society, 2009.

[123] W. Fu and J. D. McCalley, "Risk based optimal power flow," *in Proc. 2001 IEEE Power Tech* pp. 1-6.

[124] F. Xiao and J. D. McCalley, "Risk-based security and economy tradeoff analysis for real-time operation," *IEEE Trans. on Power Systems*, vol. 22, no. 4, pp. 2287-2288, 2007.

[125] G. Giebel, R. Brownsword, G. Kariniotakis, M. Denhard, and C. Draxl. The State of the Art in Short-Term Prediction of Wind PowerA Literature Overview A Literature Overview, 2nd Edition. [Online]. Available: http://www.anemos-plus.eu/

[126] S. Skogestad, "Simple analytic rules for model reduction and PID controller tuning," *Journal of Process Control*, vol. 13, pp. 291-309, 2003.

[127] R. Moreno, R. Moreira, and G. Strbac, "A MILP model for optimising multi-service portfolios of distributed energy storage," *Applied Energy*, vol. 137, pp. 554–566, 2015.

[128] S. W. Alnaser and L. F. Ochoa, "Advanced network management systems: A risk-based AC OPF approach," *IEEE Transactions on Power Systems, in press*, 2014.

[129] R. A. F. Currie, B. O'Neill, C. Foote, A. Gooding, R. Ferris, and J. Douglas, "Commercial arrangements to facilitate active network management," in *CIRED 21st International Conference on Electricity Distribution*, 2011.

[130] L. Kane, G. Ault, and S. Gill, "An assessment of principles of access for wind generation curtailment in active network management schemes," in *22nd International Conference on Electricity Distribution (CIRED)*, 2013, pp. 5.

[131] J. Mutale, G. Strbac, and D. Pudjianto, "Methodology for Cost Reflective Pricing of Distribution Networks with Distributed Generation," in IEEE/PES General Meeting 2007, 2007, pp. 1 - 5.

Appendices

A. Networks Data for 33 kV Network From the North West of England

This appendix presents the technical parameters for the 33 kV network used in this work. The impedance and the ratings of lines and transformers are presented in Table A. 1 and Table A. 2 (in per unit with respect to a base of 100 MVA). The peak active and reactive powers of loads are presented in Table A. 3.

Table A. 1 Lines Parameters

Start Bus	End Bus	S_{max} (p.u.)	R (p.u.)	X (p.u.)
200	210	0.1663	0.1389	0.1322
200	201	0.2006	0.0398	0.0513
202	203	0.3229	0.3199	0.6768
209	207	0.1663	0.4605	0.4381
201	202	0.20096	0.4104	0.5379
206	207	0.2989	0.1041	0.2249
204	206	0.2989	0.0191	0.0412
202	204	0.3229	0.0857	0.185
204	205	0.2286	0.1169	0.1139
200	202	0.2172	0.425	0.5568
210	209	0.1663	0.0562	0.0535
200	208	0.1663	0.2504	0.255
208	207	0.1663	0.4611	0.4387
208	209	0.2006	0.0554	0.0697

Table A. 2 Transformer Parameters

Start Bus	End Bus	S_{max} (p.u.)	R (p.u.)	X (p.u.)
208	1103	0.23	0.04	1
208	1103	0.23	0.04	1
202	1100	0.20	0.04	1
202	1100	0.20	0.04	1
207	1104	0.13	0.04	1.04
207	1104	0.13	0.04	1.04
203	1101	0.095	0.05	1.33
203	1101	0.095	0.05	1.33
100	200	1.5600	0.0037	0.1244

Table A. 3 Peak Demand and Reactive Power of Loads

Bus location	Active power (MW)	Reactive power (MVAr)
1100	10.6	5
1101	1.5	0.3
1102	0.1	0.04
1103	10.9	2
1104	9.2	1

B. Scenarios of Generation and Loads Used in the Multi-Period AC OPF

Table B.1 presents the scenarios of loads and generation to be adopted by the multi-period AC OPF planning tool used in Section 4.9 to find the maximum additional DG capacity connected to the 33 kV UK distribution network.

Table B. 1 Scenarios of Generation and Loads Used in the Multi-Period AC OPF

Wind (p.u.)	Loads (p.u.)				Probability (%)
	1100	1101	1103	1104	
0.05	0.5	0.5	0.3	0.3	0.07
0.05	0.5	0.5	0.3	0.5	0.1
0.05	0.5	0.5	0.5	0.5	0.19
0.05	0.7	0.5	0.5	0.5	4.36
0.05	0.5	0.7	0.5	0.5	4.59
0.05	0.7	0.7	0.5	0.5	2.96
0.05	0.7	0.7	0.5	0.7	0.88
0.05	0.5	0.5	0.7	0.5	0.46
0.05	0.5	0.5	0.7	0.7	0.2
0.05	0.7	0.5	0.7	0.7	0.15
0.05	0.7	0.7	0.7	0.7	0.15
0.15	0.3	0.3	0.3	0.3	0.3
0.15	0.5	0.5	0.3	0.3	1.35
0.15	0.5	0.5	0.3	0.5	11.9
0.15	0.5	0.5	0.5	0.5	7.93
0.15	0.7	0.5	0.5	0.5	3.76
0.15	0.5	0.7	0.5	0.5	3.04
0.15	0.7	0.7	0.5	0.5	2.11
0.15	0.7	0.7	0.5	0.7	1.11
0.15	0.5	0.5	0.7	0.5	0.98
0.15	0.5	0.5	0.7	0.7	0.91
0.15	0.7	0.5	0.7	0.7	1.11
0.15	0.7	0.7	0.7	0.7	0.84
0.25	0.5	0.5	0.3	0.5	0.46
0.25	0.5	0.5	0.5	0.5	0.26
0.25	0.7	0.5	0.5	0.5	0.02
0.25	0.5	0.7	0.5	0.5	0.6
0.25	0.7	0.7	0.5	0.5	0.25
0.25	0.7	0.7	0.5	0.7	0.25
0.25	0.5	0.5	0.7	0.5	0.26
0.25	0.5	0.5	0.7	0.7	0.31
0.25	0.7	0.5	0.7	0.7	0.19
0.25	0.7	0.7	0.7	0.7	0.04
0.25	0.7	0.7	0.9	0.7	0.03
0.35	0.5	0.5	0.3	0.5	2.68
0.35	0.5	0.5	0.5	0.5	0.57
0.35	0.5	0.7	0.5	0.5	0.42
0.35	0.7	0.7	0.5	0.5	0.19
0.35	0.7	0.7	0.5	0.7	0.15
0.35	0.5	0.5	0.7	0.5	0.08
0.35	0.5	0.5	0.7	0.7	0.04
0.35	0.7	0.5	0.7	0.7	0.03
0.35	0.7	0.7	0.7	0.7	0.01
0.35	0.7	0.7	0.9	0.7	0
0.45	0.5	0.5	0.3	0.5	5.18
0.45	0.5	0.5	0.5	0.5	2.45
0.45	0.5	0.7	0.5	0.5	1.47
0.45	0.7	0.7	0.5	0.5	1.17
0.45	0.7	0.7	0.5	0.7	0.94
0.45	0.5	0.5	0.7	0.5	0.53
0.45	0.5	0.5	0.7	0.7	0.32
0.45	0.7	0.5	0.7	0.7	0.34
0.45	0.7	0.7	0.7	0.7	0.77
0.45	0.7	0.7	0.9	0.7	1.09
0.55	0.5	0.5	0.3	0.5	1.08
0.55	0.5	0.5	0.5	0.5	0.57
0.55	0.5	0.7	0.5	0.5	0.26
0.55	0.7	0.7	0.5	0.5	0.22
0.55	0.7	0.7	0.5	0.7	0.07
0.55	0.5	0.5	0.7	0.5	0.03
0.55	0.5	0.5	0.7	0.7	0.03
0.55	0.7	0.5	0.7	0.7	0.04
0.55	0.7	0.7	0.7	0.7	0.01
0.55	0.7	0.7	0.9	0.7	0.07
0.65	0.5	0.5	0.3	0.5	0.4
0.65	0.5	0.5	0.5	0.5	0.12
0.65	0.5	0.7	0.5	0.5	0.13
0.65	0.7	0.7	0.5	0.5	0.05
0.65	0.7	0.7	0.5	0.7	0.03
0.65	0.5	0.5	0.7	0.5	0.01
0.65	0.5	0.5	0.7	0.7	0.01
0.65	0.7	0.5	0.7	0.7	0.06
0.65	0.7	0.7	0.7	0.7	0.07
0.65	0.7	0.7	0.9	0.7	0.01
0.75	0.5	0.5	0.3	0.5	1.34
0.75	0.5	0.5	0.5	0.5	0.59
0.75	0.5	0.7	0.5	0.5	0.32
0.75	0.7	0.7	0.5	0.5	0.2
0.75	0.7	0.7	0.5	0.7	0.15
0.75	0.5	0.5	0.7	0.5	0.08
0.75	0.5	0.5	0.7	0.7	0.01
0.75	0.7	0.5	0.7	0.7	0.04
0.75	0.7	0.7	0.7	0.7	0.04
0.75	0.7	0.7	0.9	0.7	0.13
0.85	0.5	0.5	0.3	0.5	7.89
0.85	0.5	0.5	0.5	0.5	6.75
0.85	0.7	0.7	0.5	0.5	2.94
0.85	0.7	0.7	0.5	0.7	1.36
0.85	0.5	0.5	0.7	0.5	0.94
0.85	0.5	0.5	0.7	0.7	0.72
0.85	0.7	0.5	0.7	0.7	0.33
0.85	0.7	0.7	0.7	0.7	0.29
0.95	0.5	0.5	0.3	0.5	0.3
0.95	0.5	0.5	0.5	0.5	1.56
0.95	0.7	0.7	0.5	0.5	0.01
0.95	0.7	0.7	0.5	0.7	0.04
0.95	0.5	0.5	0.7	0.5	0.03
0.95	0.5	0.5	0.7	0.7	0.02
0.95	0.7	0.5	0.7	0.7	0.02
0.95	0.7	0.7	0.7	0.7	0.01

C. Research Publications

- S. W. Alnaser and L. F. Ochoa, "Optimal sizing and control of energy storage in wind power-rich distribution networks", IEEE Trans. on Power Systems, submitted for second round of reviews (Paper TPWRS-01402-2014).

- S. W. Alnaser and L. F. Ochoa, "Advanced network management systems: A risk-based AC OPF approach", IEEE Transactions on Power Systems, vol. 30, pp. 409-418, 2015. DOI Link

- S. W. Alnaser and L. F. Ochoa, "Distribution network management system: An AC OPF approach", in IEEE/PES General Meeting 2013, 2013, p. 5. DOI Link

- S. W. Alnaser and L. F. Ochoa, "Towards distribution energy management systems: Maximising renewable DG", in 22nd International Conference on Electricity Distribution CIRED 2013, 2013, p. 4. DOI Link

- S. W. Alnaser and L. F. Ochoa, "Hybrid controller of energy storage and renewable DG for congestion management", in IEEE/PES General Meeting 2012, 2012, p. 8. DOI Link